REPUBLIQUE DU CAMEROON

Paix-Travail-Patrie

****

****

DEPARTEMENT DE GENIE CIVIL

****

DEPARTMENT OF CIVIL ENGINEERING

****

REPUBLIC OF CAMEROON

Peace-Work-Fatherland

****

****

DEPARTMENT OF CIVIL,

ARCHITECTURAL AND

ENVIRONNEMENTAL ENGINEERING

****

MODELLING THE GROUND SURFACE SETTLEMENT INDUCED BY UNDERGROUND EXCAVATION

Case study : Extension of metro line 12 in France

Thesis submitted in partial fulfillment of the requirements for the degree of Master in Civil Engineering

Option : Geotechnical Engineering

Présented by :

MANGUELLE THIERRY CLAUDE

Matricule **:15TP20921**

Supervisor :

Pr.Eng. SIMONETTA COLA

ACADEMIC YEAR : 2019/2020

DEDICATION

To my wonderful and loving parents

Mr MANGUELLE SIMON PIERRE

And

Madam MANGUELLE GLADYS

ACKNOWLEDGEMENT

This Thesis is the fruit of the combined efforts of several individuals who contributed either directly or indirectly to its elaboration. It is therefore with gratitude that I address my sincere thanks to:

- The President of the jury;
- The Examiner of this jury for accepting to bring his criticisms and observations to improve this work;
- My supervisors Prof. Simonetta COLA and Engineer Christian Noubissi for all their guidance, explanations, documentation and advice during this thesis work;
- Prof. George NKENG, the Director of ENSTP for his academic and administrative support during these years spent at ENSTP;
- Pr. Carmelo MAJORANA and Pr. ESOH ELAME, of the University of Padova (Rome-Italy), for his work with establishing this partnership with NASPW for the training of young Cameroonians.
- Prof. MBESSA Michel, the head of department of Civil Engineering for his tutoring and valuable advices;
- All the teaching staff of ENSTP and University of Padua for their good quality teaching and the motivation they developed in us to continue our studies;
- All my classmates who were a source of motivation and tenacity.
- My siblings: TETCHA NKOLA PRIMAEL, TIYUSHY IRVIN, ZAPA FOTSO GEORGE, for their encouragement, love, affection and support since our childhood.
- All the students of ENSTP and my friend AHMED for the confidence they always put on

LIST OF ABBREVIATIONS AND SYMBOLS

ADECO	Analysis of controlled Deformations in Rocks and Soils
α	rheological parameter
AFTES	Association Française des Tunnels et de l'Espace Souterrain
BEM	Boundary Element Method
C	Soil cohesion
c'	Effective soil cohesion
CPV	Volume Pressure Controller
d	Plate thickness
D	Tunnel diameter
DEM	Discrete Element Method
E	Young's modulus
EBP:	Earth balanced Pressure
e_0	Void ratio
E_0	Tangent modulus
E_{50}	secant modulus
EA	Axial stiffness
EI	Bending stiffness
E_{oed}	Oedometric soil modulus
E_{ur}	Unloading modulus
FDM	Finite Difference Method
FEM	Finite Element Method
G	Shear modulus
HSM :	Hardening Soil Model
HSSM :	Hardening Soil with small Strain Model
I	Moment of inertia
k_x	Horizontal permeability

k_y	Vertical permeability
MC	Mohr Coulomb
NATM :	New Australien Technique Metros
P_L	Ménard limit pressure
PMT	Pressuremeter test
TBM	Tunnel boring machine
u	Elastic displacement
ε_x	Horizontal strain
ε_y	Vertical strain
ε_z	Axial strain
ν	Poisson's ratio
σ_r	Radial stress
σ_x	Horizontal stress
σ_y	Vertical stress
σ_z	Horizontal stress
σ_θ	Tangential stress
φ	Internal friction angle
φ'	Effective soil friction angle
ψ	Dilatancy angle

ABSTRACT

The construction of underground transport infrastructures has become an unavoidable alternative in urban areas. Despite their great importance, tunnels excavated in urban areas can cause enormous damage to the surrounding infrastructure. Generally, the control of these risks is done through a monitoring procedure to record the ground displacements. Numerical methods exist to predict the ground response to tunneling, but a two-dimensional approach has been chosen that requires the application of a fictitious pressure that is generally not well known. The role played by the law used to simulate the soil behavior is fundamental. The reliability of a numerical simulation relies on the adoption of an appropriate constitutive soil models such as the elasto-plastic laws Hardening Soil Model with Small Strain (HSSM), Hardening Soil Model and Mohr Coulomb's model. In this work, 2D simulations of the extension of the metro line 12 with these three laws of behavior in the north of the city of Paris are conducted using the finite element software PLAXIS 8.6 to calibrate the observations. We made an analysis and a calibration of the different modulus of deformation of each constitutive soil models (determination of the ratios between the different modulus), a comparison of the results obtained from the different settlement tanks after modelling was then conducted with the Peck settlement tank, which allowed us to conclude that the use of the HSSM constitutive soil model is the best adapted for the excavation of our tunnel because it takes into account the variation of the modulus in the case of small deformations. An analysis of the influence of the mechanical characteristics of the soil around the tunnel on the settlement curve was carried out and it results that the modulus of deformation on the settlement curve was carried out and it was found that the modulus of deformation, the angle of internal friction and the cohesion play a major role in the prediction of the surface settlements (the value of the maximum settlement) and finally, an analysis of the influence of the apparition of plastic zones around the tunnel on the settlement curve was carried out .

Keywords : **constitutive soil models; numerical modeling; underground structure**

RESUME

La construction d'infrastructures de transport souterraines est devenue une alternative incontournable dans les zones urbaines. Malgré leur importance capitale, les tunnels excavés dans des agglomérations peuvent occasionner d'énormes dégâts au niveau des infrastructures environnantes. Généralement, le contrôle de ces risques passe par une procédure de surveillance permettant d'enregistrer les déplacements du sol. Des méthodes numériques existent pour prédire la réponse du sol au creusement de tunnel.On a opté pour une approche bidimensionnelle qui nécessite l'application d'une pression fictive généralement mal connue. Le rôle joué par la loi permettant de simuler le comportement du sol est fondamental. La fiabilité d'une simulation numérique repose sur l'adoption d'une loi de comportement appropriée à l'exemple des lois élasto-plastique Hardening Soil Model with Small Strain (HSSM), Hardening Soil Model et la loi de Mohr Coulomb. Dans ce travail , des simulations 2D du prolongement de la ligne du métro 12 avec ces trois lois de comportement dans le nord de la ville de Paris sont menées à l'aide du logiciel aux éléments finis PLAXIS 8.6 pour caler les observations.Nous avons fait une analyse et une calibration des differents modules de deformations de chaque loi de comportement (determination des rapports entre les differents modules) ,une comparaison des résultats obtenus des differents cuvettes de tassements apres modélisation a ensuite été menée avec la cuvette de tassement de Peck, ce qui nous a permis de conclure que l'utilisation de la loi de comportement HSSM est la mieux adapter pour le creusement de notre tunnel car elle prend en compte la variation du modulus dans le cas des petites déformations . Une analyse de l'influence des caracteristiques mécaniques du sol autour du tunnel sur la cuvette de tassement a été effectuée et il en resulte que les modules de deformations , l'angle de frottement interne et la cohésion jouent un role primordiale sur la prediction des tassements en surface (la valeur du tassement maximal) et en definitive, une analyse a été faite sur l'influence de l'apparition des zones plastiques sur la cuvcette de tassement .

Mots-clefs : Modèles de comportement ; modélisation numérique ; ouvrages souterrains

LIST OF FIGURES

LIST OF TABLES

LIST OF EQUATIONS

TABLE OF CONTENTS

General introduction

In urban areas, estimating the influence of tunnelling on neighbouring buildings is an important economic and environmental aspect. Indeed, the loss of volume in the tunnel is reflected on the surface, creating ground movements likely to affect more or less significantly the structures on the surface. The interaction between existing structures and underground structures is a complex phenomenon in which the behaviour of the surrounding massif represents a problem during tunnelling. However, a realistic soil model is an essential element in predicting the magnitudes and distribution of deformations. The constitutive soil model frequently used in the numerical simulation of underground construction is linear elastic perfectly plastic with a Mohr-Coulomb fracture criterion. In general, its use leads to settlement curve that are shallower and wider than those observed experimentally. In order to take into account some of the fundamental aspects of soil behaviour such as dilatance before fracture, the variation of the modulus as a function of the stress state, a module in unloading is different from that in loading, it is therefore necessary to use an elastoplastic model with isotropic work hardening. For an analysis of settlements, it also appears necessary to take into account the variation in the modulus of soils with low deformation. In order to better model the behavior of the soil during the extension of the metro line 12 of Paris, we will study the influence of the use of different constitutive soil models to different levels of complexity , nonlinearity before rupture or anisotropy on deformations around tunnels. They all stress the importance of taking into account the nonlinearity of the terrain in numerical models.

In this thesis, during the extension of the Paris Metro line 12, sensors were installed at the ground surface to record the settlements. To predict those deformations, engineers generally conduct some numerical simulations. A reliable simulation relies on the adoption of an appropriate constitutive model. The aim of this thesis is to illustrate the influence of the constitutive model on the response of the soil, to analyse and calibrate the different stiffness modulus of each constitutive soil model and analyse the influence of plasticity around the tunnel on the settlement curve .Three constitutive soil models are implemented in a two-dimensional simulation of underground construction in plane strain: a perfectly plastic linear elastic model (Mohr-Coulomb model), an elastoplastic model with isotropic work hardening (*Hardening Soil Model, Schanz et al., 1999*) and an evolution of this model taking into account

the evolution of the shear modulus as function of the level of deformation (Plaxis, 2015). The study is based on the results of pressuremeter tests. The influence of the chosen model is highlighted in terms of settlements.

Chap 1: LITERATURE REVIEW

Introduction

While urban agglomerations are becoming denser and denser, the realization of underground works, such as car parks, metropolitan tunnels, road, rail, etc. has become a priority issue in the context of policies to reorganize spaces, improve the viability and development of public transport for essentially functional and economic reasons. These structures are generally hollow at shallow depths in terrains that may have a heterogeneous nature. They may have been built either underground or in the open air and then covered with embankments (covered trenches). Their use is very diverse: electrical plants, car parks, warehouses, multi-purpose shelters, storage of fluids or radioactive waste, etc. .. The engineer is thus faced with two major problems: on the one hand to ensure the smooth running of the work while preserving the stability of the structure, and, on the other hand, to control the deformations of the surrounding massif to avoid interaction with the surrounding structures. In highly urbanized areas, the digging of structures can in fact cause major disorders to structures, with human and economic consequences.

1 .1 History of underground construction

Neanderthals were the first who start which the underground construction . Neanderthal construction sites in France have been dated to 174,000 bc, far earlier than the earliest human sites. Human underground construction likely began with cave-dwelling pre-historic people who wanted to expand their home (*Brierly and Gary, 2020*). The purpose of many ancient underground structures is a mystery, for instance erdstalls (type of tunnel which are found across Europe). All ancient civilizations practiced some form of underground construction with some also branching into rock-cut architecture. In early urban centers, underground spaces served as burial places provided protection against invaders, and enabled early public utility (*Brierly and Gary, 2020*).

The first known use of gunpowder in underground construction occurred in France in 1681. The invention of dynamite and steam and compressed air powered drills in the 18th century

revolutionized the industry. The 19th century saw innovations in shield tunneling techniques which made underground construction in soil safer. As nations urbanized the extent of underground urban construction increased significantly with improved sewers, public water systems, subways, and underground commercial spaces all being required by expanding cities. In the late 20th and early 21st century, advances in automation and geotechnical_engineering have allowed the ambition and scale of underground construction projects to increase archeology in major cities often requiring underground construction techniques as excavations must be made without disturbing existing buildings on the site. Underground museums have been created to preserve historical structures in-situ and without altering, the often historically significant building built above (*Meuller and Tom, 2020*). Archeological sites are also commonly discovered during underground construction (*Solly and Meilan, 2020*) .

1.2 Types of underground construction

The classification of underground construction is based on three aspects, one can list the underground construction based on purpose (road, rail, navigation), based on execution mode and based on the shape.

1.2.1 Underground construction based on the purpose

The classification of underground construction, based on their purpose or usefulness, highlights the following underground construction: railway tunnel, road tunnels and navigation tunnels, which are presented in the following paragraphs:

1.2.1.1 communication tunnel

(a) Road Tunnel

A road tunnel is a structure that creates a confined space through which a road passes, for example: rock tunnels; cut-and-cover tunnels, where an open trench is made that is then covered; submerged, underwater or underwater tunnels. Their design and construction are complex and can take several years, sometimes more than 10 years. Indeed, the different types of prospecting (geological, hydrogeological and geotechnical) must be carried out at several stages of study to obtain the elements necessary for the development of the project. These

studies make it possible to choose a suitable construction method, which minimizes delays and costs.

Figure 1.1. First road tunnel of Lorain

(b) Railway Tunnel

The railway tunnel is a mode of guided transport used for the movement of people and objects. It is generally characterized by a specialized infrastructure consisting of two parallel rails allowing the movement of motorized trains. Along with road, river and air modes, it is one of the modern forms of transportation.

Figure 1.2 . Villefranche Tunnel (Nice/Villefranche –sur-Mer , 1868)

(c) Canal Tunnel

A canal tunnel is a tunnel dug to allow the passage of a canal or waterway (mainly navigation) under a natural obstacle. They are usually built to reduce the number of locks. The longest tunnel in the world is the Rove tunnel in France with 7120 m, this tunnel is closed to navigation since 1963 following a collapse. The oldest tunnel-canal is the Malpas tunnel, also in France, built in 1679.

Figure 1.3 . Entrance to the Mauvages tunnel

1.2.1.2 Transport Tunnels

(a) Water Supply

Water supply includes the techniques used to bring water from its source to the place of consumption through a network of pipes or architectural structures. It is generally composed of a source (river, body of water, groundwater) from which water is pumped, the transport network (canal, pipeline), the storage (basin, water tower); finally the distribution network which brings water to the consumers (tap, fountain, etc...).

Figure 1.4 . Water supply (Article assainissement – Ooreka, 2008)

(b) Hydraulic Galleries

Hydraulic galleries belong, as well as pipes and canals, to the set of structures that allow to convey water from the dam or the water intake to the plant where it will be treated.

Figure 1.5 . Hydraulic Galleries- hydrostatium

(c) Sewers

Most often underground, a sewer is a pipe or masonry tube designed to collect and evacuate various types of water, whether natural, such as runoff and rainwater, or produced by human activity, such as wash water, drainage water, or wastewater (gray water and grey water)

Figure 1.6 . sewer of paris (les Maçons parisiens,2008)

1.2.1.3 Tunnels and Storage cavities

(a) Parkings

A parking lot, parking area, is a space or building specially designed for parking vehicles. It can be public or private, enclosed, elevated or underground. It is most often found next to public buildings (train station, airport), workplaces, shopping centers or in front of supermarkets to accommodate users.

Figure 1.7 . underground Parking

(b) liquid or gaseous storage

Underground storage is the storage of useful fluids (gas, hydrocarbons) in the subsoil, in artificial or natural cavities, either in porous geological layers, aquifers in general or those whose permeability can be increased. Underground storage of hydrocarbons has developed a lot in the last few years, and will develop in the future (reference).

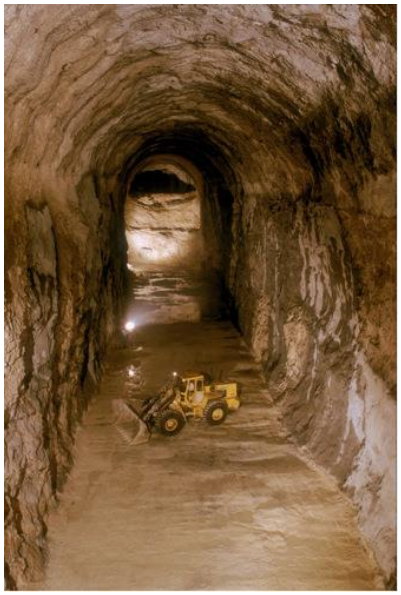

Figure 1.8. underground storage of gases and hydrocarbons .

1.2.2 underground excavation based on the construction technique

1.2.2.1 tunnels or cavities built in the open air

In urban areas, the construction of deep underground structures is carried out from the surface, which is then covered with a reinforced concrete slab and a fill. It is mainly for economic reasons, related to local factors, that leads to this solution. In particular, the work of moving the networks should not be too important**.**

1.2.2.2 tunnels built underground at shallow or high depths

Unlike open air construction, here tunnels are built deep underground or in the rock, usually by a tunnel boring machine or by the use of explosives. They are the most frequently encountered in the world.

1.2.3 underground excavation based of shape

1.2.3.1 Shafts and tunnels (constant or little variable section)

A well is originally a vertical physical cavity, connecting two levels of different depths, penetrable or not. It can be natural (well in karst cavities) or artificial.

Figure 1.9 . well of saint patrice in Orvieto Italie

1.2.3.2 Cavities

Underground cavities are voids that affect the subsoil and whose origin can be:

- human: mines, shelters, tunnels, war graves, quarries

- natural: cave , chasm

Figure 1.10 . Underground cavities bored inside rock (Fort du salbert,2018)

1.3 Methods of Tunnel construction

A tunnel construction is an underground passage provided beneath earth surface or water. Different methods of tunnel construction and their details are discussed. In most of the cases tunnel construction is expensive but it saves time and provides comfort. Large excavation of soil or rock etc. is necessary for a tunnel construction. With the availability of modern equipment, excavation and backfilling has become easier.There are various types of construction techniques developed for construction of tunnels, which are discussed below.

1.3.1 Clay Kicking Method of Tunnel Construction

This method is used for strong clayey soil conditions. This is an old method and used for small works like sewage pipes installations etc. In this method, a hole is excavated into the ground and after some depth tunnel is excavated which is done by the clay kicker which lies on a plank at 45° angle. An excavating tool is provided under clay kicker foot. The excavated using that tool is collected by other workers. This is well famous because it is the method used by Englishmen to put mines under the German empire during First World War.

Figure 1.11. clay kicking or working on the cross (Manchester's –building heroes of WWI, 2008)

1.3.2 Pipe Jacking Method of Tunnel Construction

The Pipe jacking method is used to construct tunnels under existing structures like roadways, railways etc. In this method, specially made pipes are driven into underground using hydraulic jacks , a maximum size of 3.2 meter diameter is allowed for tunnels.

Figure 1.12. pipe jacking (Tunnel construction techniques and their details Article ,2020)

1.3.3 Box Jacking Method of Tunnel Construction

Box jacking method is similar to pipe jacking, but in this case, instead of pipes, specially made boxes are driven into the soil. A cutting head is provided at the front side of the box. Excavated matter is collected within the box. Larger size tunnels can be excavated using box jacks up to 20 meters.

Figure 1.13. Box Jacking Tunnel (Tunnel construction techniques and their details Article ,2020).

1.3.4 Cut and cover Tunnelling

Cut and cover method of tunnel construction is generally used to build shallow tunnels. In this method, a trench is cut in the soil and it is covered by some support, which can be capable of bearing load on it. The cutting can be done by two methods. One is bottom up method in which a tunnel is excavated under the surface using ground support. Another method is top-down method in which side support walls are constructed first by slurry walling method or contiguous bored piling. Then roof is located on the top of the walls and excavation is carried out. Finally, base slab is constructed. Most of the Underground metro rail stations are constructed using cut and cover method.

Figure 1.14. cut and cover Tunnel (waterproof Magazine , 2019)

1.3.5 NATM method

The New Austrian tunneling method (NATM), also known as the sequential excavation method (SEM) or sprayed concrete lining method (SCL) (*Alun thomas , 2019),* is a method of modern tunnel design and construction employing sophisticated monitoring to optimize various wall reinforcement techniques based on the type of rock encountered as tunneling progresses.. The name NATM was intended to distinguish it from earlier methods, with its economic advantage of employing inherent geological strength available in the surrounding rock mass to stabilize the tunnel wherever possible rather than reinforcing the entire tunnel. The NATM integrates the principles of the behaviour of rock masses under load and monitoring the performance of underground construction during construction. The NATM has often been referred to as a "design as you go" approach, by providing an optimized support based on observed ground conditions. More correctly it can be described as a "design as you monitor" approach, based on observed convergence and divergence in the lining and mapping of prevailing rock conditions. It is not a set of specific excavation and support techniques.

Figure 1.15. understanding the New austrian Tunnel Method (Tunnel Business Magazine ,2018)

1.3.6 Bored tunnelling

The bored tunnel method is modern technology of tunneling. In this case, tunnel boring machines are used, which automatically work and makes the entire tunneling process easier. It is also a quicker process and a good method to build tunnels in high-traffic areas. Tunnels boring machines (TBM's) are available in different types suitable for different ground conditions. These machines can be used in difficult conditions such as below the water table etc. A special pressurized compartment is provided for TBM to work in below water table conditions. The workers should not enter that compartment except for repair works. Care should be taken while TBM is in working conditions. The only difficulty with this TBM is its heavy weight. So, transportation is complex and costlier.

Figure 1.16. Tunnel Boring machine (*Tunnel construction techniques and their details Article ,2020)*

1.4 Ground movements caused by tunnelling

The introduction of a cavity in a ground alters the state of stress in the massif around the excavated area. This results in movements within the massif. Depending on the intensity of this disturbance, these movements are usually accompanied by an instantaneous movement of the size at the excavation and a convergence of the tunnel walls (Fig 1.17). All these deformations already start well in front of the cut, as amply described and demonstrated with in situ measurements by Lunardi and Bindi [2004] and Lunardi [2008].

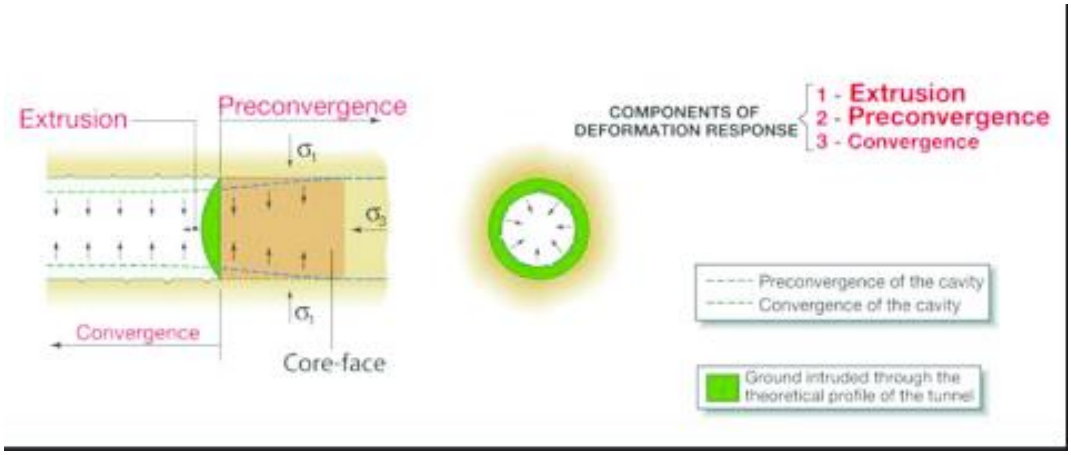

Figure 1.17. The three components of the deformation in the massif caused by the digging of a tunnel (Lunardi and Bindi, 2004)

These movements, attributable to volume loss of ground (*Schlosser, 1989*), may then spread to the ground surface with some delay, depending on the response time of the mass and the tunnel cover. However, Chapeau [1991] pointed out that for shallow tunnels (C/D < 2); the damping can be so small that an error in the excavation procedure can result in block failure of the entire neck. For greater cover heights, on the other hand, the vaulting effect, described by Lunardi [1997], can intervene and avoid this harmful phenomenon. The three-dimensional settlement curve, well represented by Attewell [1987] and Lebais et al [1995], can cause significant damage to existing structures. For this reason, a priority issue in the construction of tunnels in urban areas is the limitation of these deformations. In this regard, Lunardi [2008] proposed a method, known as ADECO, pointing out that tunnel deformations and surface settlements would be limited by a strict control of the deformations of the face core.

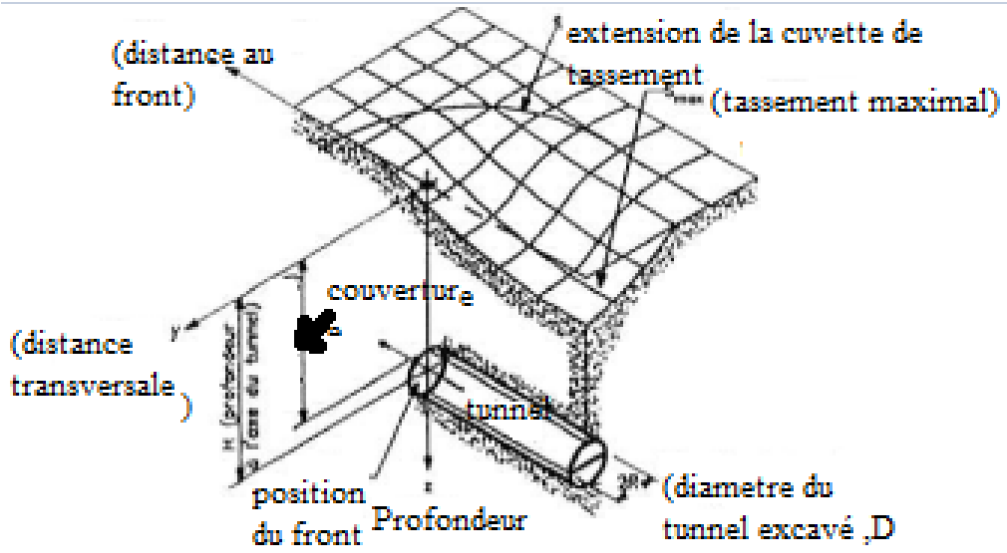

Figure 1.18 . 3D settlement curve (Leblais et al. 1995)

Horizontal displacements in the massif are measured, in the longitudinal and transverse directions, using inclinometers. The transverse inclinometric deformations, derived from the measurements presented by Bernat [1996], show that the soil on the surface tends to converge towards the center of the basin; in addition, a "belly" appears at the height of the excavation towards the void created. In the case of the pressurized front-end TBM (*Ollier, 1997*), this belly appears in the opposite direction. The effect of this excavation method is also visible in the longitudinal inclinometric deformation where the soil is driven forward during excavation.

1.5 predictive Methods

The tunnelling causes more or less significant disturbances in the internal balance of the surrounding massif, thus creating deformations and ground displacements. In urban areas, the settlements resulting from this phenomenon can affect the stability of neighbouring structures. These disorders can have significant human and economic consequences. Several approaches are thus used to seek to study and predict the evolution of these movements in the massif. In this section, the different methods will be presented through examples from the literature.

1.5.1 Empirical or semi-empirical methods

These methods, in general, aim to estimate primarily surface settlements from a small number of parameters, such as tunnel depth, diameter, nature of the mass, and volume or convergence loss caused by excavation. A large database of settlement measurements is available in the literature (*Schmidt [1969], Peck [1969], Attewell [1977], Clough and Smith [1981], O'Reilly and New [1982], Rankin [1988*]). These measurements showed that the cross-sectional distribution of colonies on the tunnel surface can be represented by a Gaussian curve. The analytical formulation of the regulation is given by the equation of peck (1.1).

$$\mathbf{S(x) = S_{max}.\ exp\left(\frac{-x^2}{2i^2}\right)} \qquad \mathbf{(1.1)}$$

In this expression, x is the distance from the point under consideration to the tunnel axis, Smax is the maximum settlement, and i is the abscissa of the basin inflection point. The settlement profile is also characterized by its half-width Lc = 2.5.i (Figure 1.19) and its total volume : Vs = 2.5.i.Smax

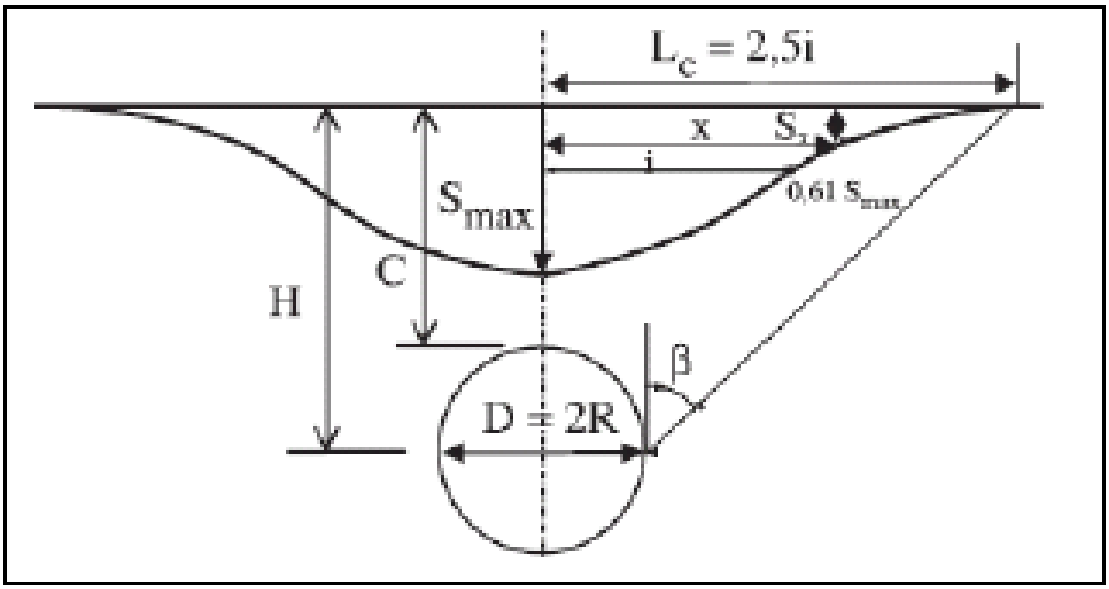

Figure 1.19 . settlement curve of Gaussian profil

Several empirical correlations have been proposed by the authors, linking "i" to the geometric parameters of the work (C, D and H defined in Figure 1.19) according to the nature of the soil. The different formulas were presented by Dias [1999] in his thesis. Selby [1988] and New and O'Reilly [1991], correlated the value of i with the depth of the tunnel axis Z, using the equation i= K.Z. Bilotta, Russo, and Viggiani [2002] collected about 90 cases of transverse profile measurements of settlements in soft ground. Through a least squares optimization of the interpolations of the measurements with the Gaussian curve, they obtained for the different cases the values of the parameter i. In this way, they could then study the variation of K and obtain a mean value of 0.43. The analysis also targeted the volume loss with respect to the theoretical excavated volume (V'). Average values of V' were thus proposed depending on the excavation technique (TBM or NATM). A similar study was recently presented by Fillibeck and Vogt [2011]. By analyzing more than 300 cross-sectional settling measurements, they propose relationships between V' and i and soil type, deformation modulus, tunnel depth and excavation technique. Based on the confidence intervals, these values can therefore be chosen to predict the order of magnitude of the maximum final settlement. Many other authors, such as Sagaseta and Moya [1980], Farmer [1977], Poupelloz [1984], Descoeudres [1979], have written empirical formulas to estimate the value of the maximum settlement S_{max} as a function of the geometry of the excavation and the coefficients to be taken into account according to the type of ground encountered.

1.5.2 Analytical Methods

1.5.2.1 Principles and examples of analytical methods

In the literature, many analytical formulations are provided. In the majority of cases, the authors were interested in studying the change in the stress field caused by tunneling. However, formulations have also been proposed for the evaluation of the displacements in the massif. These are based on the general principles of mechanics as well as on strong assumptions concerning the geometry of the problem (circular tunnel with horizontal axis at great depth), the stratigraphy (a single homogeneous layer), the constitutive model (Tresca or Mohr-Coulomb) and the initial state of the stresses (non-heavy, isotropic and homogeneous soil). Furthermore, the formulas are expressed in the plane and in the framework of small strain analyses. These assumptions represent one of the main weaknesses of these methods. Based on

the above assumptions, the radial displacement (as a function of distance from the r-axis) of an unsupported tunnel and the relative volume loss (V_t) are defined in equation (1.2), in the case of linear elasticity.

$$U(r) = -\frac{1+v}{E} P \frac{R^2}{r} \quad \text{and} \quad V_t = 2\frac{1+v}{E} P\pi R^2 \qquad \textbf{(1.2)}$$

Where, $P = \sigma_V = \sigma_h$, v: poison coefficient ,r : the distance from the tunnel axis and E :young modulus .

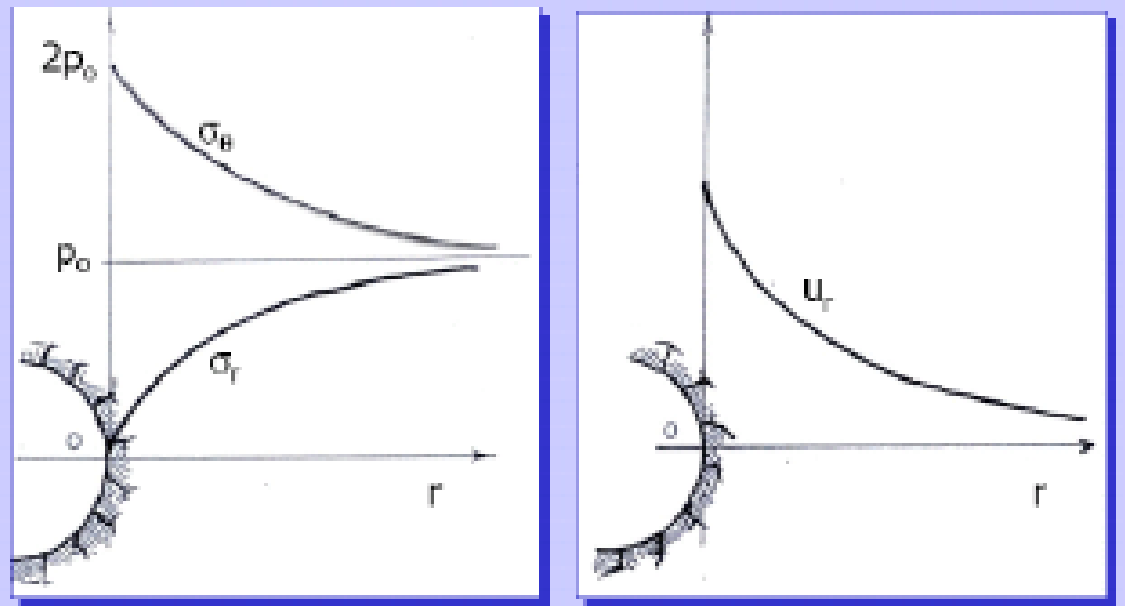

Figure 1.20. curve of stresses and radial displacement as a function of the distance r considered.

Panet [1969], Poupelloz [1984], Sagaseta [1987] and Verruijt [1997] have proposed formulations for surface settlements and horizontal displacements in the framework of an elastic medium. Poulos [1974], Berry [1977] are interested in the case of an anisotropic solid. Studies have also been carried out on an elastoplastic medium. We can mention those of Panet [1973, 1976], Detourney [1987] and the method of De Beer and Buttiens, presented by Poupelloz [1984], in which a field of stresses and displacements is defined, by defining a boundary radius around the excavation between the plastic and elastic zones. Plastic deformations are also considered by Rowe et al. [1983] and Lee et al. [1992] who, by combining these deformations around the waist with the effects of pre-convergence and void of the ground bearing contact, defined an annular void parameter, called GAP. Depending on

this parameter, the surface settlement can be calculated using empirical relationships. This notion of annular void was then taken up by Loganathan and Poulos [1998]. Their solution considers that the radial displacement around the tunnel, excavated to the shield, is not uniform. From this reflection, they propose a settlement equation along a cross section, in which the only soil parameter to be known is the Poisson's ratio.

1.5.2.2 Convergence -confinement Method

Still in the context of analytical approaches, an often used method is the so-called "convergence confinement" (*Panet, 1995*), designed to simplify the three-dimensional tunneling problem into a two-dimensional plane deformation problem of the soil-support interaction. It is commonly introduced in 2D numerical calculations of tunnel excavation projects, in order to estimate the deformations of the mass (convergence and settlement) and to validate the supports. In this paragraph, the principles of this method will be presented. The approach adopted to apply them to a 2D calculation will be explained in the rest of the work. On the basis of the hypotheses exposed in the previous paragraph, this method consists in simulating the advance of the size by reducing a fictitious pressure (P_i) applied to the walls of the excavation is presented in (figure 1.21).

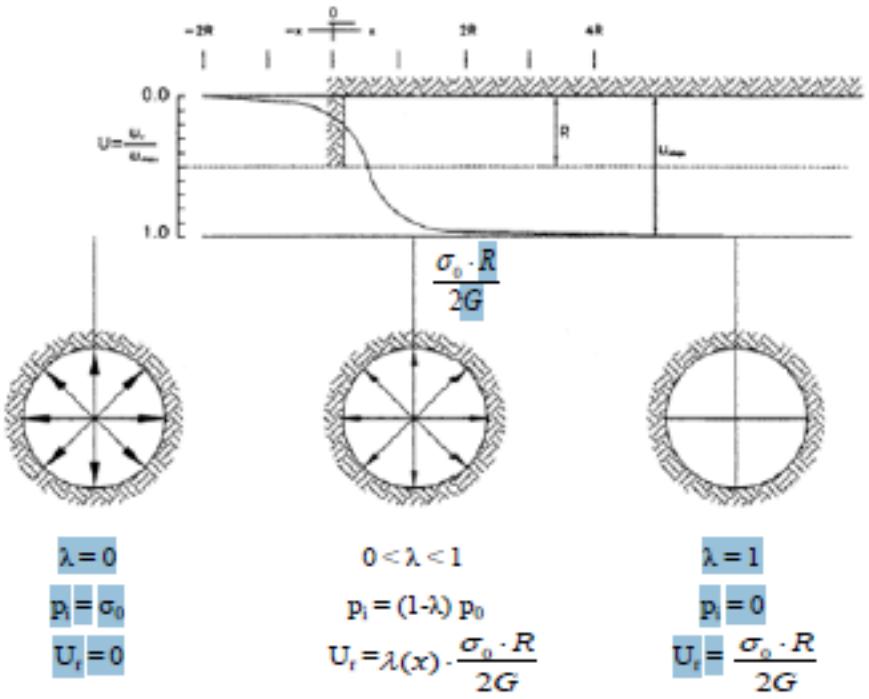

Figure 1.21. variation in the rate of deconfinement, pressure and radial displacement as a function of distance from the face.

This pressure varies according to the following relationship:

$$P_i = (1 - \lambda)\sigma_0 \qquad \textbf{(1.3)}$$

Where σ0 is the initial stress in the mass and λ is a dimensionless parameter, called "deconfinement rate", which varies from 0, for a section far in front of the waist, to 1 for a section far behind (case of an unsupported tunnel, Figure 1.21). If we consider a section between the two mentioned above, the problem becomes three-dimensional since we must consider the influence of the face. In this case, the choice of tèghe value of the deconfinement rate, which is directly related to the distance of the considered section size, is the main difficulty of the method.

In an elastic-linear medium and in the case of an unsupported tunnel, λ= 0.25 is generally used for a cross-section corresponding to the size (AFTES, Working Group 7 [2002]). Many authors have also been interested in the formulation of the radial displacement in elastoplastic media: Panet and Guenot [1982] related the deconfinement rate, and thus the displacement, to the value of the plastic radius, Bernaud, Corbetta and Minh [1991] proposed a principle of similarity in order to determine the function $U_r(x)$from the corresponding elasticity curve, Carranza-Torres et al. [2000] provided an exponential formulation of the radial displacement in the case of a massif with a Hoek-Brown fracture criterion . Another way to represent the convergence-confinement method is the cavity characteristic line (Figure 1.22). It describes the existing relationship between the internal pressure pi and the radial displacement U_r . If the mass remains in an elastic domain, the curve follows the "typical" AC line. On the other hand, if by increasing the value of the deconfinement rate the limit of the elastic domain is reached, from point B and a λ > λelastic, the curve loses its linearity and the final displacement will be larger (still in the case of an unsupported tunnel).

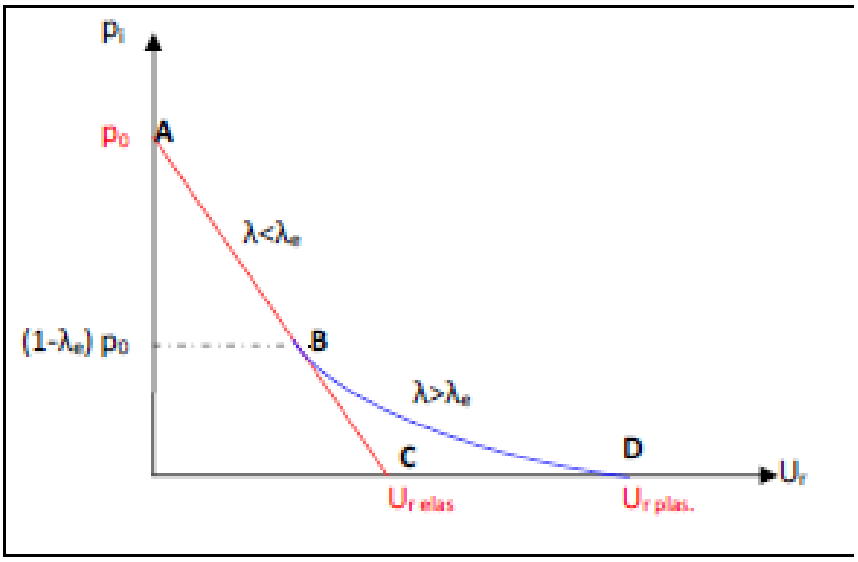

Figure 1.22. characteristic line of the cavity

The advantage of this representation is that on the same graph one can add, in the case of a tunnel this time coated, the confinement line of the supports (Figure 1.23).

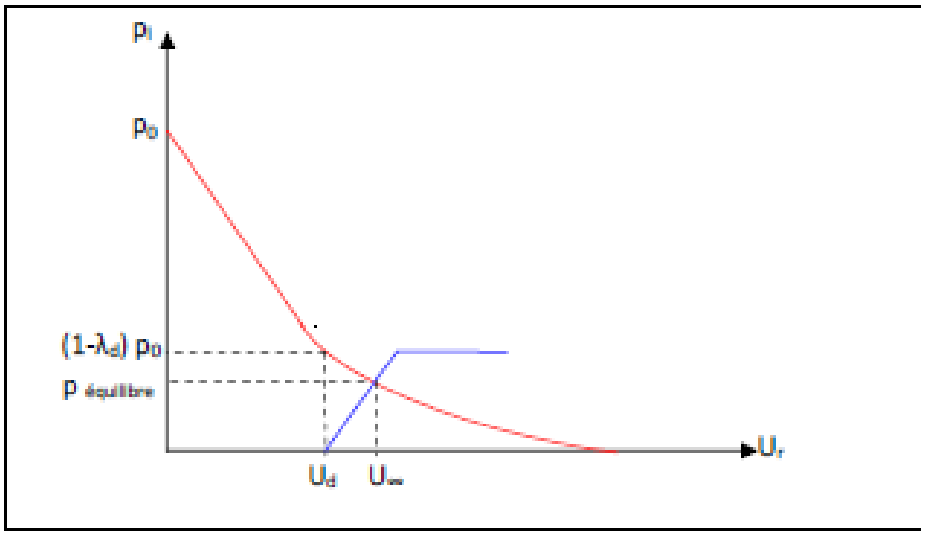

Figure 1.23. Support confinement line

The supports, installed at a distance of d (unsupported distance) behind the face, oppose the convergence of the walls by exerting pressure on the contour of the excavation. The point of intersection of the two curves represents the equilibrium of the support-cavity system. In the correspondence of this point, we find the final radial displacement of the tunnel (U_∞) and the

final load taken by the supports (P equilibrium). The support curve depends on the geometric and mechanical characteristics of each type of reinforcement (bolts, concrete rings, hangers, etc.). In the recommendation of the AFTES Working Group No. 7, the values of the stiffness modulus of the different types of supports are presented. One of the difficulties of this approach is to determine the radial displacement (U_d) at the time of installation of the supports, the starting point of the confinement curve. This displacement is the sum of the movement , which occurred in front of the cutting face (pre-convergence) and in the unsupported zone (d). To this U_d value corresponds a certain deconfinement rate λ_d. The validity of the method and its application in tunnel projects are based on the correct estimation of λ_d. Starting from the reflection that this value is lower than the one corresponding to the case of the unsupported tunnel (the rigidity of the lining in fact limits the convergence behind but also in front of the face), reduction factors to be applied to λ have been proposed as a function of d/R (elastic mass). They were determined in the context of the so-called implicit methods proposed by Bernaud and Rousset [1992] and Nguyen and Guo [1993]. Various extensions of this method have been proposed by different authors. Shahrour and Ghorbanbeigi [1996] have shown that it is possible to apply the convergence-confinement method to shallow tunnels in clay using 2D numerical calculations based on the results of a 3D model.

1.5.3 Numerical Methods

The third group of tools used to predict the effects of tunneling processes are various numerical tools. These tools represent the most comprehensive solutions for tunneling simulation. They give the possibility to include most of the complexity of the technology without introducing subjective assumptions. Depending on the approach used, they can be divided into groups. Below, the three main groups are presented (sorted from most to least popular):

- Finite Element Method (FEM) and Finite Difference Method (FDM)
- Boundary Element Method (BEM)
- Discrete Element Method (DEM)

Obviously, there are several other methods but their application is limited to very specific problems, which are mostly related to geotechnical engineering. In fact, a numerical method

used to solve a problem is, in most cases, predetermined by the user's choice of software. The different packages give the user a number of features mainly common to all. (Osmański, 2016).

1.5.3.1 Boundary Element Methods

The boundary element method (BEM) is a numerical technique used to solve boundary value problems expressed in the partial differential equation (PDE) term. It is composed of two main integral equations, one for the definition of a domain boundary and the second equation, which relates a solution, obtained at the boundary to that of the domain. Few examples of the boundary element method (BEM) applied to tunneling are found in the literature. Most of them show analyses performed in two-dimensional space.

The first application presented by (Swoboda, 1986) concerns the model in two-dimensional space, explaining how to couple beam elements and boundary elements. (Swoboda M.B.) Rheological analysis of tunnel excavation using coupled FEM and BEM. A similar study was performed by Varadarajan et al. (1987), who performed elastoplastic analysis using coupled FEM and FEM-BEM, while jointed rock analysis was performed by Xiao et al. (1994). Nonlinearity was discussed in the paper by Venturini and Brebbia (1984). While Prazerers et al (2012) presented a new approach to simulate conventional tunneling with BEM in three-dimensional space.

1.5.3.2 Discrete Element Methods

A numerical method used to calculate the motion of a large number of small particles is called the discrete element method (DEM) or discrete element method. In the analysis of soil mechanics problems, this method is used to simulate the mechanical behavior of subsurface materials as the interaction between their particles. Considering the material not as a continuum but as very small individual particles, the number of mathematical equations describing their motion and interaction increases enormously. Thus, the computational effort required to solve a problem.

Rapidly increases the reduction of just-to-local applications, mainly two-dimensional problems.

1.5.3.3 Finite Element and Difference Methods

Simulation of the tunnelling process using FEM and FDM are the most popular. Their popularity is derived from a user-friendly interface of modern packages, a wide range of features to study both ultimate and serviceability limit states, and a relatively low computational effort required to obtain results. FEM is a numerical technique in which boundary value problems for partial differential equations are solved by finding the approximate solutions. In the literature, there are a multitude of examples showing the application of both methods to simulate the process of tunneling in two-dimensional and three-dimensional space (Osmański, 2016).

1.6 Presentation of similar work on the study of the influence of the constitutive soil Models

Yousef HEJAZI, Daniel DIAS &Richard KASTNER from INSA Lyon have set up models of constitutive soils at different complexisty levels of clays. The study is not based on a real site. However, mechanical parameters are deduced from triaxial tests and then used to model the excavation of a shallow tunnel in flat deformations.

1.6.1 Parameters calibration

The simulations are based on an intensive process of laboratory and in situ tests. These experiments allow the characterization of the overconsolidated clay in London (Gasparre, 2005). The selected samples concern the execution of the terminal 5 of the Heathrow airport (London). According to the geological section of this area, the following lithography can be distinguished: a layer of gravel up to 2.5 m deep. Below this layer is a clay layer from which three different lithological units can be distinguished. In order to simplify the model, only one layer is taken into account, whose parameters are represented in table 1.1.

Table 1.1 . The parameters chosen for the three Constitutive Soil models

Modèle	C kN/m²	φ (°)	ψ (°)	ν	E kN/m²	E_{50}^{ref} kN/m²	E_{oed}^{ref} kN/m²	E_{ur}^{ref} kN/m²	m	G_0 kN/m²	$\gamma_{0.7}$
MC	7	20,5	4,81	0,28	31×10^3	-	-	-	-	-	-
HSM	7	20,5	4,81	0,28	-	$32,5\times10^3$	$32,5\times10^3$	$97,5\times10^3$	0,5	-	-
HSsmall	7	20,5	4,81	0,28	-	$32,5\times10^3$	$32,5\times10^3$	$97,5\times10^3$	0,5	65×10^3	10^{-4}

1.6.2 Simulation Numerique

The numerical simulation of the excavation of a shallow tunnel was carried out using the finite element code Plaxis2D, a plane deformation model was created. The water table is 2.5 m deep. The mesh (Figure 1.24) is 100 m long and the tunnel is located at H = 53.75 m from the substrate (constant depth assumed). The tunnel is circular and its diameter is D = 7.7 m. The cover height for the reference calculation is 2D.

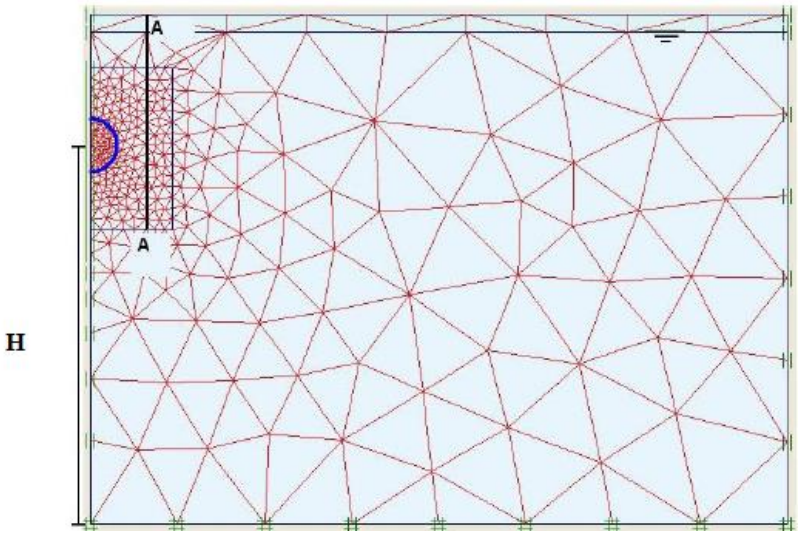

Figure 1.24 . Geometrie and mesh in finite element

1.6.3 Presentation of the Results of Modelisation

The settlement curve and the corresponding horizontal displacements (according to section A-A – Figure) resulting from the numerical simulations are shown in the figure 1.25.

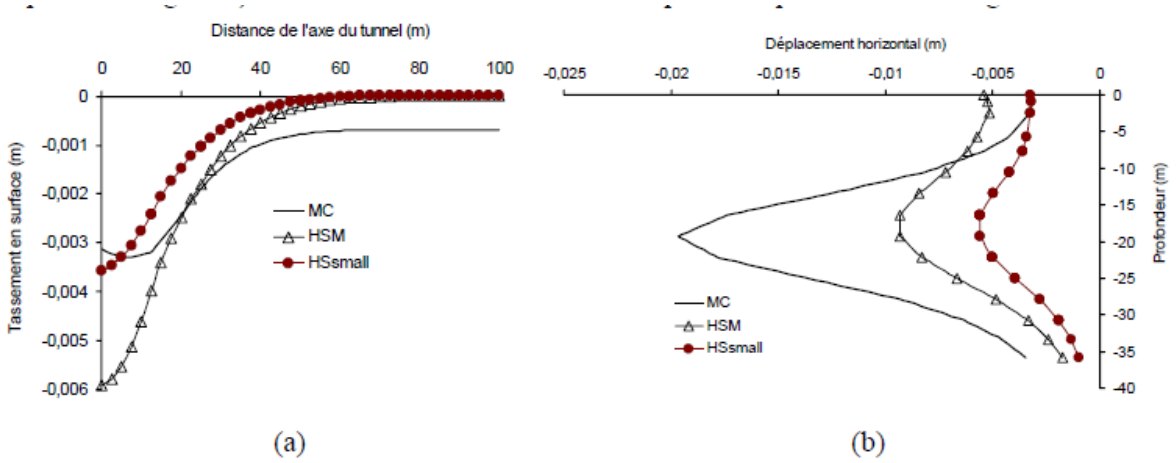

Figure 1.25. (a) Surface settlement ; (b) horizontal displacement according an inclinometer 1D far from the axis. – (reference of calculation)

The impact of the constitutive model can be seen in the difference in movement response. Despite a consistent longitudinal extension of the mesh, it can be seen that using the MC model; settlements are still observed (Figure 1.25 a) at 100 m from the axis, which seems unrealistic. This problem can be justified by the fact that even in low deformation areas, the shear modulus in the MC model is constant. The model based on higher stiffness in small deformations comes closest to the experimental observations (deeper and narrower settlement basin, Addenbrooke et al., 1997); in contrast to the Mohr-Coulomb model which induces a basin that does not fit the Gauss equation. There is also a 40% difference between the maximum settlement estimated by HSM and HSsmall, which shows the importance of taking into account the variation in shear modulus.

Conclusion

At the end of this chapter, the objective was to introduce, the types of underground constructions; present the different methods of tunnel construction; the behavior of the soil due to tunneling, present the predictive methods to estimate the response or settlement of the soil at the surface and present a similar work on the study of the influence of constitutive soil models on the prediction of the settlement curve. It can be said that this similar work presented above has limitations because it was not performed on a real site that is why we will perform this work on a real site which is none other than the extension of line 12 in France in order to confirm the reliability of this work .

Chapter 2 :METHODOLOGY

Introduction

The excavation of underground constructions such as tunnels induces a change in the stress state of the soil, which can be physically identified by the settlement at the soil surface. The response of the soil to the construction of tunnels with modern methods is the result of complex operations. To highlight a methodology for this work is to describe the steps to be followed in order to make a correct modeling of the excavation of a tunnel. In this work, the methodology to be followed begins with the general recognition of the study area, including its general physical and socio-economic characteristics, followed by a collection of data for modelling and a description of the geotechnical test performed to obtain the geotechnical parameters. A two-dimensional modeling of our tunnel will fill this part. Finally, the presentation of the PLAXIS software used for our numerical modeling will complete the development of this part.

2.1 General recognition of the site

The general recognition of the site involves documentary research in order to know the general physical characteristics of the site (geographical location, relief, climate, geology, hydrology and demography). This reconnaissance is important for a better analysis of the site by observing how the different formations present on the site have evolved over time.

2.2 Collection of Data

The aim is to obtain the data necessary to understand and solve problem. This include geotechnical data, hydrogeological and geological data, data related to the tunnel boring and lining and finally the monitoring data.

2.2.1 Geotechnical data

These data are derived from the results of the full identification of materials taken from the site or from in-situ tests that were carried on site.

2.2.2 Geological and hydrogeological data

The aim here is to obtain the different layers with their thicknesses presents on the site. They are obtained thanks to the documentation more precisely from the document "feedback of the extension of the metro line 12 of Paris".

2.2.3 Data related to the tunnel boring machine and lining

The tunnel was bored using a tunnel boring machine, the characteristics of which is very important to know. These characteristics were gotten through research and documentation.

2.2.4 Monitoring Data

During the excavation of tunnels, sensors (extensometers) were installed to measure the displacements or deformations of the ground (monitoring data) and made it possible to obtain observation points. Thanks to these, we will be able to plot the Peck's settlement curve.

2.3 Description of the Pressuremeter Test

This test, performed in the field, appeared fifty years ago in the practice of soil mechanics, with the filing of a patent on January 9, 1955, by Louis Menard (1931-1978). It has become, at least in France, a common test widely used today. It allows a different approach to geotechnical problems and the realization of a greater number of tests than the laboratory allows.

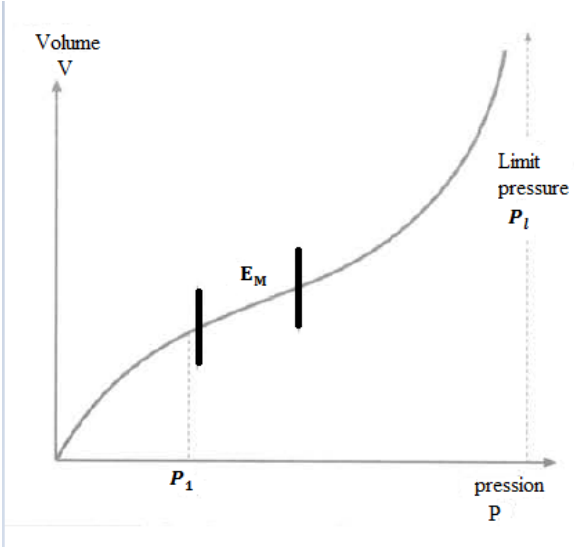

Figure 2.1 . Pressuremeter type curve (revue Française Géotechnique N°114, 2008)

The Menard pressure meter essentially consists of a cylindrical probe inserted into a pre-bored hole of slightly larger diameter than the probe. This is radially expandable under the effect of a pressure supplied by a volume pressure regulator (CPV) located at ground level. The probe consists of three cells: a central cell full of water and two <<holds >> cells so that the stresses and strains induced by the central cell in the soil are radial. It is connected to the CPV by flexible tube. The controller gives the borehole diameter increase by measuring the volume of the central cell. A static load test is therefore performed by increasing the pressure in equal pressure steps. The interpretation of the load curve allows to deduce:

- ❖ a deformation modulus, in the so-called pseudo-elastic phase, because it is practically linear, but not reversible;

- ❖ Limit pressure which corresponds to the appearance of large deformations of the cylindrical cavity.

A typical pressiometric curve is given in figure 2.1; it has three parts:

- The first one corresponds to a re-contact between the probe and the borehole wall. It can be said that the soil reworking and its decompression are partially corrected; or a pressure P1 is reached,

- the second one is not linear but is close to it; it thus allows the calculation of a so-called pressiometric modulus, noted E_m, defined on a range of constraints whose upper limit does not exceed a value called critical pressure value (or creep) beyond which:

- the third part of the curve quickly presents an asymptotic aspect which leads to define the limit pressure Pl.

Mohr Coulomb material parameters were gotten by equations derived by Menard, Yee and Varaksin (*Yee and Varaksin, 2012*) for friction angle and cohesion gotten from Cassan correla-tions.

- Friction angle in sand: $\varphi = \frac{2*\ln\left(\frac{P_l}{2,5}\right)}{\ln(2)} + 24$ **(2.1)**

- Friction angle in rocks: $\varphi = \frac{7*\ln\left(\frac{P_l}{4}\right)}{\ln(2)} + 40$ **(2.2)**

- Cohesion (C): $C = \frac{P_l}{5}$, $Pl<0.3MPa$ **(2.3)**

$$C = \frac{P_l}{12} + 0.03,\ 0.3<Pl<1.0MPa \quad \textbf{(2.4)}$$

$$C = \frac{P_l}{35} + 0.085,\ 1.0<Pl<2.5MPa \quad \textbf{(2.5)}$$

2.4 2D finite element modelling assumptions

In addition to the use of the elastoplastic constitutive model for terrain modeling, possibility to model soil-structure interactions, taking into account the excavation phase and loading, the 2D finite element method allows access to the entire displacement field in the earth mass, both at the surface and at depth. This method is therefore particularly suitable for the study of buildings and structures with significant loading or unloading, when constructions are based on deep foundations or for the study of interactions with underground structures. With respect to the assumptions made for the calculation of the forces in the segments, the modeling of the segments and the scaling of the settlement calculations are different.

❖ **Phasing of finite element calculations for the determination of settlements**

The phasing of the finite element calculations for the estimation of settlements is as follows

- **Step 1**: Initialization of the constraints, considering the earth's thrust coefficient at rest K0 for determining the effective horizontal stresses;

- **Step 2**: Set up any loading/unloading ;

- **Step 3**: Passing the simulated shield by:

  - The application of the deconfinement rate λ=0.9 corresponding to the deconfinement rate at the skirt exit for an unsupported tunnel , via the parameter ΣM_stage of PLAXIS,

  - The application of the total confinement pressure (taking into account a pressure gradient of 12 KN/m3/m) explicitly introduced in PLAXIS. This pressure is corrected by the rate λ ; thus the introduced pressure will be : PPLAXIS=P/λ =P/0.9 ;

- **Step 4**: Installation of the segments and deactivation of the confinement pressure

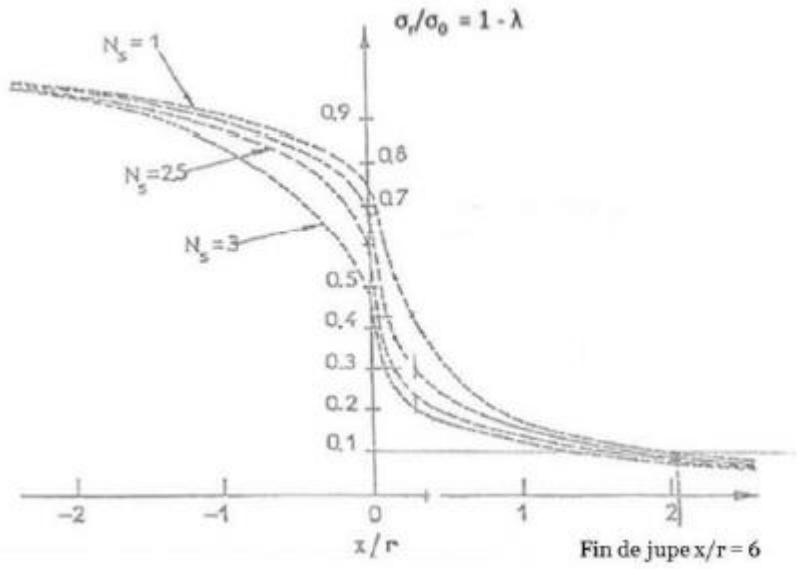

Figure 2.2. Panet deconfinement curves

2.5 Modelling tunnelling in 2D

The effect of tunneling on the stresses and strains of the massif is three-dimensional. Only three-dimensional calculations can simulate, taking into account all the complexity of the interaction phenomena between the soil, the pre-support in front of the working face and the tunnel support. However, the three-dimensional approach still requires quite a lot of computing time. For this reason, in most tunnel project studies, 2D calculations are performed. They are based, in most cases, on the principle of the so-called convergence-confinement method, described in the bibliographic section. According to this method, a fictitious pressure is exerted on the contour of the excavation. The relationship between this pressure and, for example, the surface settlement is illustrated in Figure 2.3. The pressure, which is initially equal to the initial ground stresses, gradually decreases until it passes from the front to the plumb of the section. At this point, some of the load is taken up by the soil and an Sfront colony appears at the surface. The load is then evenly distributed on the supports installed behind the working face. A state of equilibrium is finally reached and the surface settlement stabilizes on the Sfinal value.

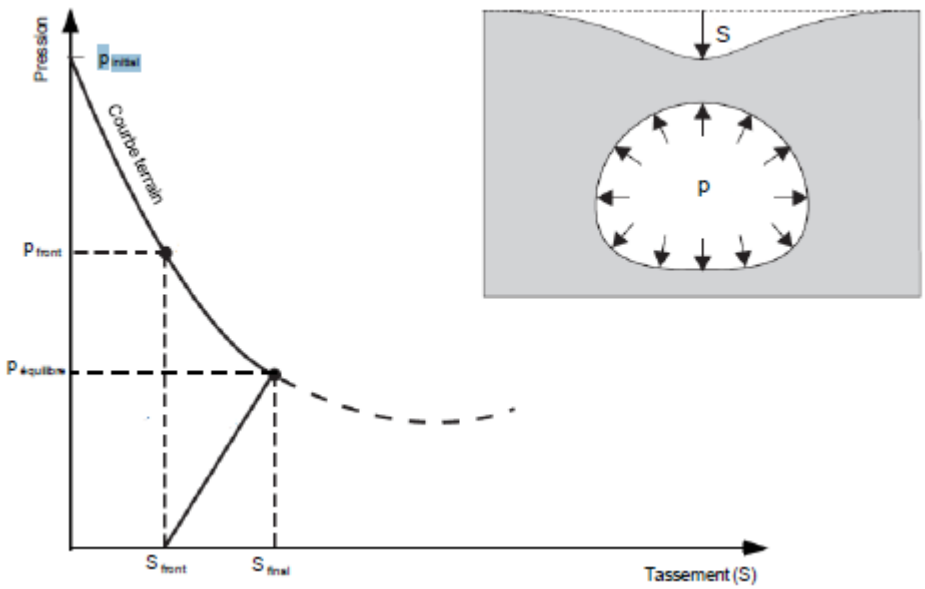

Figure 2.3. Convergence-confinement method, relationship between tunnel contour pressure and surface settlement.

The Plaxis 2D calculation code allows this methodology to be integrated through a step-by-step construction of the tunnel that is based on the concept of the deconfinement rate λ. This parameter is very influential on both the decays (which increase with λ) and the forces in the supports (which decrease with λ). It represents the percentage of stress reduction that takes place before full supports are placed. The main steps in this approach are as follows:

1) **Initialisation of contraints.**

From the characteristics of the terrain (γ, K0) and hydraulic conditions, the initial stresses of the massif are calculated.

2) **Excavation of the tunnel**

The excavation of the tunnel is simulated by the removal of the ground inside the tunnel. During this phase, a certain percentage of stress relaxation λ is applied.

3) **Installation of supports**

The linings are activated and the deconfinement is completed. The loads are divided between the ground and the linings and the final equilibrium can be achieved.

Tunnel construction can be mainly divided into two phases, the tunnelling phase and the ring building phase.

- The tunnelling phase is simulated by a deactivation of the soil element at the face of the tunnel during the progression of the TBM. A face pressure is assumed to be the same as the excavation chamber. A value of 195kPa insures the stability of the tunnel face during the excavation process. A gradient of 12kN/m represents the weight of the excavated soil and water mixture in the excavation chamber.

- At the tail shield, reinforced concrete linings are placed and the gap with surrounded soil is filled with mortar. This procedure is simulated with the application of an injection pressure of 266kPa. The applied pressure is then removed after the installation of the linings.

The segmental linings in this analysis are modelled as a continuous cylindrical shell, with the width, the thickness and the deformation modulus of the segmental rings equal to 1m, 40cm and 20GPa respectively.

2.6 presentation of PLAXIS 2D

Plaxis is a finite element software that has been developed specifically for the two-dimensional analysis of deformation and stability in geotechnical engineering projects. The simple graphical input procedures enable a quick generation of complex finite element models, and the enhanced output facilities provide a detailed presentation of computational results. It has been developed with the principal aim to find solution to various aspects of complex geotechnical structures and construction processes using robust and theoretically sound computational procedures. It is a package of 04 modules that are INPUT, CALCULATION, OUTPUT, CURVES.

2.6.1 The finite element method

The finite element method (FEM) is a numerical technique used for solving the differential equations governing a boundary value problem (Zienkiewicz, 1977). The study area is divided into discrete areas, often triangular or rectangular, defined by node points located at the vertices and sometime along the element edges as seen in (figure 2.4).

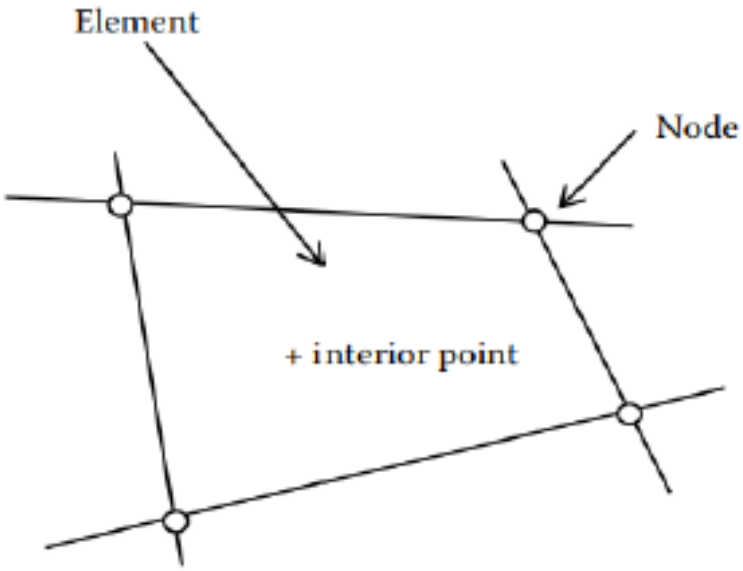

Figure 2.4. Finite element (Clayton et al, 2014)

The method divides the continuous space subjected to analysis in small parts, i.e. the Finite Elements (the assemble of Finite Elements is also called the mesh), and solves the differential equations governing a particular phenomenon (mechanical problem, flow in a river, seepage, coupled analysis, etc.) by integrating in a numerical way the equations written in a discretized form for all the element.

The procedure of FEM consists of:

- Subdivision of soil continuum in Finite Elements (meshing);
- Define the properties of materials according to perfect-plastic or elasto-plastic model
- Calculation of initial stress state assuming elastic behaviour and applying a gravitational load to the nodes of elements

2.6.2 PLAXIS Input module

The analysis of a new project with the software must starts by the creation of a geometry model. This geometry model is a 2D representation of the real three-dimensional and consist

of three components which are points, lines and clusters. A geometry model should include a representative division of subsoil into distinct soil layers, structural objects, construction stage and loadings.

Points are from the start and end of lines. Points can also be used for the positioning of anchors, point forces, point fixities and for local refinements of the finite element mesh.

Lines are used to define the physical boundaries of the geometry, the model boundaries and discontinuities in the geometry such as walls or shells, separations of distinct soil layers or construction stages. A line can have several functions or properties.

Clusters are areas that are fully enclosed by lines. PLAXIS automatically recognizes clusters based on the input of geometry lines. Within a cluster the soil properties are homogeneous. Hence, clusters can be regarded as parts of soil layers. Actions related to clusters apply to all elements in the cluster.

After the creation of a geometry model, a finite element model is automatically be generated. In a finite element mesh three types of components can be identified, and described as follow:

- Elements

During the generation of the mesh, clusters are divided into triangular elements. A Choice can be made between 15-node elements and 6-node elements. The powerful 15-node element provides an accurate calculation of stresses and failure loads. In addition, 6-node triangles are available for a quick calculation of serviceability states. Considering the same element distribution, the meshes composed of 15-node elements are actually much finer and much more flexible than meshes composed of 6-node elements, but calculations are also more time consuming.

In addition to the triangular elements, which are generally used to model the soil, compatible plate elements, geogrid elements and interface elements may be generated to model Structural behaviour and soil-structure interaction.

• Nodes

A 15-node element consists of 15 nodes and a 6-node triangle is defined by 6 nodes. Adjacent elements are connected through their common nodes. During a finite element calculation, displacements (u_X and u_Y) are calculated at the nodes. Nodes may be pre-selected for the generation of load displacement curves. The distribution of nodes over the elements is shown in figure 3.2.

• Stress points

In contrast to displacements, stresses and strains are calculated at individual Gaussian integration points (or stress points) rather than at the nodes. A 15-node triangular element contains 12 stress points while a 6-node triangular element contains 3 stress points as indicated in figure 2.13 Stress points may be pre-selected for the generation of stress paths or stress-strain diagrams.

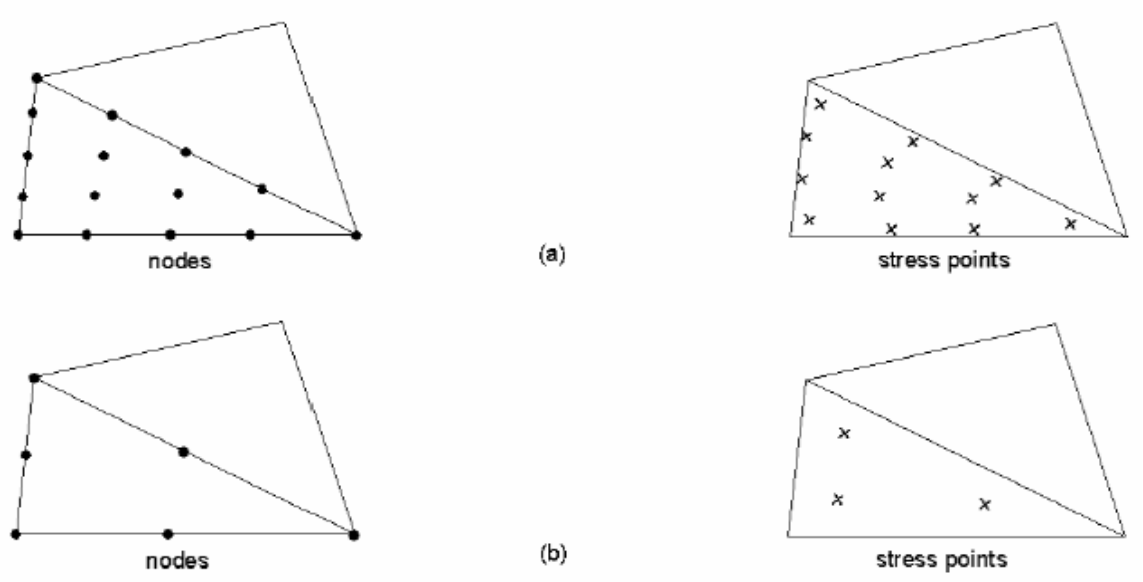

Figure 2.5. Nodes and stress points (Plaxis manual, 2012)

There are different inputs data as geometry object, text and values and selections.

2.6.2.1 Input of geometry object

After applied the general setting, the input window appears. The creation of a geometry is done through the uses of points and lines procedure but also several geometry object available from the menu or from the toolbar. At Figure 2.6, it can be observed a view of the Plaxis interface.

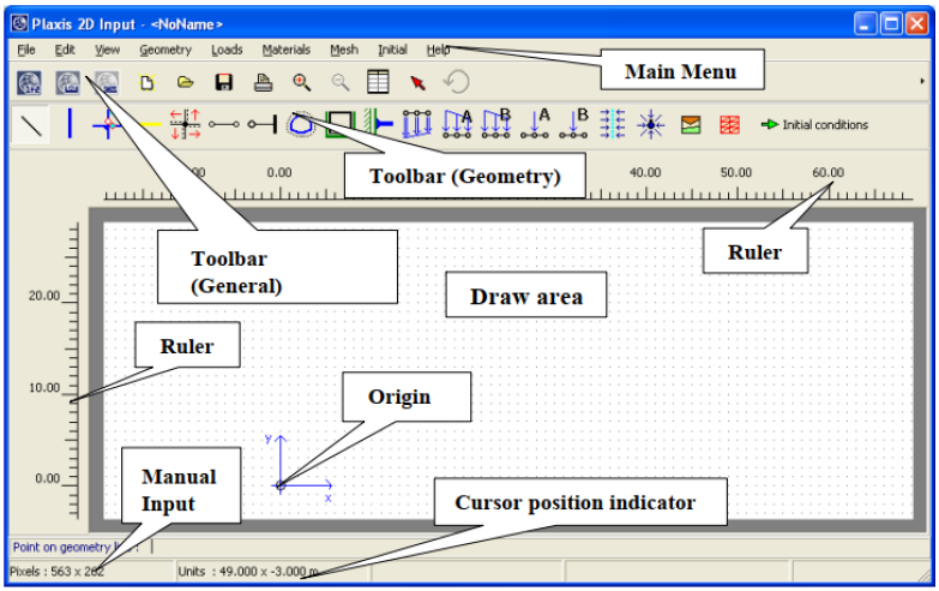

Figure 2.6. Plaxis 2D interface (Plaxis manual 2012)

2.6.2.2 Input of text and values.

Each software required the input of text and values. The required input is specified in the edit boxes. There are multiple edit boxes for a specific subject grouped in windows. An example of edit boxes is present at(Figure 2.7).

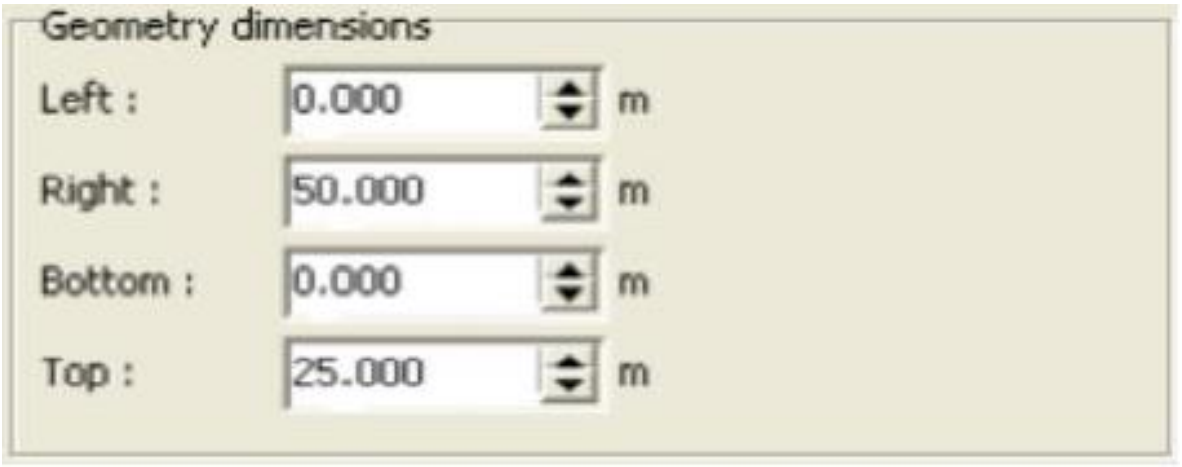

Figure 2.7. Spin edits (Plaxis manual, 2012)

2.6.2.3 Input of selections

Selections are made by means of radio buttons, check boxes or combo boxes. Some samples are presented in figure 2.8.

- Radio buttons: only one item may be active in a radio buttons window

- Check boxes: in a check boxes window, more than one item may be selected in the same time

- Combo boxes: it is use to choose one item from a predefined list of possible choice

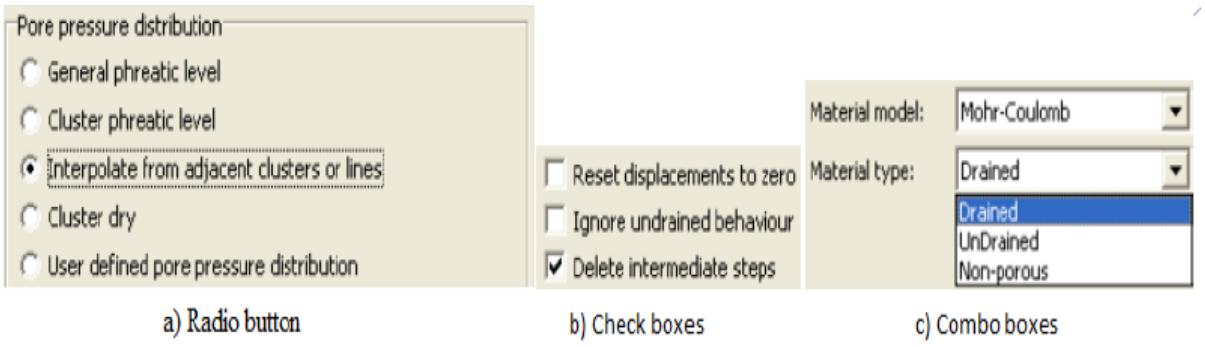

Figure 2.8. Input selections (Plaxis manual, 2012)

There are also structural inputs in which the required inputs are organised in a way to make it as logical as possible.

2.6.3 Plaxis calculation program

The calculation program is started after the generation of the real finite element. There are several types of calculation and to perform a real finite element calculation, it is necessary to define the type to use, but also the type of loading.

2.6.3.1 Types of calculation.

There are four main types of calculation: the plastic calculation, the consolidation analysis, the Phi-c reduction used for a safety analysis and the dynamic calculation. The dynamic calculation required the presence of the PLAXIS dynamics module which is an extension of Plaxis 2D. The calculation program takes into account only deformation analysis.

- Plastic calculation

It is the one appropriate in most practical geotechnical application. Plastic calculation should be selected to carry out an elastic-plastic deformation analysis in which it is not necessary to take the decay of excess pore pressures with time into account. It does not take time effect into account, except when the Soft Soil Creep model is used.

- Consolidation analysis

Consolidation analysis should be selected when it is necessary to analyse the development or dissipation of excess pore pressures in water-saturated clay-type soils as a function of time. Plaxis allows for true elastic-plastic consolidation analyses. In general, a consolidation analysis without additional loading is performed after an undrained plastic calculation. It is also possible to apply loads during a consolidation analysis. However, it should be taken when a failure situation is approached, since the iteration process may not converge in such situations. It is

possible to apply construction in time using a consolidation analysis. Moreover, consolidation analyses can be performed in the framework of large deformations.

• Phi-c reduction

The Phi-c reduction is used for a safety analysis by reducing the strength parameters of the soil. It should be selected when it is desired to calculate a global safety factor for the situation at hand. A safety analysis can be performed after each individual calculation phase and thus for each construction stage. It is considered as a special type of plastic calculation, when a safety analysis is performing, no loads can be increase simultaneously. These three basics types of calculation can be performed as an updated mesh analysis by taking into account the effect of large deformations.

2.6.3.2 Types of loading input

It can be distinguishing three types of loadings. They have to be specifying after choosing the calculation type. They are staged construction, total multipliers and incremental multipliers.

• Staged construction

Staged construction enables an accurate and a realistic simulation for various loading, construction and excavation processes. The option can also be used to reassign material data sets or to change the water pressure distribution in the geometry. A staged construction analysis can be executed in a Plastic calculation as well as a Consolidation analysis. Staged construction is the most important type of loading input.

• incremental multipliers

It is used to specify an incremental load multiplier that is applied to the current configuration of the external load. Before entering an increment of external load, a time increment can be entered. This is done only for a consolidation analysis or if the soft soil model is used. Their combination determines the loading rate that is applied in the calculation.

- total multipliers

This type is used to specify the ultimate values of external loads. When the total multiplier loading is selected, the ultimate values of external loads will be applied exactly at the end of calculation.

2.6.4 Plaxis output program

The output program contains all facilities useful to view and list the results of generated input data and finite element calculations. It allows to obtain a large amount of data such as stresses, stresses, pore pressures and displacements for soils, and displacement and forces for geogrid material.

2.6.5 Plaxis curve program

The curve program is used to generate the stress paths, stress-strain diagrams and load displacement curves of pre-selected point in the geometry. These curves allow to visualise the variation of some quantities for various calculation and by this observed the local and global behaviour of the soil.

Conclusion

The objective of this chapter was to present the procedure for modelling a tunnel in 2D with the aim of obtaining the different settlement curve during the extension of the Paris metro line 12 with an earth pressure tunnel boring machine. This methodological approach focuses firstly on the general characteristics of the project through the general recognition of the Study Area to know its general physical characteristics and socio-economic (demography), the collection of geotechnical data, geological, the characteristics of the tunnel boring machine and coating and complete by monitoring data. To implement a numerical model, it is important to select appropriate software. In this work, in order to study the problem in a simplified manner, the Plaxis 2D software is the one chosen for the analysis and it has been briefly presented in this chapter. The procedure used to build the 2D numerical model in Plaxis2D software, the different assumptions made and how to obtain different results were also presented.

Chapter 3 : NUMERICAL ANALYSES OF THE TUNNEL

Introduction

The extension of line 12 to Mairie d'Aubervilliers will bring the center of Aubervilliers to within 10 minutes of Paris. It will thus contribute to the renewal of Aubervilliers town center and to a better service to the Plaine Saint-Denis. This chapter deals with the implementation of the methodology presented in chapter 2. To do this, the project site will be presented at the outset, giving its general physical characteristics (location, climate, relief, hydrology, geology) and its socio-economic characteristics (demography). Then comes the presentation of the application project on the geotechnical, geological and hydrogeological data as well as the characteristics of the TBM and the tunnel lining, and the monitoring data. The settlement pit of the different soil constituents of the Line 12 Paris extension excavated in an elasto-plastic soil are presented and compared to the settlement pit obtained by the empirical method (Peck's formula). Our numerical analysis of the tunnel is based on the finite element method (FEM). An analysis using Mohr's Coulomb, HSM and HSSM constitutive laws will be done successively by presenting the selected modeling parameters, the three constitutive soil models and the results and at the end we have done an analysis around the tunnel.

3.1 Presentation of the site

It consisting to present the study area through its location, geology, relief and soil, climate, hydrology, population .

3.1.1 Localisation of the site

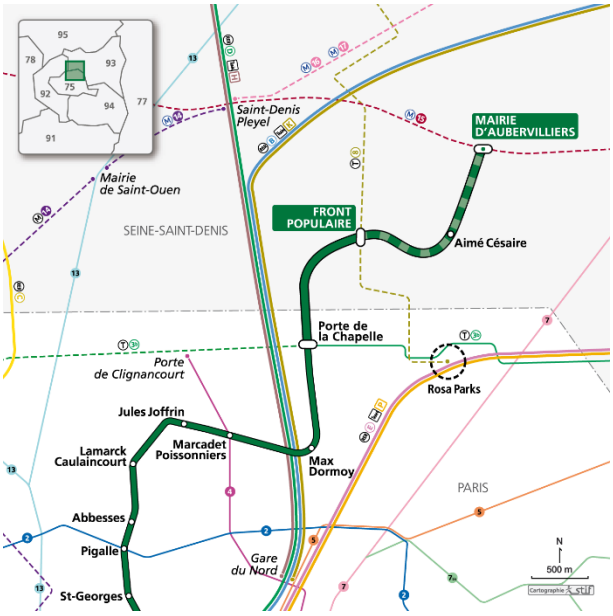

Figure 3.1. paris metro line 12 Northern extension

Following an initial extension phase that was completed in December 2012 , line 12 now links Mairie d'Issy with the Front populaire station located in between the towns of saint-Denis and Aubervilliers .A furthet extension to the North of this line is currently being considered .

This is the first phase of the extension of the line to Mairie d'Aubervilliers provided for in the 2000-2006 state-region plan contract. Its financing was validated by the STIF Board on 5 April 2006. The construction site then started, in the second half of 2007 with the deviations of networks, to allow the commissioning of the first Front Populaire station in 2012. The tunnel was nevertheless dug from the first stage to Mairie d'Aubervilliers, but the construction of the other two stations of the aime Cesaire and Mairie d'Aubervilliers extension was postponed to the second stage, with a view to opening at the end of 2017. The work of the first stage had a cost of 198.5 million euros (48% Region, 27.5% State, 8.5% General Council, 16% RATP - on subsidized loan from the Region)

3.1.2 Climate

The climate of Seine-Saint-Denis is similar to the climate of Paris. The department, like the whole of the Ile-de-France, is subject to a degraded oceanic climate, where the oceanic influence prevails over the continental climate. Generally speaking, the summers are rather cool. (18 °C on average), and winters are rather mild (6 °C on average) with rainfall of the

same magnitude in all seasons (in terms of precipitation) and lower rainfall (647 millimeters) than on the coast.

The location of the department in the very densely urbanized area of the Paris conurbation explains a very slight temperature increase of one or two degrees depending on the climatic conditions compared to the rural areas of Île-de-France, especially in calm, anticyclonic weather. This difference is particularly noticeable at daybreak and **tends to increase over the** years. The average annual temperature is 11°C, the coldest month is January with +4.7°C; the warmest months are July and August with +20°C (daily average). The average number of days with temperatures above 25°C is 43, of which 9 exceed 30°C.

3.1.3 Relief

Seine-Saint-Denis is located northeast of Paris. Its surface area is 236 km2, which makes it one of the smallest French departments. Seine-Saint-Denis, together with the two other small departments bordering Paris (Hauts-de-Seine and Val-de-Marne), forms the small ring of the Paris region.

It is located in the Paris Basin and includes an important part of France . The department is essentially made up of a low plateau, the Plaine de France, structured by the wide valleys of the Seine and the Marne and surmounted by a relief of mounds, with the plateau of Romainville, culminating at 131 m in Les Lilas, eastern extension of the hill of Belleville - Ménilmontant, plateau of Vaujours, culminating at 130 m height, and the plateau of Avron (115 m), which materialize the end of the massif of Aulnoye or that of the plateau of Brie. The latter are separated by the depressions of Gagny and Rosny-sous-Bois, which correspond to an old bed of the Marne. In the north of the department is the Butte-Pinson, which announces the first foothills of the Montmorency plateau.

3.1.4 Geology

The geology of the department is that of the sedimentary Parisian Basin. A succession of clay and marl horizons are interspersed with marl and limestone formations (such as the limestones of Saint-Ouen-sur-Seine or those of Brie), often gypsum, which were exploited for a long time in open-air gypsum quarries or in galleries (in Romainville, Rosny-sous-Bois or Gagny, for example). Today, only the gypsum of the Aulnoye massif, on the plateau

overlooking Vaujours and Coubron, is still exploited for the Placoplatre factories of Vaujours .

3.1.5 Hydrology

The department is bounded on the northwest by the Seine, at the top of the Gennevilliers loop. It is crossed by the Marne at its southeast end. Two canals built at the beginning of the 19th century by the City of Paris, the Ourcq Canal and the Saint-Denis Canal, and the Chelles Canal inaugurated in 1865 to facilitate navigation from Vaires-sur-Marne to Neuilly-sur-Marne, also irrigate it.

3.1.6 Demography

According to the latest Insee estimates, the population is 1,670,149 inhabitants as of January 1, 2020. Infant mortality is one of the highest in metropolitan France (4.8 ‰ in 2011-2013, compared to an average of 3.3 ‰ in Metropolitan France and 3.8 ‰ in Île-de-France). Nevertheless, infant mortality continues to decline (it was 5.9% in 2008). Moreover, Seine-Saint-Denis has the highest fertility rate in metropolitan France with 2.50 children per woman. This is mainly due to the high proportion of immigrants (28.4% in 2012), especially from developing countries where fertility is relatively higher.

3.2 Presentation of the Projet

The extension of the Paris metro line 12 toward "la Mairie d'Aubervilliers" started in 2008. As shown in Figure 3.2, the project is divided into two parts. The first part started at the "Porte de la Chapelle" station and ended at the "Aimé-Césaire" station and was completed in 2012 with the construction of the "Front Populaire" station. The second part started at the "Aimé-Césaire" station and ended at the receiving shaft at Valmy. With a length of 2.8km and a diameter of 9.15 m, the tunnel was bored by an earth balanced pressure (EBP) shield and the two stations (Aimé-Césaire and Mairie d' Aubervilliers) are still under construction. The expansion is expected to be completed by the end of 2021, according to RATP.

During the excavation, sensors were installed at the ground surface to record the settlement. The objective of the monitoring was to control the deformation of the soil to prevent the nearby structures and infrastructures from possible risks.

3.2.1 Geotechnical context

From the result of the Pressuremeter test, deformation modulus is derived. The mechanical characteristics (wet volume weight, coefficient of the land at rest K_0, Young's modulus E, fish coefficient υ, effective cohesion c' and the angle of friction φ') of the different layers are summarized in the table 3.1.

Table 3.1. mechanical characteristics of the different layers encountered during the extension of line 12 (according to geotechnical synthesis memory XELYS)

Soils	γ KN/m^3	E_{CT} Mpa	C_{CT} Kpa	φ_{CT} (°)	E_{LT} Mpa	C' (Kpa)	φ' (°)	P_l Mpa	E_M Mpa	α	υ
Fill	20	10	0	25	10	0	25	0,6	8,5	$^1/_2$	0,35
Alluvions	20	5	0	10	5	0	10	0,4	4	$^1/_2$	0,35
Saint –Ouen Limestone	19	80	30	25	40	0	30	1,5	12	$^1/_2$	0,3
Ducy limestone	19	20	5	20	39	0	30	0,7	6,5	$^1/_2$	0,3
Beauchamp upper sand	21	100	20	30	60	0	35	4,0	38	$^1/_3$	0,3
Beauchamp median sand	20	140	60	15	100	60	15	3,1	28	$^1/_2$	0,3
Beauchamp Lower sand	21	120	20	30	60	0	35	4,1	35	$^1/_3$	0,3
Marls and Sandstones	21	240	50	30	120	30	30	4,5	48	$^1/_2$	0,30

3.2.2 Geological and hydrogeoligical Context

3.2.2.1 Geological context

At the scale of the project, the stratigraphic succession remains globally unchanged and consists of embankments, infragypsous marls, monceau sands, saint Ouen limestones, Ducy limestones, upper Beauchamp sands / medians / inferior, marls and caillasses. The tunnel is

hollowed out in the upper Beauchamp sands ,median Beauchamp sand and Lower Beauchamp sand . The thicknesses of these different layers of soil are presented in the table 3.2.

Table 3.2 . tchiknesses of the differents layers

Layers	Level [NGF][mm]	Thickness[m]
Fill	32,6	1,8
Alluvions	30,6	2,0
Saint ouen	21,7	8,9
Ducy	20,2	1,5
Upper Beauchamp sand	16,6	3,6
Median Beauchamp sand	13,9	2,7
Lower Beauchamp Sand	9,6	4,3
Marls and sandstones	0	9,6

The phreatic nappe , the ground surface and the axe of the tunnel are respectly at level 32,1 m, 34,4 and 13,9 m from the substratum .

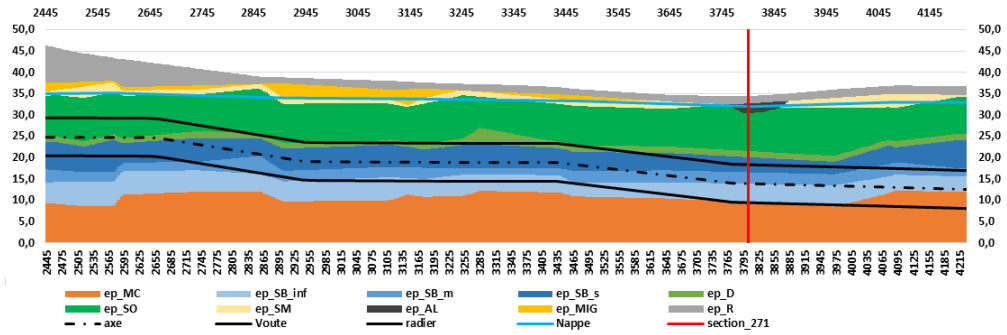

Figure 3.2. Geotechnical profile of the section of the extension of the Paris Metro line (from S.Mahdi & al., 2019)

3.2.2.2 Hydrogeological context

The excavation is carried out under the water table, with hydraulic loads of between 50 and 200 Kpa at the level of the tunnel axis , the permeability of geological horizons are presented in table 3.3 .

Table 3.3. permeability of geological horizons

SOIL	Retained permeabilities (m/s)	Lefranc permeabilities given as an indication (m/s)
Saint-Ouen Limestone	10^{-5}	$10^{-7} - 10^{-6}$
Ducy Limestone	10^{-3}	$10^{-6} - 10^{-5}$
Beauchamp Upper Sand	10^{-5}	$10^{-7} - 10^{-6}$
Beauchamp median Sand	10^{-7}	$10^{-7} - 10^{-6}$
Beauchamp Lower Sand	10^{-5}	$10^{-7} - 10^{-6}$
Marls and sandstone	10^{-4}	$10^{-8} - 10^{-7}$

3.2.3 General features of the tunnel Boring machine and the linings

The excavation of the tunnel of the Paris line 12 was carried out with an earth pressure tunnel boring machine and the installation of a lining consisting of rings in prefabricated linings of 400 mm thickness inside the skirt.

3.2.3.1 Description of the tunnel Boring Machine (Elodie)

With a total of 70 people mobilized for its operation, it has been working 24 hours a day, 5 days a week since October. This tunnel boring machine named Elodie on Monday, September 07, 2009 plant of 1350 tons and 82 m long was built in Germany by the company Herrenknecht. The tunnel boring machine company was manufactured, in particular for the extension project of line 12 of the metro and will be led by the works group <Vinci construction and eiffage tp>>

Figure 3.3. Boring Tunnel Machine (ELODIE)

The main characteristics of the tunnel boring machine used in the analyses are the subject of this note.

- Cutting Wheel diameter : 9170mm
- Front body diameter of the shield: 9150mm
- Front body length : 2620mm
- Central body diameter of the shield: 9135mm
- central body length : 3255mm
- Diameter Shield skirt : 9120mm
- Skirt length : 4895mm
- Total shield length including skirt: 10770mm

- Annular vacuum on diameter : 55mm
- Maximum working pressure (containment) : 4 bars
- Annular void filling: Jam mortar injects through the skirt

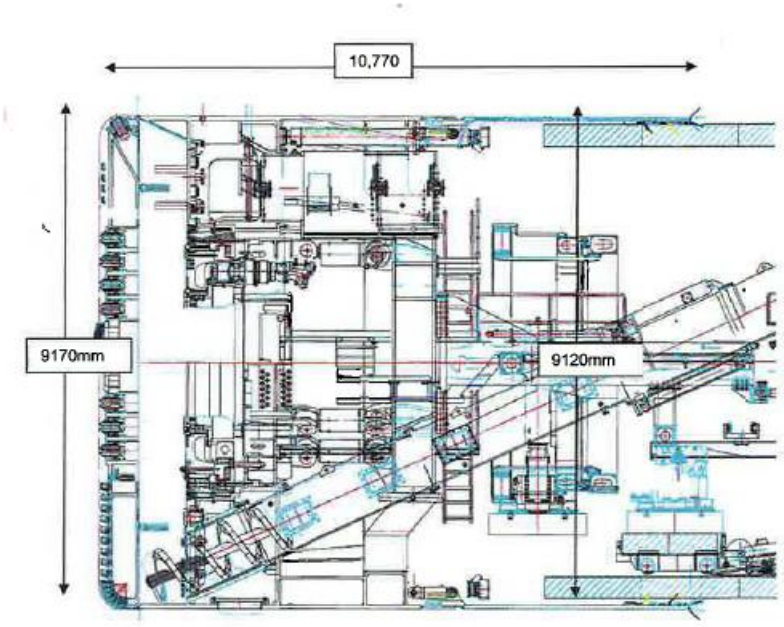

Figure 3.4. Tunnel boring Machine box L 12 shield

3.2.3.2 Reinforced Concrete lining Modelling

The lining is modelled in PLAXIS by curved beams with elastic behaviour, it is modelled as a continuous concrete cylinder in the longitudinal direction; on the other hand, the partial joints between linings are modelled via an overall reduction in inertia; a flat-rate reduction of 0.80 is considered; the concrete of the lining is class C 40/50. The parameters defining the lining in PLAXIS are shown in the table 3.4 .

$$I_e = I_J + \left(\frac{4}{n}\right)^2 . \frac{e^3}{12} \qquad \textbf{(3.1)}$$

With $I_J = \frac{\alpha^3 e^3}{12}$ **(3.2)**

Where n is the number of elements , I_J : joint inertia , e: segment thickness , I_e :inertia reduced of the ring and $\alpha = 0{,}665$.

Table 3.4. lining parameters

Joint inertia	Inertia reduced of the ring	modulus	Normal stiffness	Flexural rigidity	Equivalent tchikness	Weight	Poison ratio
$I_J[m^4/mL$	$I_e[m^4/mL$	E [Gpa]	E.A [KN /m]	EI_e[KN/m]	d_{eq}[m]	w [KN/m/m]	v [-]
1,568 E-03	3,939 E-03	11,7	4,6961 E+06	4,624 E+04	0,34	11,6	0,2

3.2.4 Monitoring Data

3.2.4.1 Presentation of the Monitoring data

A total number of 580 sensors have been installed at the ground surface to record soil movement during the excavation and construction processes. 20% of the sensors are unusable due to a variety of reasons, including loss of data, corrupted data, and loss of location. Among the remaining sensors, 300 survey points were located on the facades of buildings and 163 survey points on the road, with an average density of 0.25 point per meter along the tunnel axis.

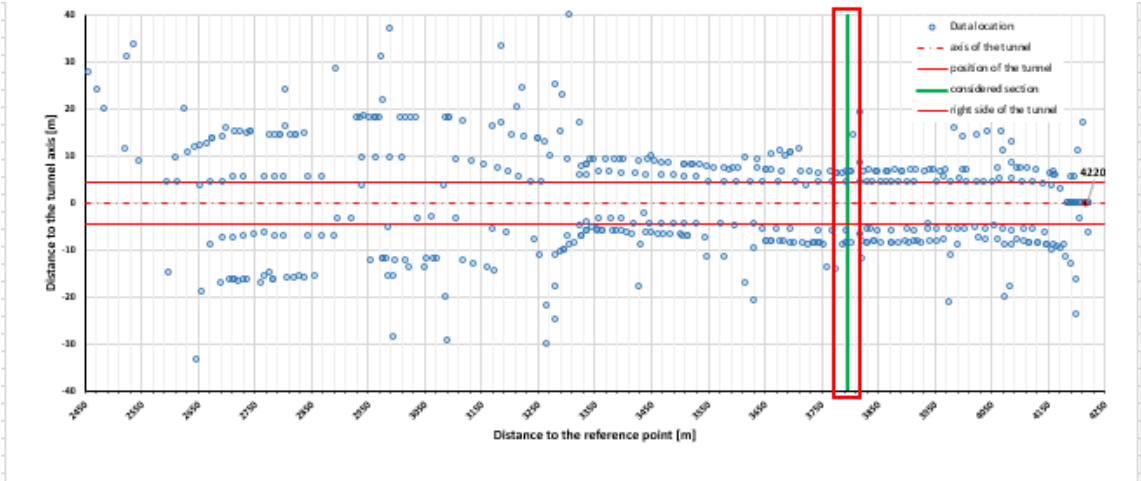

Figure 3.5. Representation of Data location

The vertical displacement of the ground surface as a function of time behaves like the Pearl curve model (Zhang, et al., 2019). The Pearl curve is a typical three-stage S-curve. The early development is slow, and then it enters a phase of rapid development when the cutter chamber of the TBM is located at the considered section. The late phase change speed is slow. Figure 3.6 presents the measurements taken from sensor 2_3819 in regarding the progression of the TBM. This sensor is located on the road, at 4220m from the reference point and 11m to the receiving shaft. -10-8-6-4-202Vertical displacement [mm] Date2_

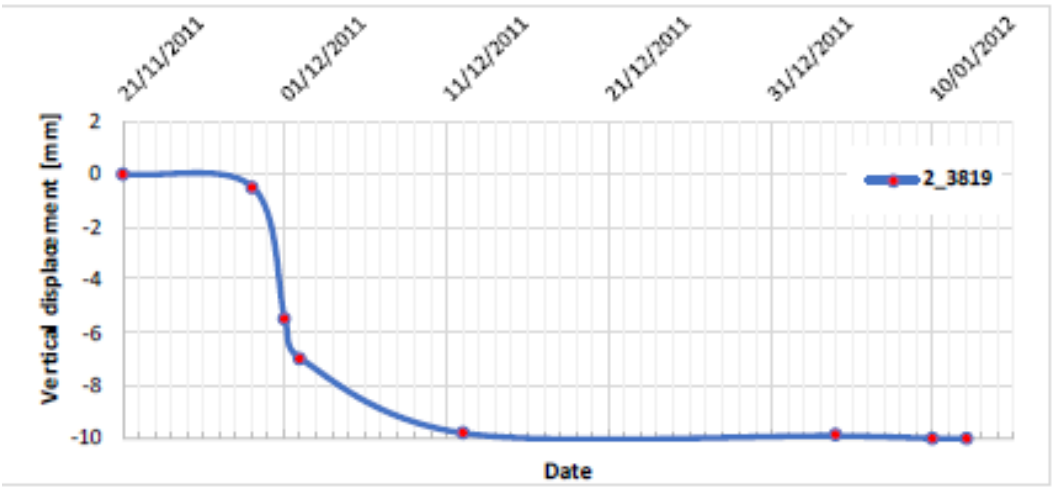

Figure 3.6. Vertical displacement evolution in time recorded by the sensor 2_3819

3.2.4.2 Monitoring data fitting

The settlement profile induced by the excavation of a tunnel is generally described by a Gaussian curve (Peck, 1969). O'Reilly and New (1982) characterized the shape of that curve using two parameters, the maximum settlement at the tunnel axis (S_{max}) and the inflection point (i).

The tunnel path is divided into 5m sections, at each section; the transversal settlement trough is defined by the peck-formula as presented in equation (3.3) where x represents the distance to the tunnel axis.

$$S = S_{max}.\, exp\left(\frac{-x^2}{2i^2}\right) \qquad (3.3)$$

The fitted curve is obtained throw the least square method. The transversal settlement is fitted for each section. Figure 3.7 presents the settlement curve of section 271, at 3795m from the reference point (the starting point of the first part of the extension).

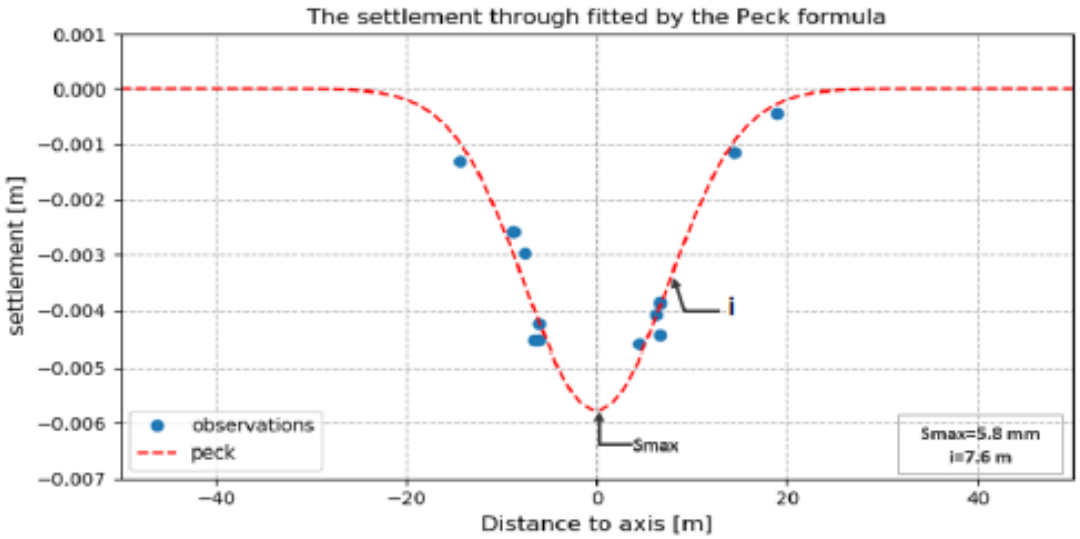

Figure 3.7. fitting settlement curve with peck Formula

3.3 Presentation of the results Numerical simulation of the extension tunnel line 12 Paris with PLAXIS 2D

3.3.1 Presentation of constitutive soils Models

3.3.1.1 Presentation of the Mohr-coulomb Model

Mohr coulomb described here is officially called the linear elastic perfectly plastic model with Mohr coulomb failure criterion. For simplicity, this model is a combination of Hooke's law and the generalized form of coulomb's failure criterion .the basic principle of the MC model is that strains are broken down into an elastic part and a plastic part. The stiffness behavior below the failure contour is assumed linear elastic according to Hooke's law, given by a constant Young's modulus and poisson's ratio. Hence, the model has a limited capability to accurately model deformation behavior before failure (Brinkgreve, 2005).

(a) Basic parameters of the Mohr coulomb Model

The Mohr-coulomb model requires five parameters, which are generally familiar to most geotechnical engineers and which can be obtained from basic tests on soil samples .These parameters with their standard units are listed below:

- **E : Young's modulus** $[KN/m^2]$
- **υ : poisson's ratio** $[-]$
- **ϕ : Friction angle** $[°]$
- **C: cohesion** $[KN/m^2]$
- **ψ: dilatancy angle** $[°]$

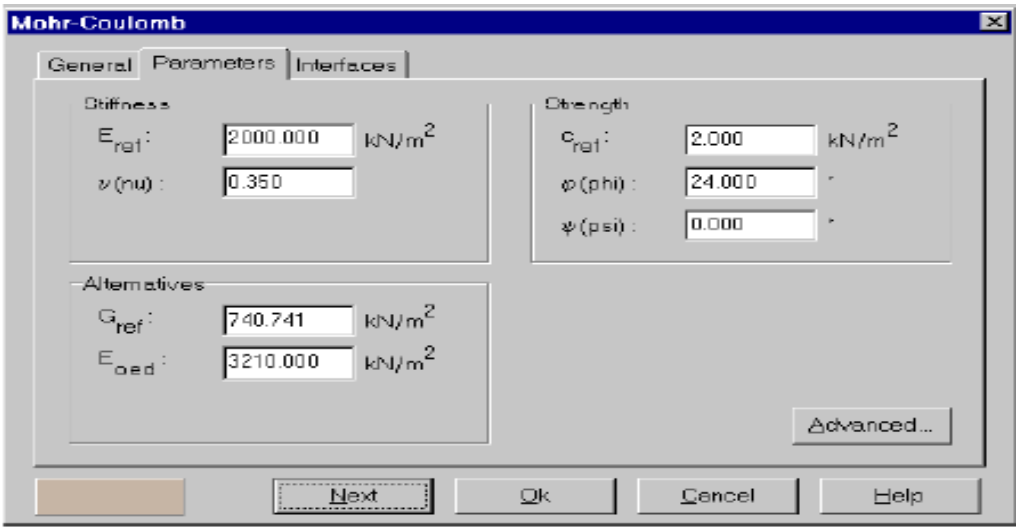

Figure 3.8. parameter tab sheet for Mohr-coulomb Model

(i) Young's modulus (E)

Plaxis uses the Young's modulus as the basic stiffness modulus in the elastic model and the Mohr-coulomb model, but some alternative stiffness modulus are displayed as well .A stiffness modulus has the dimension of stress. The values of the stiffness parameter adopted in a calculation require special attention as many geomaterials show a non-linear behaviour from the very beginning of loading. In soil mechanics, the initial slope is usually indicated as E_0 and the secant modulus at 50 % strength is denoted as E_{50} (see Figure 3.9).For materials with a large linear elastic range, it is realistic to use E_{50} , but for loading of soils, one generally uses E_{50} .Considering-unloading problems, as in the case of tunnelling or excavations, one needs E_{ur} instead of E_{50}.

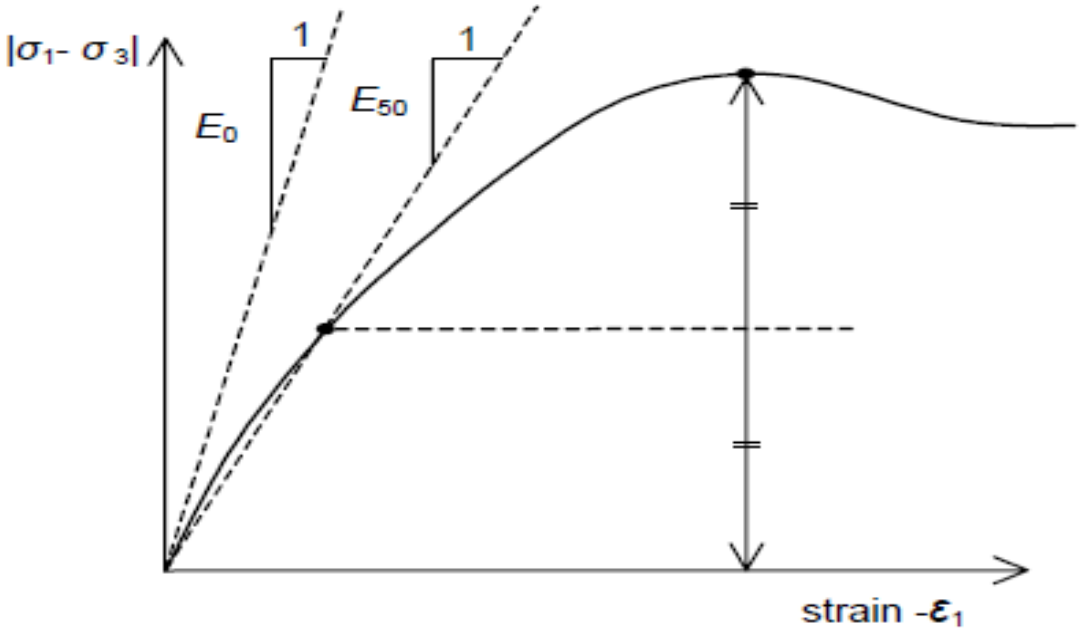

Figure 3.9. Definition of E_0 *and* E_{50} for a standard drained triaxial test result

For soils , both the unloading modulus , E_{ur} , and the first loading modulus E_{50} , tend to increase with the confining pressure .Hence , deep soil layers tend to have greater stiffness than shallow layers .Moreover , the observed stiffness depends on the stress path that is followed .The stiffness is much higher for unloading and reloading than for primary loading .Also , the observed soil stiffness in terms of a Young's modulus may be lower for (drained) compression than for shearing .Hence , when using a constant stiffness modulus to represent soil behaviour one should choose a value that is consistent with the stress level and the stress path development.

(ii) Cohesion (c)

The cohesion strength has the dimension of stress .Plaxis can handle cohesionless sands ($c = 0$), but some options will not perform well .To avoid complications, non –experienced users are advised to enter at least a small value (use c > 0,2 kpa).

Plaxis offers a special option for the input of layers in which the cohesion increases with depth.

(iii) Dilatancy angle (ψ)

The dilatancy angle is specified in degrees .A part from heavily over-consolidated layers , clay soils tend to show little dilatancy ($\psi = 0$) .The dilatancy of sand depends on both the

density and on the friction angle .For quartz sands the order of magnitude is $\psi = \phi - 30°$ .For ϕ values of less than 30 ° however , the angle of dilatancy is mostly zero .A small negative value for ψ is only realistic for extremely loose sands .For further information about the link between the friction angle and dilatancy ,see Bolton (1986).

(iv) Friction angle (ϕ)

The friction angle, ϕ (phi) is entered in degrees .High friction angles, as sometimes obtained for dense sands, will substantially increase plastic computational effort.

The computing time increases more or less exponentially with the friction angle .Hence, high friction angles should be avoided when performing preliminary computations for a particular project. The friction angle largely determines the shear strength as shown in Figure 3.10 by means of Mohr's stress circles.

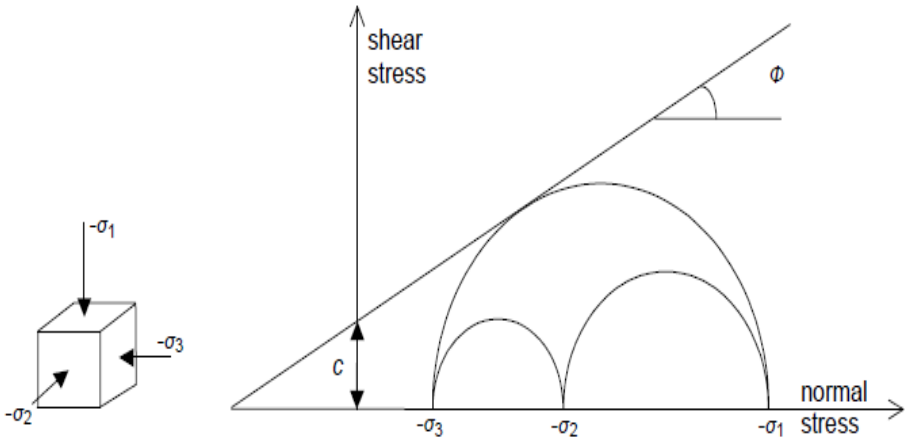

Figure 3.10. stress circles at yield; one touches coulomb's envelope

(v) Poisson's ratio

Standard drained triaxial tests may yield a significant rate of volume decrease at the very beginning of axial loading and, consequently, a low initial value of poisson's ratio (υ_0).For some cases, such as particular unloading problems, it may be realistic to use such a low initial value, but in general when using the Mohr coulomb model the use of a higher value is recommended.

The selection of a poisson's ratio is particularly simple when the elastic model or Mohr-coulomb model is used for gravity loading (increasing $\sum M_{Weight}$ from 0 to 1 in a plastic calculation) .For this type of loading PLAXIS should give realistic ratios of $K_0 = \sigma_h/\sigma_V$ .As both models will give the well-know ratio of $\sigma_h/\sigma_V = \upsilon/(1-\nu)$ for one dimensional compression it is easy to select a poisson's ratio that gives a realistic value of K_0 .Hence , ν is evaluated by matching K_0 .In many cases one will obtain ν values in the range between 0,3 and 0,4 .In general , such values can also be used for loading conditions other than one-dimensional compression .For unloading conditions however , it is more common to use values in the range between 0,15 and 0,25.

(b) Advanced Parameters

When using the Mohr-coulomb model, the <advanced > button in the parameter tab sheet may be clicked to enter some additional parameters for advanced modelling features .As a result, an additional window appears as show in Figure 3.11. The advanced features comprise the increase of stiffness and cohesive strength with depth and the use of a tension cut-off .In fact, the latter option is used by default, but it may be deactivated here , if desired .

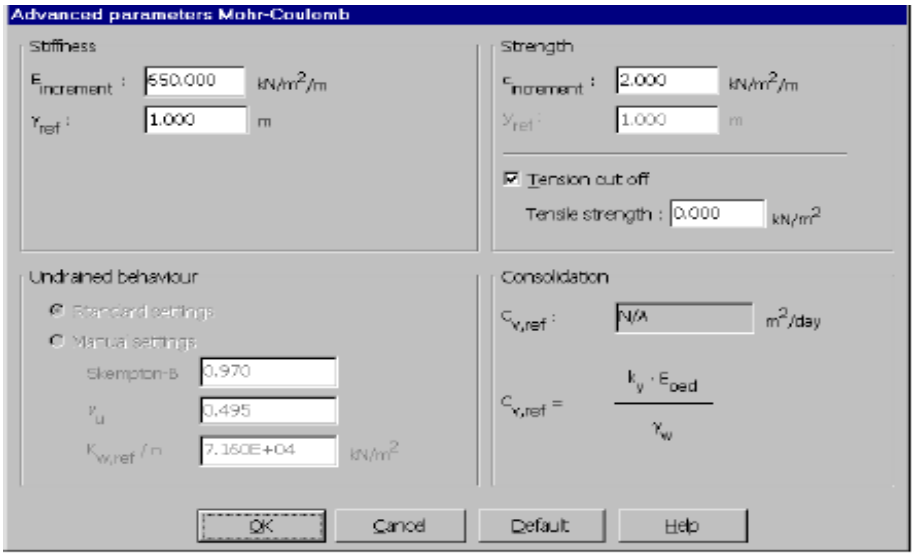

Figure 3.11. Advanced-Mohr coulomb parameter window

(i) Increase of stiffness ($E_{increment}$)

In a real soils , the stiffness depends significantly on the stress level , which means that the stiffness generally increases with depth .When using the Mohr-coulomb model, the stiffness is a constant value .In order to account for the increase of the stiffness with depth the $E_{increment}$ .Value may be used , which is the increase of the Young's modulus per unit of depth (expressed in the unit of stress per unit depth) .At the level given by the y_{ref} parameter , the stiffness is equal to the reference Young's modulus , E_{ref}, as entered in the paramaters tab sheet .The actual value of Young's modulus in the stress points is obtained from the reference value and $E_{increment}$ .Note that during calculations a stiffness increasing with depth does not change as a function of stress state .

(ii) Increase of cohesion ($C_{increment}$)

PLAXIS offers an advanced option for the input of clay layers in which the cohesion increases with depth .In order to account for the increase of the cohesion with depth the the $C_{increment}$ value may be used , which is the increase of cohesion per unit of depth (expressed in the unit of stress per unit depth) .At the level given by the y_{ref} parameter , the cohesion is equal to the (reference) cohesion , C_{ref} , as entered in the parameters tab sheet .The actual value of cohesion in the stress points is obtained from the reference value and $C_{increment}$.

(iii) Tension cut-off

In some practical problems an area with tensile stresses may develop .According to the coulomb envelope show in Figure ….this is allowed when the shear stress (radius of Mohr circle) is sufficiently small .However , the soil surface near a trench in clay sometimes shows tensile cracks .This indicates that soil may also fail in tension instead of in shear .Such behaviour can be included in PLAXIS analysis by selecting the tension cut-off .In this case Mohr circles with positive principal stresses are not allowed when selecting the tension cut-off the allowable tensile strength may be entered .For the Mohr –coulomb model and the Hardening –soil model the tension cut-off is , by default , selected with a tensile strength of zero.

3.3.1.2 Presentation of Hardening soil Model (HSM)

(a) Hardening Soil model principles

The Hardening Soil Model (HSM) is based on the double work hardening models developed by Schanz et al. [1999]. The plastic criterion adopted is that of Mohr-Coulomb (MC). Plastic work hardening before fracture is taken into account instead of the purely elastic behaviour assumed in the MC model. The rigidity of the soil is described using three stiffnesses:

• E_{50} : triaxial stiffness in loading (more precisely the module cutting at 50% of the resistance, (Fig. 3.15);

• E_{oed} : Oedometric stiffness;

• E_{ur} : Triaxial stiffness in unloading-reloading.

The module in unloading can therefore be distinguished from that in loading.

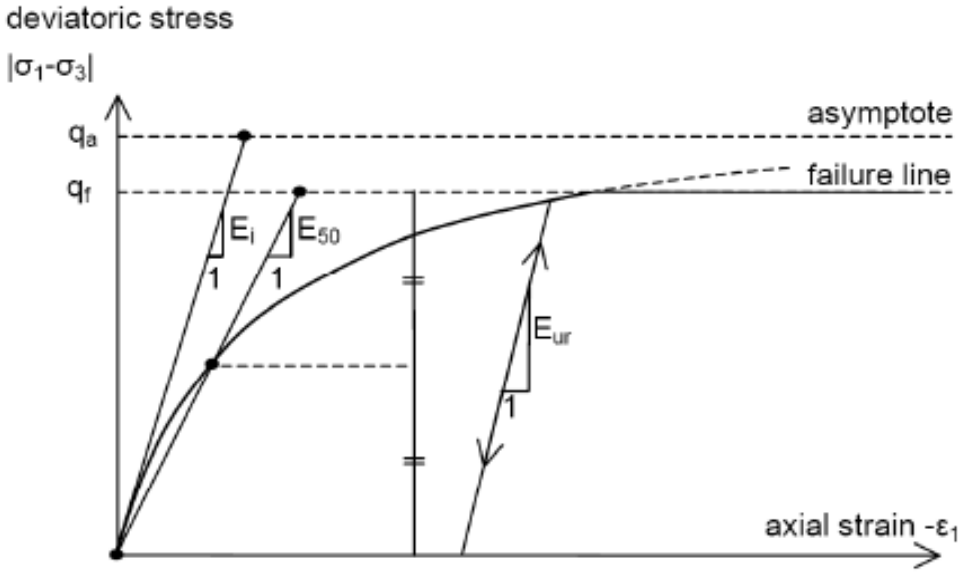

Figure 3.12. Hyperbolic curve for stress-strain relationship

(b) Hyperbolic curve for stress-strain relationship

The HSM model derives from the hyperbolic model of Duncan-Chang [1970] because it takes up, by improving, the hyperbolic formulations and it is adapted to all types of soils. The relationship between axial deformations (ε_1) and deviatoric stress (q) is given by the equation (3.6).

$$\varepsilon_1 = \frac{q_a}{2E_{50}} * \frac{q}{q_a - q} \qquad \textbf{(3.4)}$$

Where q_a is the asymptote of the breaking stress (Fig. 3.13). It is related to the maximum breaking stress (q_f) by the equation (3.7).

$$q_a = \frac{q_f}{R_f} \quad \text{avec} \quad q_f = (c' cot\varphi' - \sigma_3').\frac{2.\sin\varphi'}{R_f(1-\sin\varphi')} \qquad \textbf{(3.5)}$$

With $R_f = 0{,}9$ for most soils

The modulus E_{50} depends on the level of stress and it determines the magnitude of the two deformations: elastic and plastic. It is given by the expression:

$$E_{50} = E_{50}^{ref}\left(\frac{c'.\cos\varphi' - \sigma_3'.\sin\varphi'}{c'.\cos\varphi' + P^{ref}.\sin\varphi'}\right)^m \qquad \textbf{(3.6)}$$

In this expression, E_{50}^{ref} is the reference module that corresponds to the reference containment pressure (100 kpa by default). For the m parameter, a typical value of 0.5 for sand and 1.0 for clay are suggested.

The elastic modulus E_{ur} determines, with the Poisson coefficient υ_{ur} , the behavior of the soil during unloading-reloading. It also depends on the stress level and its definition is as follows:

$$E_{ur} = E_{ur}^{ref} \left(\frac{c'cot\varphi' + \sigma_3'}{c'cot\varphi' + P^{ref}}\right)^m \qquad (3.7)$$

The load surface is described by two mechanisms with isotropic work hardening controlling respectively the volume and deviatoric deformations (Figure 3.13).

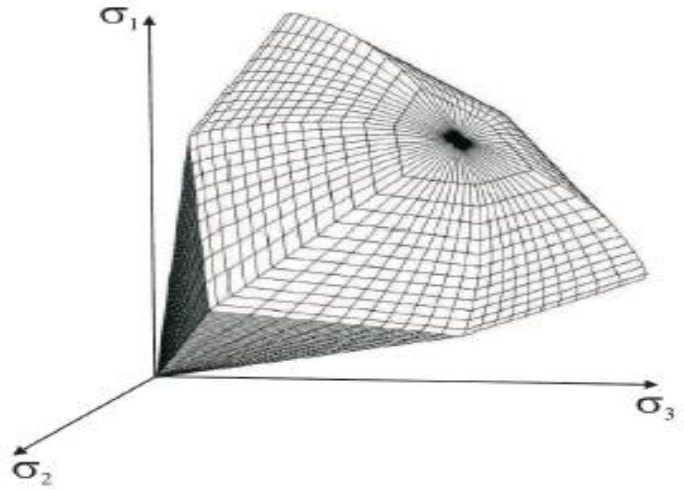

Figure 3.13. Load surface adopted by the HS model (schanz et al (1999)))

(c) Parameter of Hardening Soil Model

The parameters of the Hardening Soil model are grouped into three categories:

(i) Plastic parameters of Mohr coulomb

- c' : cohesion of soil
- φ' : internal friction angle
- ψ : dilatancy angle

(ii) Basic parameters of stiffness

- E_{50}^{ref} : triaxial Young modulus
- E_{oed}^{ref}: oedometric young modulus
- E_{ur}^{ref} : loading /unloading young modulus ($E_{ur}^{ref} = 3.E_{50}^{ref}$ par défaut)
- m : exponent of the stress level (a value of 0.5 is often used)

(iii) Advanced Parameters

- υ_{ur} : fish coefficient for unloading / reloading (0.2 by default)
- P^{ref} : confinement pressure of reference (100 Kpa by default))
- ${K_0}^{nc}$: K_0 in the case of normal consolidation (${K_0}^{nc} = 1 - \sin\varphi'$, by default)
- R_f : fracture approach ratio q_f/q_a (0,9 by default)

By making the simplifying assumption that $E_{50}^{ref} = E_{oed}^{ref}$and keeping the other recommended default values, we see that the HSM model has no more free parameters than the Mohr-coulomb criterion. Thanks to its simplicity, it is thus adapted to the realization of calculations of project in engineering office and to the characterization of the behavior of grounds, where a limited number of mechanical parameters could be defined (case of the extension of the subway of the line 12 Paris)

3.3.1.3 Presentation of Hardening soil model with small stiffness Model (HSSM)

The work of (Atkinson & Sallfors, 1991) taken over by (Reiffsteck, 2002), (Obrzud, 2010) and (PLAXIS, 2015) in particular has shown that conventional geotechnical tests, with the triaxial apparatus or the pressiometer, lead to the imaisation of stiffness for high levels of deformation (of the order of several percent). The stiffness is much higher for small deformations and an S-profile describes these variations as a function of the level of deformation (Figure 3.14). The Hardening Soil model with small-strain stiffness (HS small)

developed by (*Benz, 2007*) allows this effect to be taken into account through a formulation formulation inspired by the Brick model described by (*Simpson, 1992*). The stiffness of the soil depends directly on the level of deformations, in this case shear deformations.

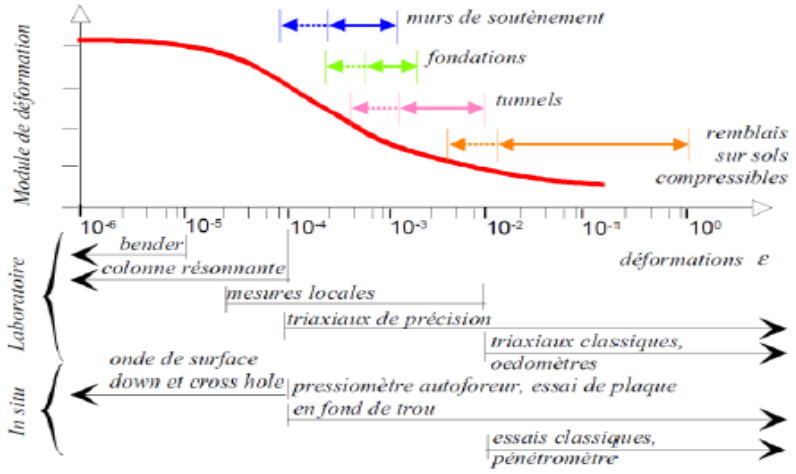

Figure 3.14. Areas of use of test equipment for the determination of strain modules (Reiffsteck, 2002)

This variant adds two parameters to the HSM model to describe the behaviour in the field of small deformations:G_0 : initial shear modulus and $\gamma_{0,7}$ the shear deformation for which the shear modulus secant is about 70% of G_0 . The shear modulus secant follows a hyperbolic decreasing according to:

$$G_S = \frac{G_0}{1+0{,}385\frac{\gamma}{\gamma_{0,7}}} \qquad \textbf{(3.8)}$$

The decay is stopped when the tangent shear modulus G_t reaches G_{ur} . G_{ur} is defined from Young's modulus and fish coefficient to equation (3.9).

$$G_{ur} = \frac{E_{ur}}{2(1+\upsilon_{ur})} \qquad \textbf{(3.9)}$$

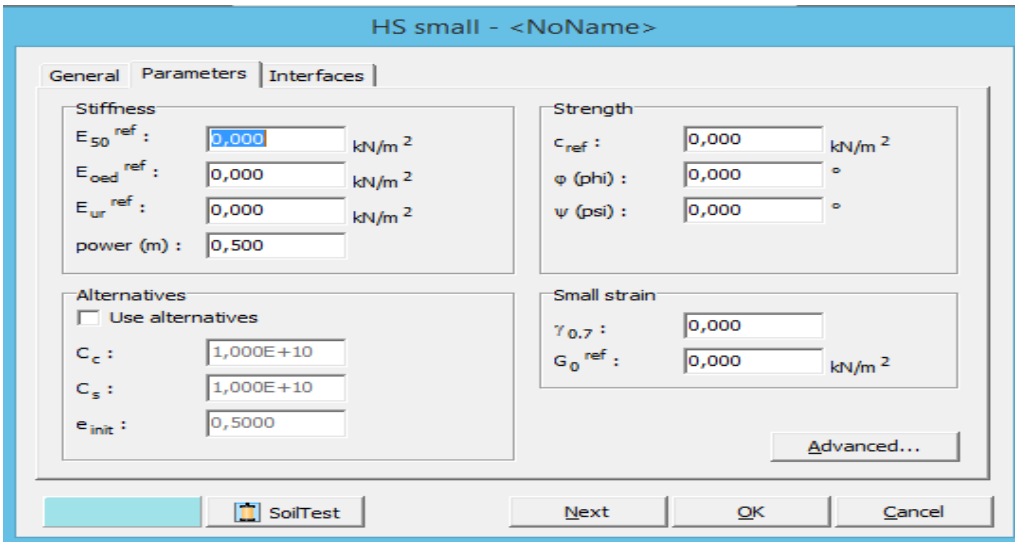

Figure 3.15. Parameters of Hardening soil model with small stiffness

3.3.2 Profiles parameters

3.3.2.1 Definition of parameters

The parameters proposed below are based on the available surveys. Depending on the construction methods used and the sensitivity of these parameters, it will be necessary to specify them by specific tests with a tightened mesh allowing to integrate heterogeneity as accurately as possible. These parameters will also have to be specified during the work phase according to the geology and mechanics actually encountered. The pressure coefficient of the resting land K_0 is determined, considering the normally consolidated formations, by the formula of Jacky: $K_0 = 1 - \sin(\varphi')$ with φ' is the effective friction angle. The coefficient is defined from Ménard's tables.

Based on the above results, we propose the table 3.5.

Table 3.5. Parameters needed for the three constitutive soils models calculation

γ (KN/m^3)	Wet weight by volume
K_O	Land thrust coefficient at rest
C (Kpa) / C' (KPa)	Short term cohesion /long-term cohesion
φ' (°)	Internal friction angle in the long term
ν	Long term fish coefficient
α	Menard's rheological coefficient
E_m	Menard's Modulus
ψ	Dilatancy angle
E young	Young Modulus

- According to the literature ,The relationship between the Menard's Modulus and the oedometric Modulus is given by the equation (3.10).

$$\mathbf{E_{oed} = K * \left(\frac{E_m}{\alpha}\right)} \qquad \mathbf{(3.10)}$$

Where, **K** is a dimensionless coefficient between 1 and 4 (From the litterature) ,α is the Menard's rheological coefficient

- We have done a calibration of the parameters E_{oed} ,E_{50} and E_{ur} depending on the constitutive soil Model (HSM and HSSM) used , the confinement pressure and the best settlement curve obtained.

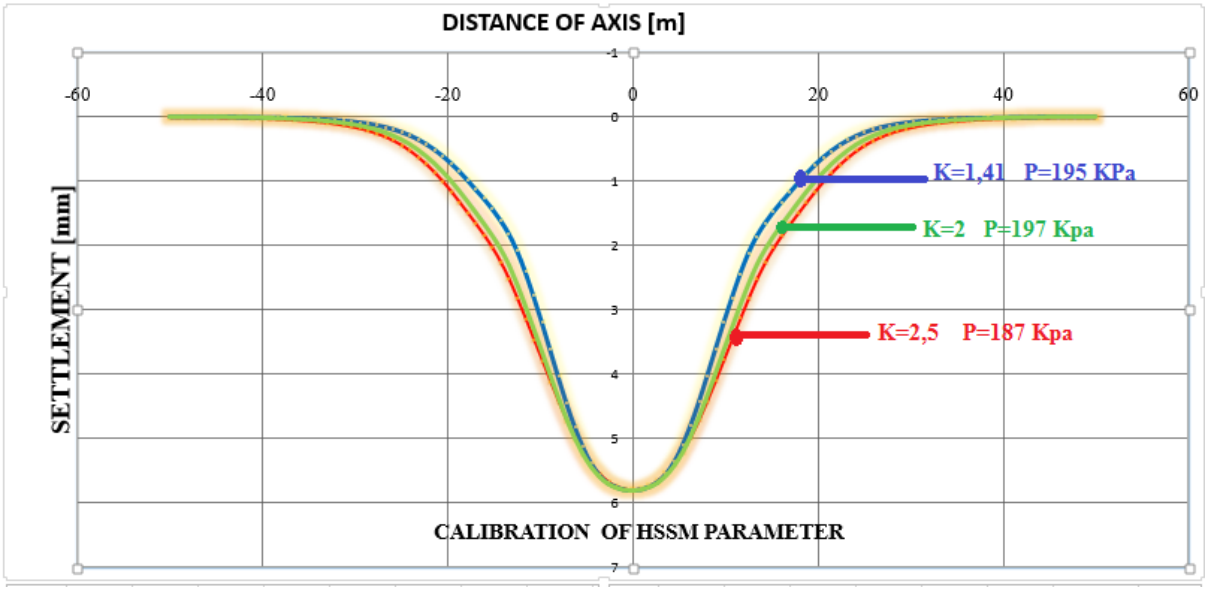

Figure 3.16 . An Illustation of the choice of the value **K** for HSSM

3.3.2.2 Mohr Coulomb parameters

Base on the result from in situ and laboratory tests and from previous experiences on different project, parameters describing the soil behavior using Mohr coulomb, HSM and HSSM are presented in table 3.6 , table 3.7 and table 3.8 respectly .

Table 3.6. Values of parameters selected for Mohr Coulomb Model

Formation/ Section 271		Pressuremeter						Long term				
		γ [kN.m^{-3}]	Em [MPa]	Pl* [MPa]	α [-]	c' [kPa]	φ' [°]	γ [kN.m^{-3}]	Eyoung [MPa]	ψ' [°]	ν [-]	K_0 [-]
Fill	R	20	8,5	0,6	0,50	0	25	20	10	0	0,35	0,58
Alluvions	AL	20	4	0,4	0,50	0	10	20	5	0	0,35	0,83
Saint-Ouen limestone	CSO	19	12	1,5	0,50	0	30	19	40	0	0,3	0,58
Ducy limestone	CD	19	6,5	0,7	0,50	0	30	19	39	0	0,3	0,58
Beauchamp upper sand	SB sup	21	38	4,0	0,33	0	35	21	60	5	0,3	0,50
Beauchamp middle sand	SB med	20	28	3,1	0,50	60	15	20	100	0	0,3	0,74
Beauchamp lower sand	SB inf	21	35	4,1	0,33	0	35	21	60	5	0,3	0,50
Marls and Sandstones	MC	21	48	4,5	0,50	30	35	21	120	5	0,3	0,50

3.3.2.3 Hardening soil Model parameters

The elastoplastic HSM constitutive model is used to simulate the soil behavior. The equations (3.11) ,(3.12) , (3.13) present the different correlations between the modulus.

$$E_{oed} = \mathbf{4} * \left(\frac{E_m}{\alpha}\right) \quad \textbf{(3.11)}$$

$$E_{oed} = E_{50} \quad \textbf{(3.12)}$$

$$E_{ur} = 3 * E_{50} \quad \textbf{(3.13)}$$

Where,

- E_{50}:deformation modulus at 50% of the deviatoric stress,
- E_{ur} :the unload-reload deformation modulus,
- E_{oed} :the oedometric deformation modulus,
-

Table 3.7. Values of parameters selected for Hardening Soil Model

Formation/ Section 271		γ [kN.m⁻³]	Pressuremeter Em [MPa]	Pl* [MPa]	α [-]	Long term c' [kPa]	φ' [°]	γ [kN.m⁻³]	Eyoung [MPa]	ψ' [°]	ν [-]	K₀ [-]	E oed [MPA]	E50 [MPA]	Eur [MPA]
Fill	R	20	8,5	0,6	0,50	0	25	20	10	0	0,35	0,58	68	68	204
Alluvions	AL	20	4	0,4	0,50	0	10	20	5	0	0,35	0,83	32	32	96
Saint-Ouen limestone	CSO	19	12	1,5	0,50	0	30	19	40	0	0,3	0,58	96	96	288
Ducy limestone	CD	19	6,5	0,7	0,50	0	30	19	39	0	0,3	0,58	52	52	156
Beauchamp upper sand	SB sup	21	38	4,0	0,33	0	35	21	60	5	0,3	0,50	456	456	1368
Beauchamp middle sand	SB med	20	28	3,1	0,50	60	15	20	100	0	0,3	0,74	224	224	672
Beauchamp lower sand	SB inf	21	35	4,1	0,33	0	35	21	60	5	0,3	0,50	420	420	1260
Marls and Sandstones	MC	21	48	4,5	0,50	30	35	21	120	5	0,3	0,50	384	384	1152

3.3.2.4 HSSM parameters

The elastoplastic HSSM constitutive model is used to simulate the soil behavior. The equations (3.14) ,(3.15) ,(3.16) and (3.17) present the different correlations between the modulus.

$$E_{oed} = \mathbf{1,41} * \left(\frac{E_m}{\alpha}\right) \quad \textbf{(3.14)}$$

$$E_{oed} = 1{,}2 * E_{50} \quad \textbf{(3.15)}$$

$$E_{ur} = 2 * E_{50} \quad \textbf{(3.16)}$$

$$E_0 = 8 * E_{50} \quad \textbf{(3.17)}$$

Where,

- $\mathbf{E_{50}}$: deformation modulus at 50% of the deviatoric stress,
- $\boldsymbol{E_{ur}}$: the unload-reload deformation modulus,
- $\boldsymbol{E_{oed}}$:the oedometric deformation modulus,
- $\mathbf{E_0}$: The elastic modulus at a certain characteristic shear strain level where the modulus reduces to 70%.
- $\mathbf{E_m}$: Menard 's modulus

The soil parameters used in the constitutive model come from the project documents. Table 3.10 presents the geotechnical parameters associated to the non linear elastoplastic model HSSM. All the layers are assumed to be in drained condition except the medium sand of Beauchamp, which is considered in undrained condition due to its very low permeability.

Table 3.8. Values of parameters selected for Hardening soil Model with small strain

Formation/ Section 271			Pressuremeter			Long term													
		γ	Em	Pl*	α	c'	φ'	γ	Eyoung	ψ' [°]	ν	K_0	Eoed	E50	Eur	G0	$\gamma_{0,7}$	E0
		[kN.m^{-3}]	[MPa]	[MPa]	[-]	[kPa]	[°]	[kN.m^{-3}]	[MPa]		[-]	[-]	[Mpa]	[Mpa]	[Mpa]	[Mpa]	[kN.m-3]	
Fill	R	20	8,5	0,6	0,50	0	25	20	10	0	0,35	0,58	23,97	19,975	39,95	107,865	0,0002	159,8
Alluvions	AL	20	4	0,4	0,50	0	10	20	5	0	0,35	0,83	11,28	9,4	18,8	50,76	0,0002	75,2
Saint-Ouen limestone	CSO	19	12	1,5	0,50	0	30	19	40	0	0,3	0,58	33,84	28,2	56,4	146,64	0,0002	225,6
Ducy limestone	CD	19	6,5	0,7	0,50	0	30	19	39	0	0,3	0,58	18,33	15,275	30,55	79,43	0,0002	122,2
Beauchamp upper sand	SB sup	21	38	4,0	0,33	0	35	21	60	5	0,3	0,50	160,74	133,95	267,9	696,54	0,0002	1071,6
Beauchamp middle sand	SB med	20	28	3,1	0,50	60	15	20	100	0	0,3	0,74	78,96	65,8	131,6	342,16	0,0002	526,4
Beauchamp lower sand	SB inf	21	35	4,1	0,33	0	35	21	60	5	0,3	0,50	148,05	123,38	246,75	641,55	0,0002	987
Marls and Sandstones	MC	21	48	4,5	0,50	30	35	21	120	5	0,3	0,50	135,36	112,8	225,6	586,56	0,0002	902,4

3.3.3 Influence of the mesh in the PLAXIS modelisation

Some elements play a very important role in the results of the plaxis 2D software modelling, for example the choice of the mesh.

In this part, we used the hardening soil model throughout our simulation. Therefore, we used the parameters given in Table 3.7 and 3 different meshes . We compared them according to the time needed to perform the calculations and the accuracy given by each mesh and the results obtained are present in table 3.9.

Table 3.9 . Analysis of different meshes

Mesh	**1**	**2**	**3**
Number of elements	439	1839	5589
Number of nodes	3711	15123	45383
Number of stress points	5268	22068	67068
Calcul time phase1	2s	4s	29 s
Calcul time phase 2	11s	50s	326s
Calcul time phase 3	1s	2s	15s
Total calcul time	14s	56s	370s
Increase in calculation time compared to mesh size 1	0%	75%	96,21%
Decrease in overall error compared to mesh 1	0%	0,35%	0 ,52%

We can conclude that the finer the mesh, the longer the computation time and the more accurate it is.For our numerical simulation, we took a mesh with 1216 number of elements, 10077 number of nodes and 14592 number of stress points (Figure 3.17). This mesh is finer at the layers around the tunnel.

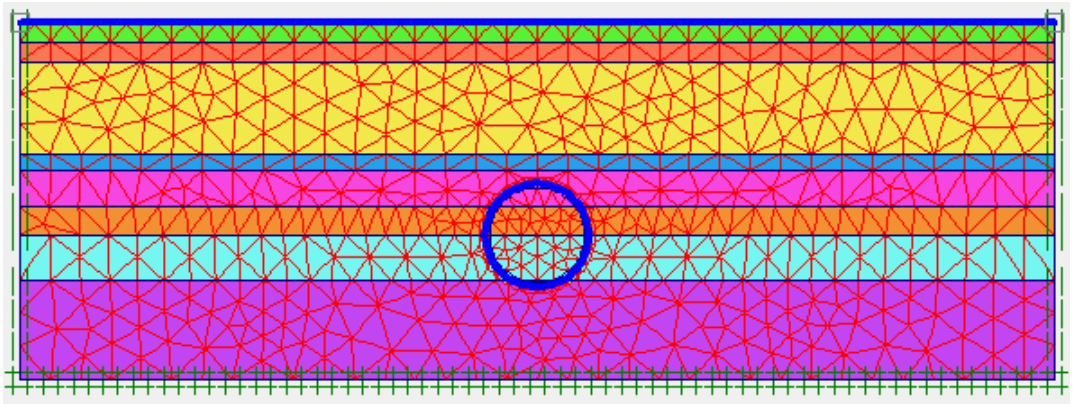

Figure 3.17 . Mesh of our numerical modelisation

3.3.4 Presentation of the results

The numerical simulation of the tunnelling was carried out using the Plaxis2D finite element calculation code, a plane deformation model was created. The water table is 2.3 m deep. The extent of the mesh is 100 m in length and the tunnel is located at H = 13.9 m from the substratum (assumed constant depth). The tunnel is circular and its diameter is D = 9.15 m. Boundary conditions and displacements were fixed at the lateral and lower boundaries. To simulate the construction phases and their effects on the ground surface, the following modelling steps were applied to all of the sections:

- Initialize the in situ stresses, σo ;by turning on gravity (normally referred to as the Ko procedure);

- Activate the structure (the plate that replace soil)

- Excavate tunnel and apply a radial pressure of λ ($\sigma 0' - Pf'$) with λ = 0.9. In the program, λ is a confinement ratio describing the proportioning of the overburden stresses applied to the lining based on the distance between the tunnel face and the point where the tunnel lining is erected. While excavating the tunnel, using Plaxis to define the confinement pressure at the axis of the tunnel, we will simulate the

value of the water pressure at the axis so that it corresponds to the confinement pressure at the axis of this section.

❖ Install the tunnel linings by defining cluster dry.

3.3.4.1 Numerical soil Model for the three constitutive soil Models

After the modelling of the profile with PLAXIS 2D, we obtain the following geometry figure 3.18 consisting of a tunnel,a plate which represent the soil ,linings and 8 soil layers, which are represented respectly:

- Fill **R**
- Alluvions **AL**
- Saint-ouen Limestone **CSO**
- Ducy Limestone **CD**
- Beauchamp Upper Sand $\mathbf{SB_{sup}}$
- Beauchamp middle Sand $\mathbf{SB_{med}}$
- Beauchamp Lower sand $\mathbf{SB_{inf}}$
- Marls and Sandstones **MC**

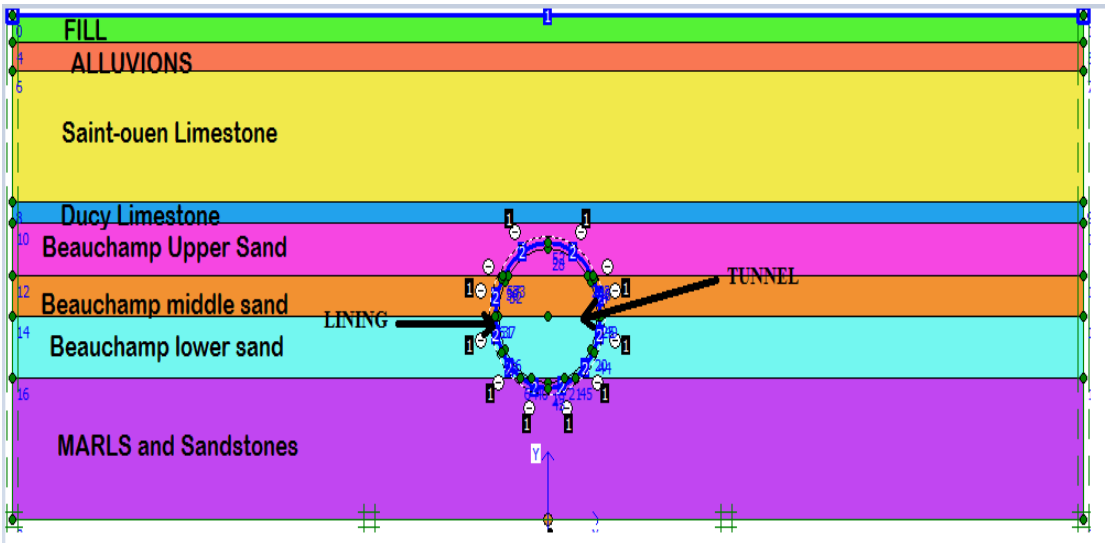

Figure 3.18. Geometry of the 2D model plane deformations

3.3.4.2 Mohr- Coulomb constitutive soil Model

After modeling the profile with PLAXIS 2D, we imposed a confining pressure of 197 Kpa at the tunnel axis and we obtain the following results:

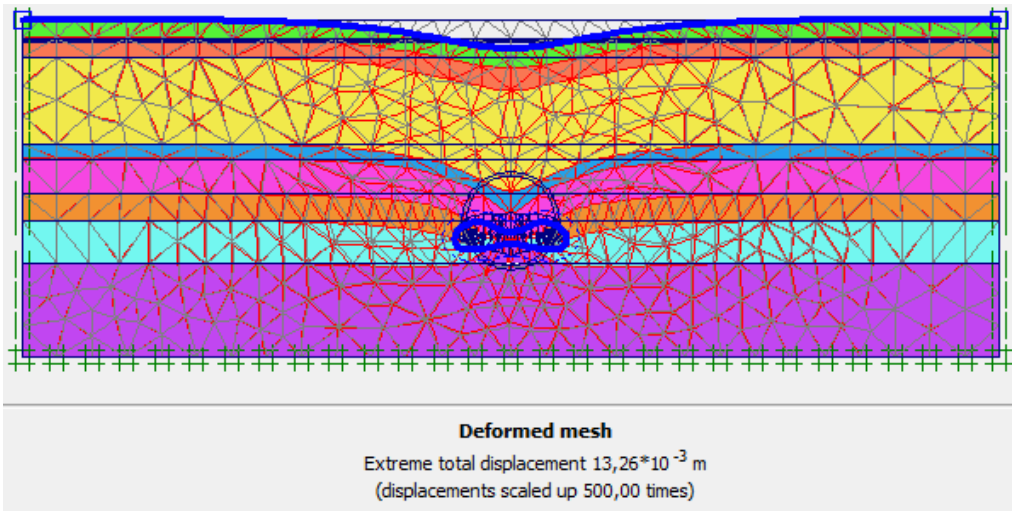

Figure 3.19. View 2D - Planar deformations of the mesh of the soil profile.

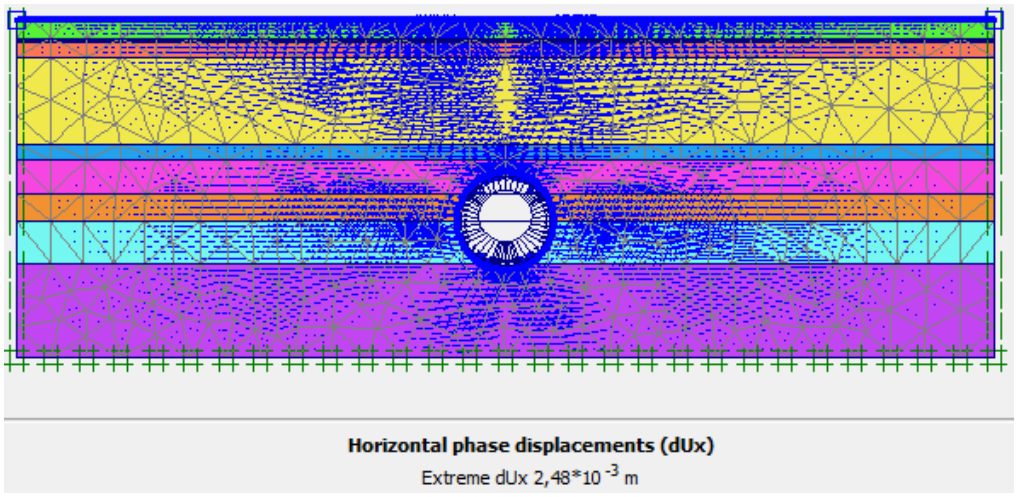

Figure 3.20. Horizontal movements in the terrain as the TBM passes through of the soil profile

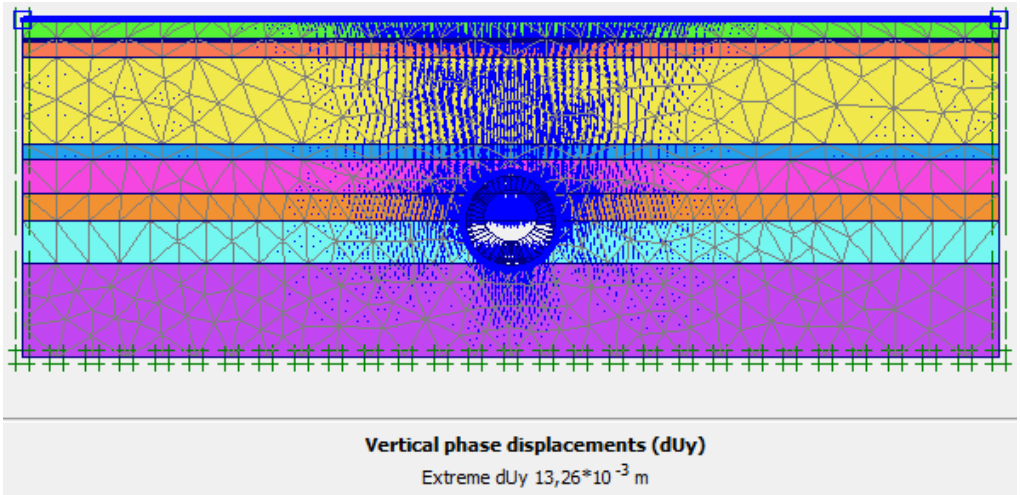

Figure 3.21. Vertical movements in the terrain as the TBM passes through of the soil profile

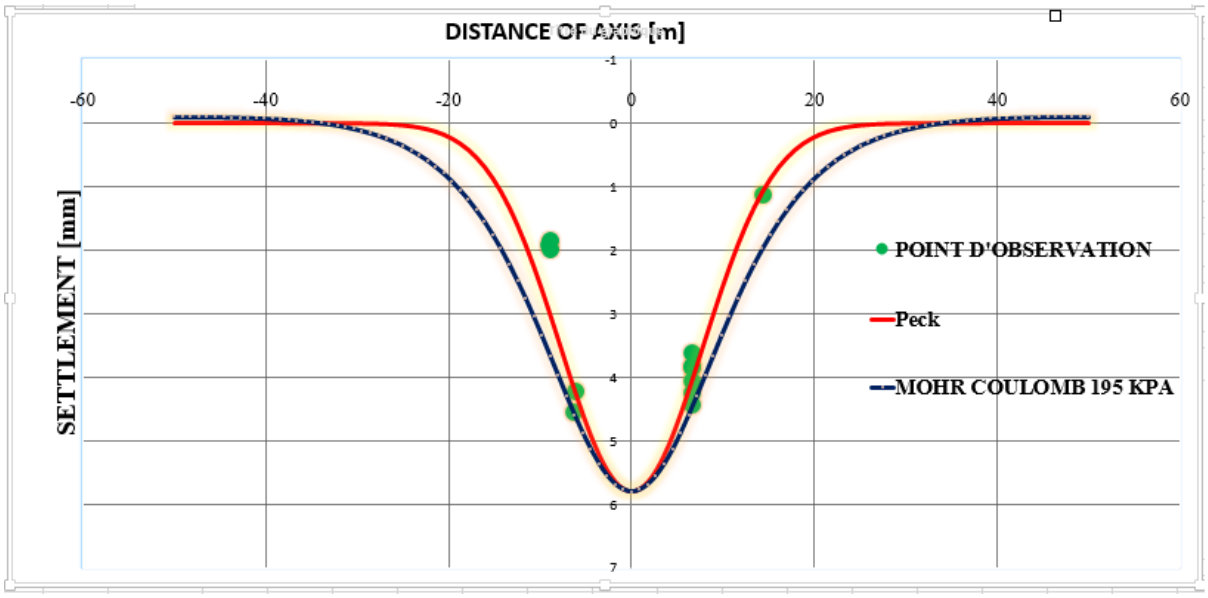

Figure 3.22. Mohr Coulomb settlement Curve

3.3.4.3 Hardening Soil Model

After modeling the profile with PLAXIS 2D, we imposed a confining pressure of 195 Kpa at the tunnel axis and we obtain the following results.

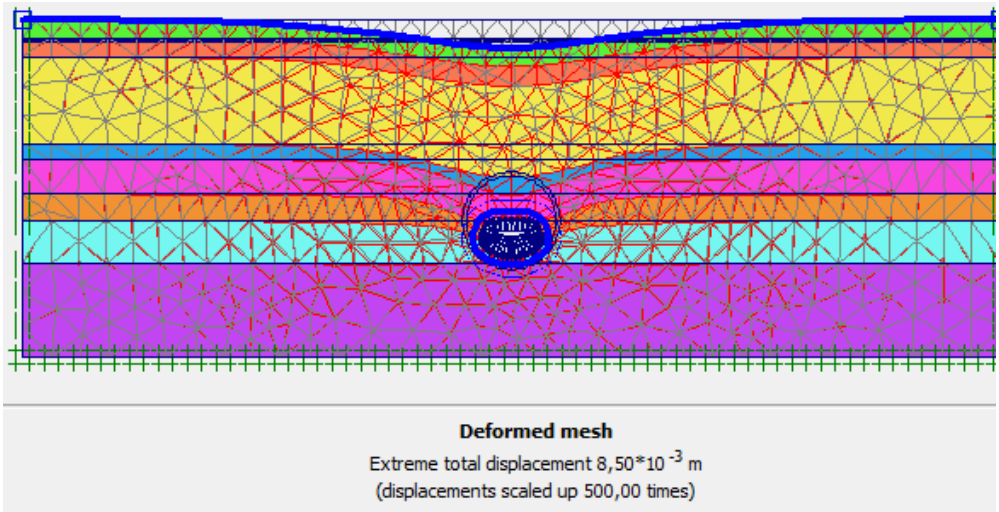

Figure 3.23. View 2D - Planar deformations of the mesh of the soil profile

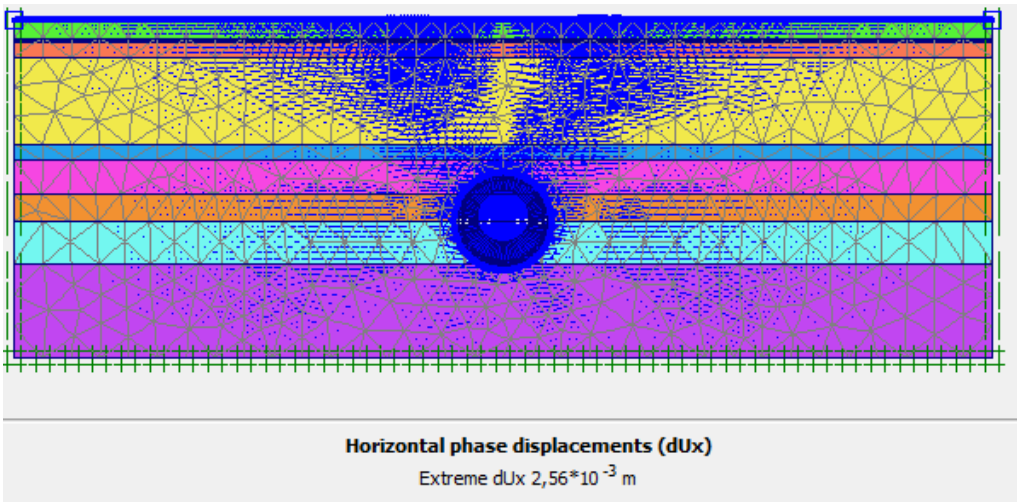

Figure 3.24. Horizontal movements in the terrain as the TBM passes through of the soil profile

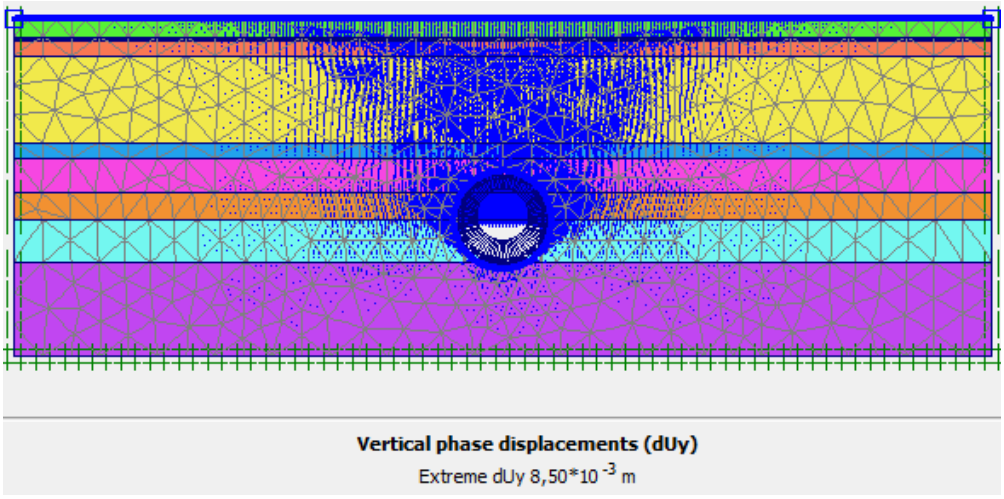

Figure 3.25. vertical movements in the terrain as the TBM passes through of the soil profile

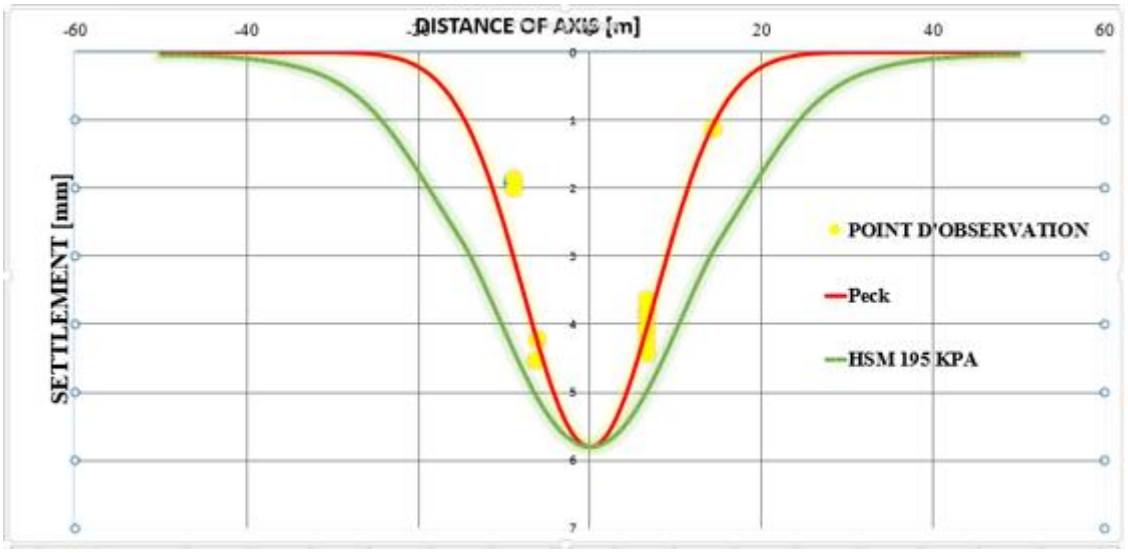

Figure 3.26. Hardening Soil model settlement curve

3.3.4.4 Hardening Soil Model With Small strain

After modeling the profile with PLAXIS 2D, we imposed a confining pressure of 195 Kpa at the tunnel axis and we obtain the following results.

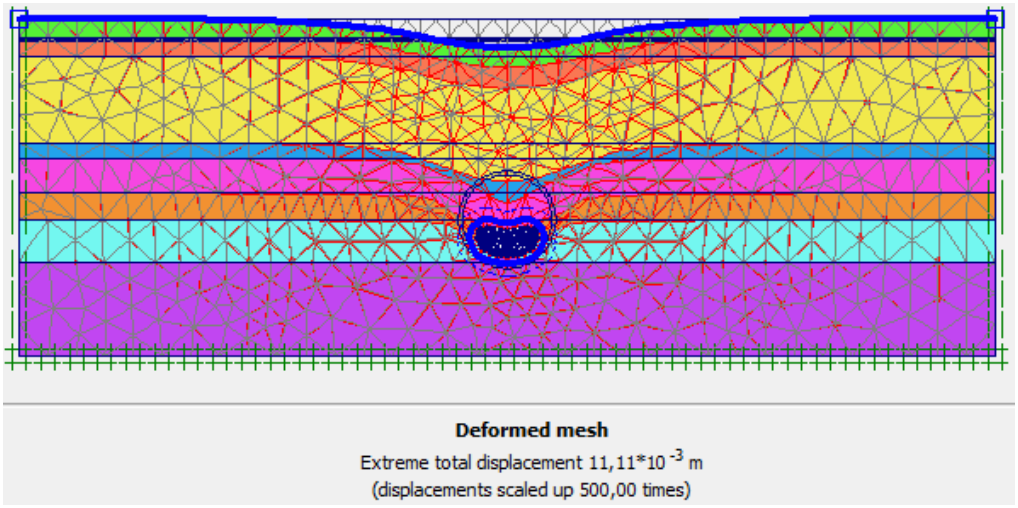

Figure 3.27. View 2D - Planar deformations of the mesh of the soil profile

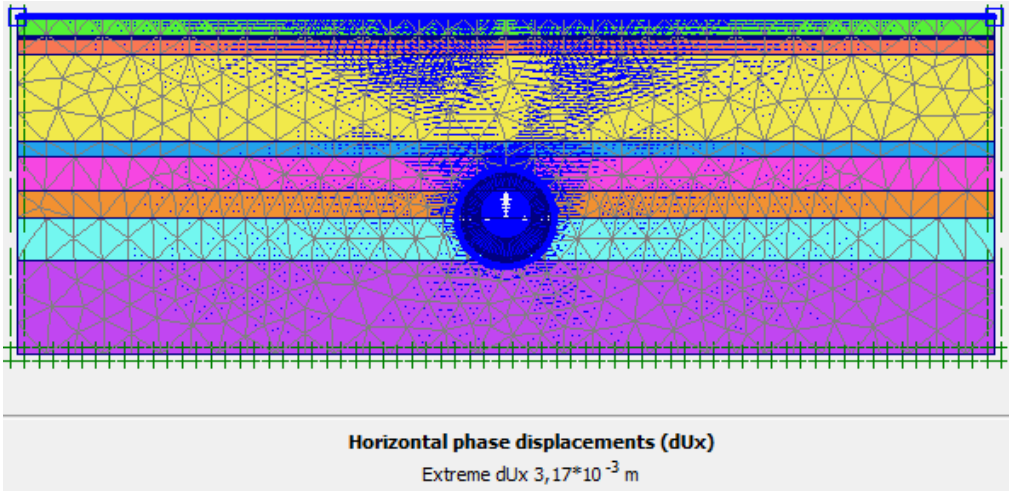

Figure 3.28. Horizontal movements in the terrain as the TBM passes through of the soil profile

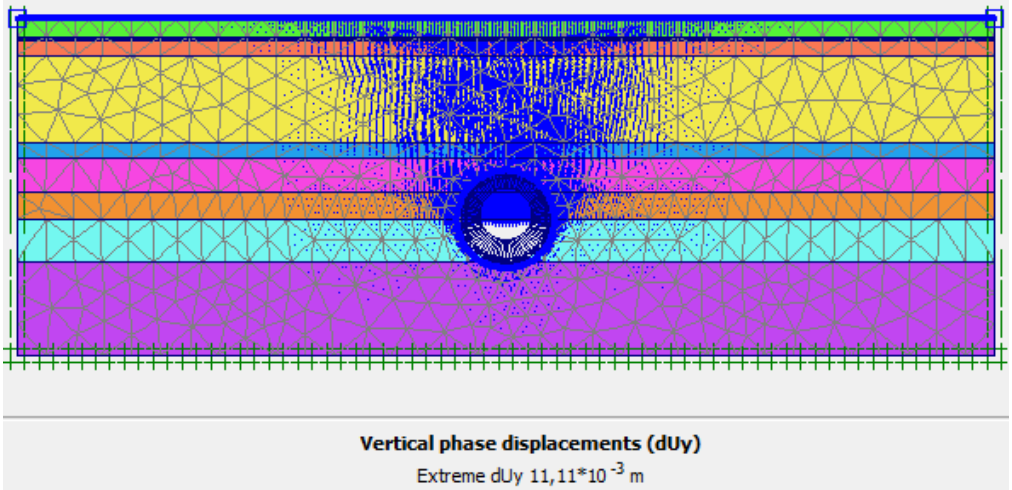

Figure 3.29. vertical movements in the terrain as the TBM passes through of the soil profile

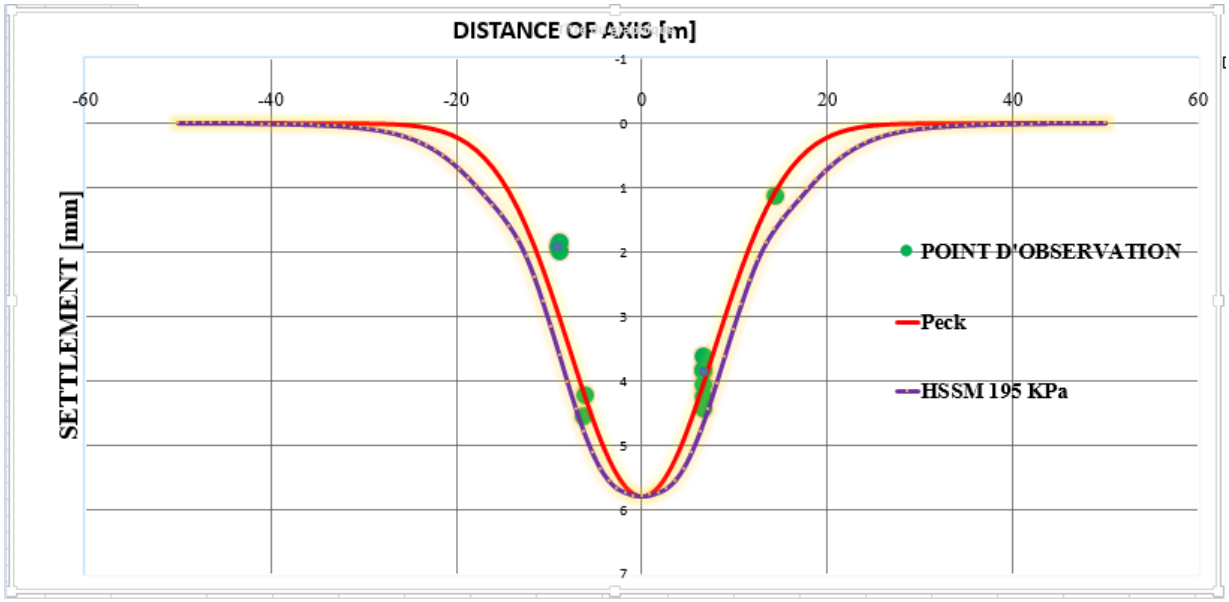

Figure 3.30. Hardening Soil with small strain settlement curve

3.3.5 Analyse of soil and phenomenon around the tunnel on the settlement curve

3.3.5.1 Analysis of the influence of mechanical caracteristics of soil around the tunnel on the settlement curve

A parametric study is performed in the layer of soil above the tunnel (Upper Beauchamp sand) to determine the impact of the three parameters (E, ϕ, c) of each constitutive soil models on surface settlement. For each variable, the simulation performed with the default values is compared to five simulations for which this parameter is varied. Thus, we have five cases for each variable.

(a) Mohr coulomb Parameters

Table 3. 10. Defaut parameters used for Mohr Coulomb Model

Variable	E(Mpa)	φ(°)	C(Kpa)
Reference value	60	35°	0,1

Table 3. 11 . Influence of Young modulus **E** on the maximum settlement with MC model

E_i(Mpa)	69	67	65	63	**60**	57	55	53	50	45	40	35
S_{max}(mm)	5,71	5,73	5,75	5,77	**5,8**	5,83	5,85	5,87	5,91	5,98	6,06	6,14

Table 3.12. Influence of cohesion C on the maximum settlement

C (Kpa)	**0,1**	1	2	3	4	5	10	20	50	60
S_{max}(mm)	**5,8**	5,79	5,79	5,79	5,79	5,79	5,79	5,78	5,78	5,78

Table 3.13 . Influence of friction angle on the maximum settlement

ϕ (°)	40	39	38	37	36	**35**	34	33	32	31	30
S_{max}(mm)	5,86	5,85	5,83	5,82	5,81	**5,8**	5,78	5,77	5,75	5,74	5,73

We can see that ,when we reduce the Young's modulus, the surface settlement increases and when we reduce the friction angle , the maximum settlement decrease , but the cohesion give us the same maximum settlement .

(b) Hardening Soil Model parameters

Table 3.14. different parameters used for HSM model

Variable	E_{50}(Mpa)	φ	c
Reference value	456	35°	0,1

Table 3.15. Influence of the secant modulus on the maximum settlement

E_{50} (Mpa)	456	400	350	300	250	200
S_{max}(mm)	5,8	5,8	5,82	5,84	5,87	5,9

Table 3.16. Influence of friction angle on the maximum settlement

ϕ (°)	40	39	38	37	36	**35**	34	33	32	31	30
S_{max}(mm)	5,81	5,80	5,80	5,80	5,80	**5,8**	5,80	5,80	5,80	5,80	5,80

Table 3.17. Influence of the cohesion on the maximum settlement

$C(Kpa)$	**0,1**	5	10	15	20	25	40	50	60
S_{max}(mm)	**5,8**	5,75	5,73	5,70	5,68	5,65	5,61	5,58	5,55

We see that when we reduce the secant modulus , and cohesion in the HSM model, the settlement increases , but the variation of the friction angle give the same value of the maximum settlement.

(c) Hardening model with small strain parameters

Table 3.18. different parameters used for HSSM model

Variable	E_{50}(Mpa)	φ	c
Reference value	133,95	35°	0

Table 3.19. Influence of the secant modulus on the maximum settlement

E_{50} (Mpa)	133,95	100	80	60	40	20
S_{max}(mm)	5,8	5,97	5,98	5,99	5,96	5,94

Table 3.20. Influence of the cohesion on the maximum settlement

C(kpa)	**0,1**	5	10	15	20	25	40	50	60
S_{max}(mm)	**5,8**	5,75	5,70	5,64	5,59	5,54	5,45	5,38	5,27

Table 3.21. Influence of the friction angle on the maximum settlement

ϕ (°)	40	39	38	37	36	**35**	34	33	32	31	30
S_{max}(mm)	5,75	5,76	5,77	5,78	5,79	**5,8**	5,81	5,82	5,83	5,84	5,85

We can see that when we reduce the cohesion , the internal friction angle and the secant modulus in the HSSM model, the surface settlement increases .

3.3.5.2 Analyse of the influence of apparition of plasticized zones around the tunnel

During the modeling of our tunnel, we observe the appearance of plastic zones at the level of the surface of the ground which are represented by small red squares (case of mohr coulomb) and around the tunnel at the level of the two layers of ground: Lower Beauchamp sand and upper beauchamp sand. These plastic zones are related to the plastic or nonlinear parameters (cohesion, friction angle, dilatancy angle). When we decrease these parameters, we increase the plasticized zone. In our study we will base our analysis on the zones that are above the tunnel (Upper Beauchamp Sand) and determine the influence of these zones on the settlement curve.

(a) Mohr coulomb Model

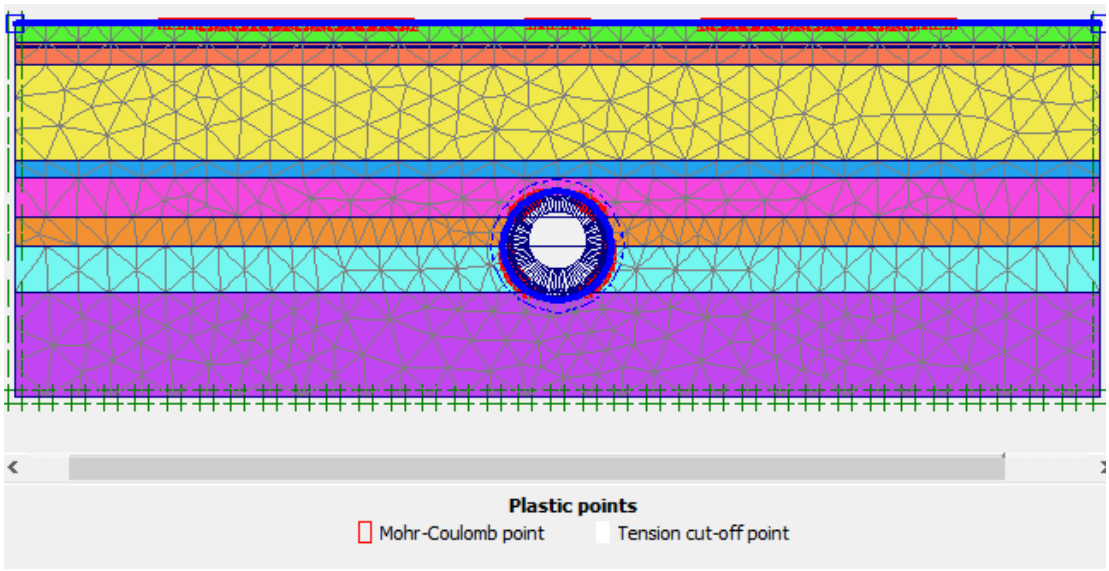

Figure 3.31. Plasticized zones with Mohr coulomb model

We observe the apparition of plastic zones on the surface of the soil (Fig. 3.31). This is due to the fact that the shear modulus is always constant even in areas of low deformation, which puts the soil in tension in these areas.Concerning the plastic zone at the level of the Upper Beauchamp sand, we will only decrease the value of the angle of internal friction, because the cohesion and dilatancy angle are almost null, and this refers to Table 3.13.

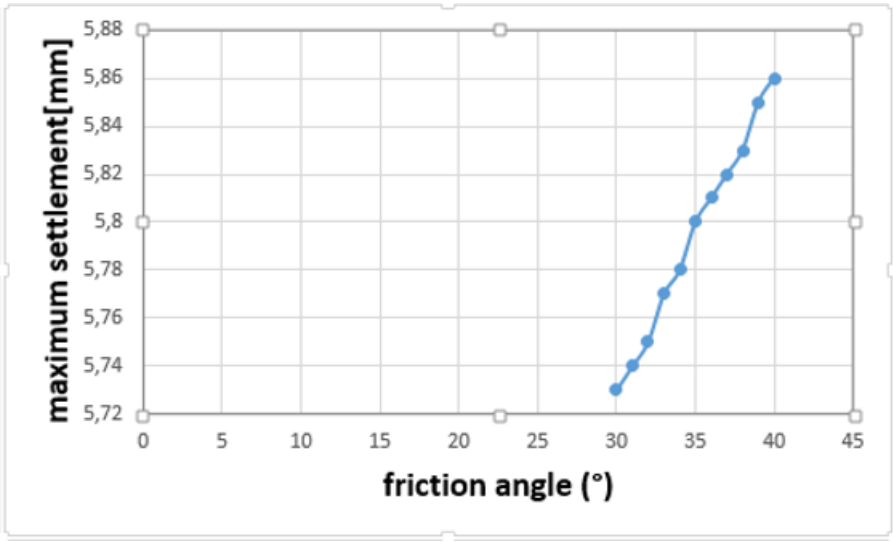

Figure 3.32. variation of the maximum settlement function of internal friction angle(MC).

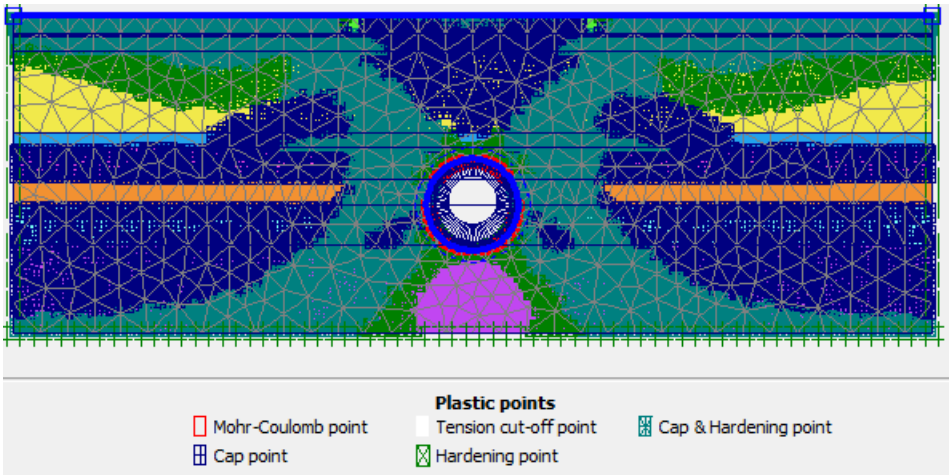

Figure 3.33. Plasticized zone in Upper Beauchamp sand with $\phi = 30°$

- When we reduce the friction angle ,we observe that the plasticized zone increase and the settlement decrease.

(b) Hardening Soil Model

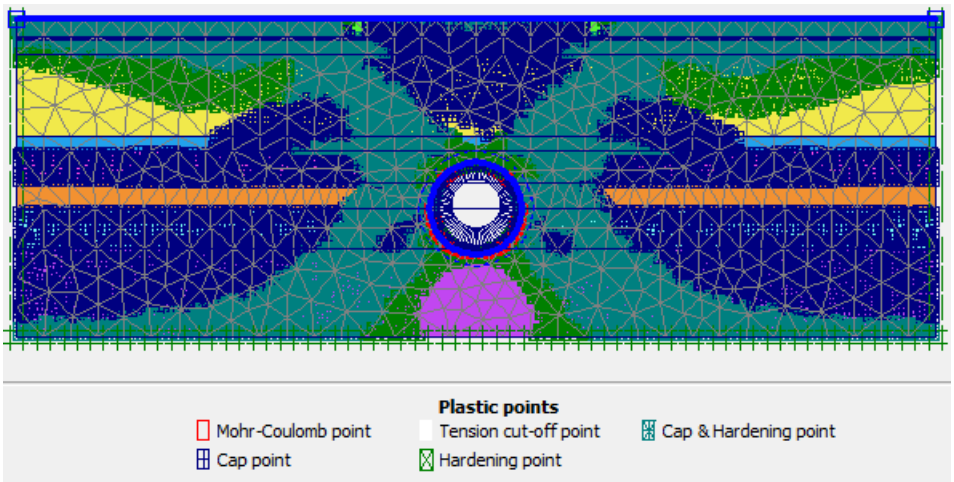

Figure 3.34. Plasticized zones with Hardening Soil Model

We observe the apparition of plasticized zones at the level of the Upper Beauchamp sand, we will only decrease the value of the internal friction angle because the cohesion and dilatancy angle are almost null and this refers us to table 3.16.

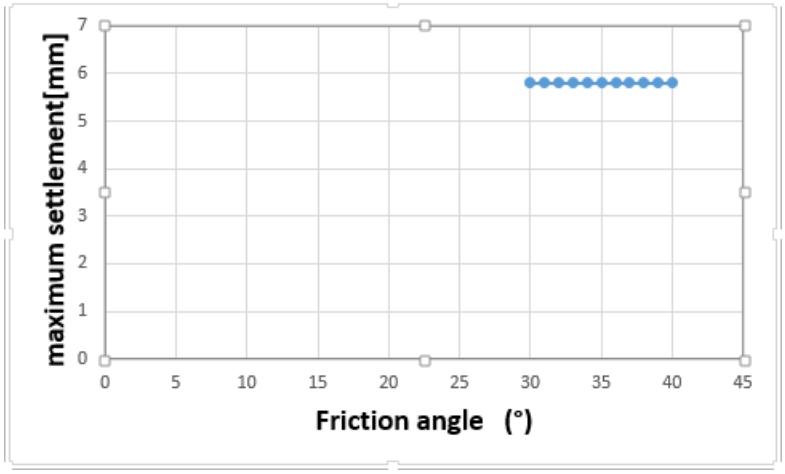

Figure 3.35. variation of the maximum settlement function of internal friction angle (HSM)

- When we reduce the friction angle , we increase the plasticized zone and the settlement remain constant (**Fig 3.35**).That means the increasing of plasticized zone in HSM doesn't change the settlement curve .

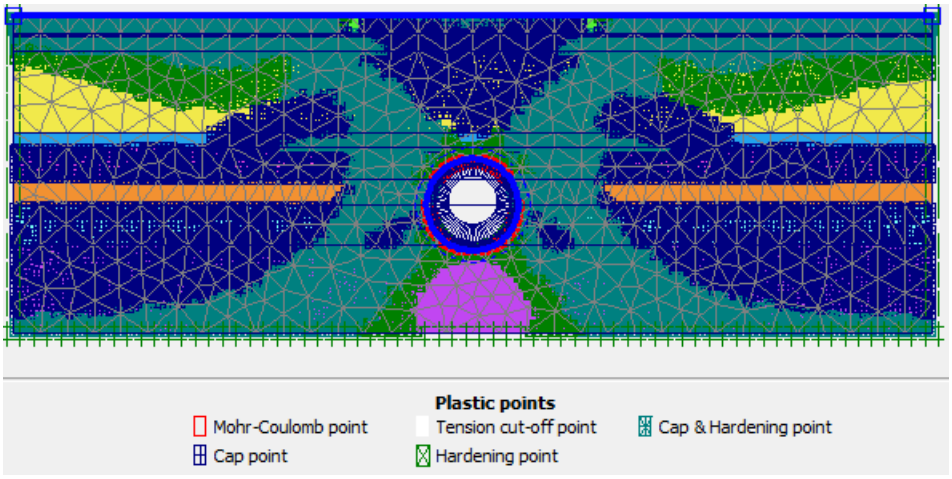

Figure 3.36. Plasticized zone in Upper Beauchamp sand with $\phi = 30°$

(c) Hardening Soil Model with small strain

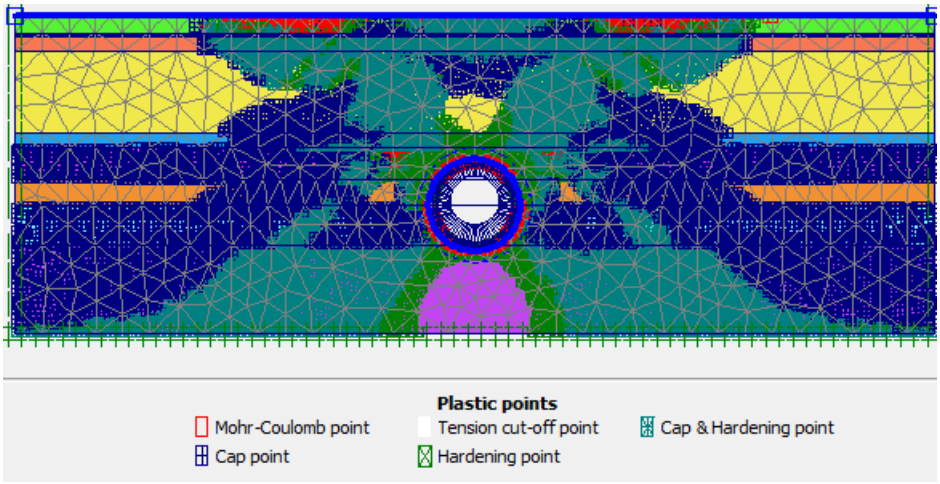

Figure 3.37. Plasticized zones with Hardening Soil Model with small strain .

We observe the apparition of a plasticized zones at the level of the Upper Beauchamp sand, we have only decrease the value of the internal friction angle because the cohesion and dilatancy angle are almost null and this refers us to table 3.21.

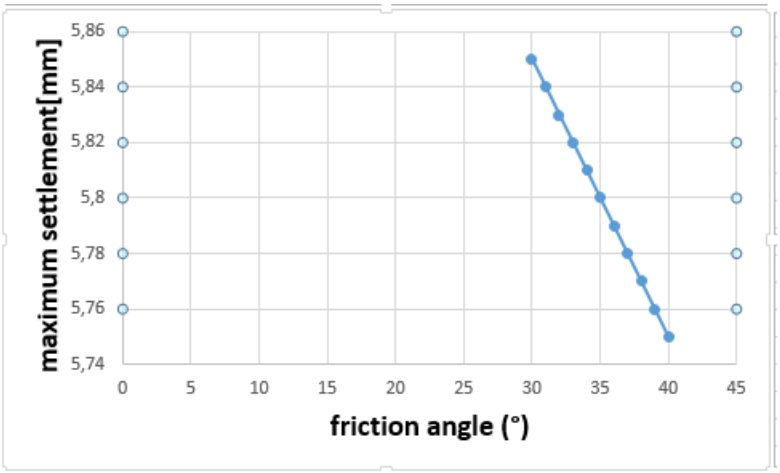

Figure 3.38. variation of the maximum settlement function of internal friction angle (HSSM)

When we reduce the friction angle from 40° to 30° we observe that the plasticized zone increase (fig 3.39) and the maximum setllement increase . (fig 3.38)

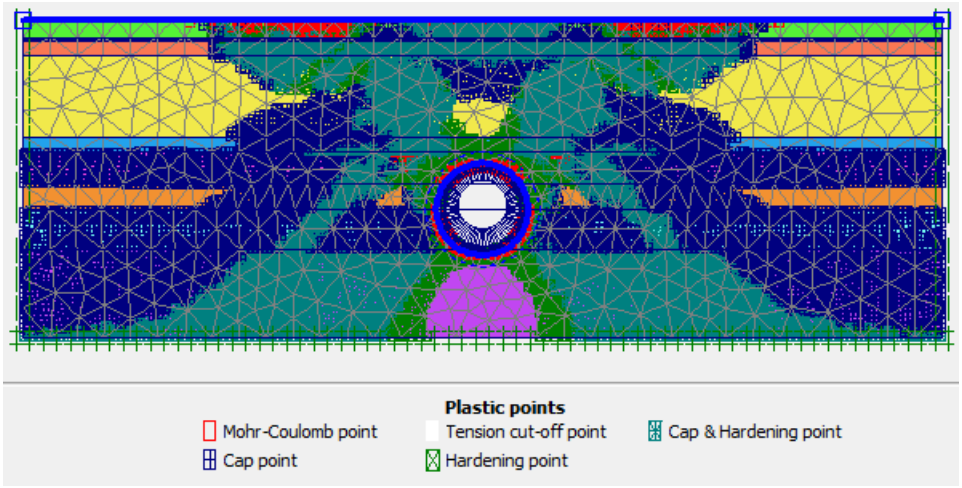

Figure 3.39. Plasticized zone in Upper Beauchamp sand with $\phi = 30°$

3.3.6 Synthesis of the results

After having obtained the different settlement curves of the constitutive soil models, we will compare them to the Gaussian curve of peck's and compare them with each other.

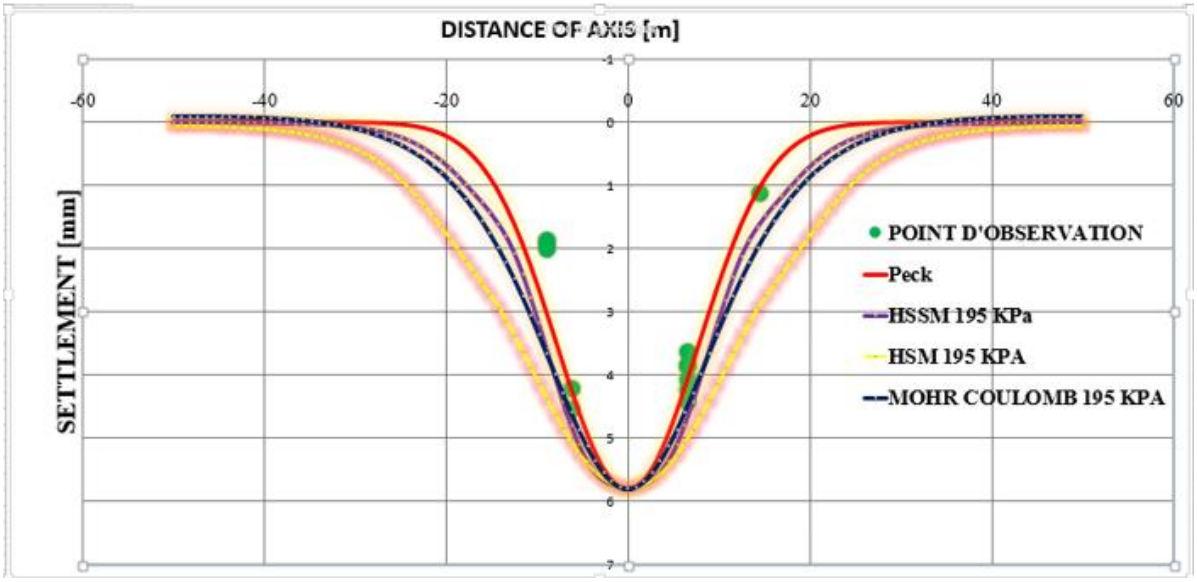

Figure 3.40 . Constitutive soil model settlement curves and peck's curve

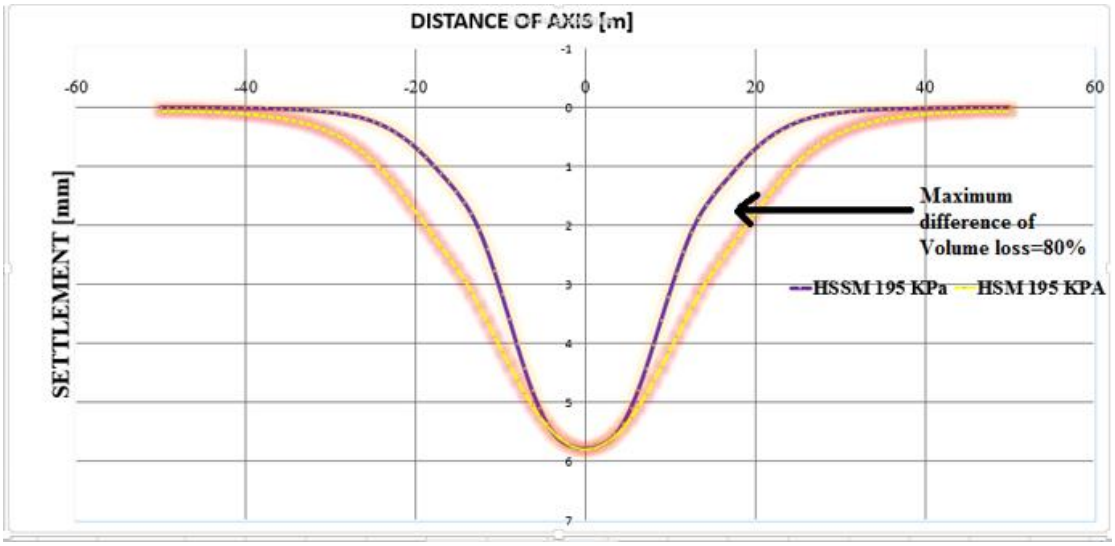

Figure 3.41 : HSM and HSSM settlement curves

- The impact of the constitutive soil model is manifested by a difference in movement response. Despite a consistent longitudinal extension of the mesh, it is found that using the MC model, ground uplift is still observed (Fig. 3.25) at 40 m from the tunnel axis, which seems unrealistic. This problem can be justified by the fact that even in areas of low deformation, the shear modulus in the Mohr coulomb model remains constant.

- The Constitutive soil Model MC is more conservative than the law of HSM, both in terms of compaction on the surface and therefore in terms of confine pressure and in estimation of the loss of volume .(Fig 3.41)

- The MC Model is more conservative and the HSM model can be considered more realistic compared to the REX available on line 12

- The model based on a higher stiffness in small deformations (HSSM) comes closest to experimental observations (deeper and less wide settlement curve – Addenbrooke et al., 1997) has the inverse of MC, which induces a curve that does not correspond to the Gauss equation. We also observe the maximum volume loss difference between HSM and HS Small settlement curve is 80% **(**Fig 3.41), which shows the importance of taking into account the variation of the shear modulus.

Conclusion

Finally, the results of the methodology of the previous chapter were developed and applied to the case study, which was the extension of line 12 of the Paris metro. After a general presentation of the site in terms of its geographical location, geology, hydrology, climate, relief and demography, a presentation of the project through its geotechnical, geological, hydrogeological context and the characteristics of the TBM and the lining used, followed by an overview of the parameters selected for the modeling. As a result, a numerical modeliing of the soil profile with the three constitutive soil models was performed and it follows that the settlement curve of the MC model is more concordant but not realistic and does not follow the peck formula, the settlement curve of HSM is realistic because it describes a good behavior of the soil but is very broad because it does not manage the variation of the modulus in small deformations and finally the settlement curve of HSSM is the one that best fits the Gaussian curve because it takes into account the variation of the modulus in the case of small deformations. Concerning the study of the influence of the mechanical characteristics of the soil around the tunnel, we observed that for the Mohr coulomb model, when we reduce the Young's modulus , the surface settlement increases. In the case of HSM , when we reduce the secant modulus and the cohesion, the settlement increases and for HSSM ,when we reduce the three parameters , the surface settlement increases.

GENERAL CONCLUSION AND OUTLOOK

This work focused on the influence of the choice of the constitutive soil model on the prediction of the settlement curve at the soil surface. Excavation of underground structures such as tunnels induces a change in the stress state of the soil, which can be physically identified by the settlement at the soil surface. The response of the soil to the construction of tunnels with modern methods is the result of complex operations. To highlight a methodology of this work is to describe the stages of extension of line 12 in Paris. The study area is located in the department of Seine-Saint Denis in Paris, more precisely between Porte de la Chapelle and Mairie d'Aubervilliers.In this thesis , we made a calibration of the different modulus of rigidity of each model of constitutive soil models , after that we made a numerical simulation with the software PLAXIS 8.6 2015 with the three models : Mohr coulomb model, hardening soil model and hardening soil model with small strain, after having obtained the three curve of settlement of the three constitutive soil models, we compared them with the curve of settlement of peck (Gaussian curve). The comparison criterion used here is the width and shape of the curve of the different models obtained and it appears that although the Mohr Coulomb model is the most used, it seems limited because its shear modulus is always constant, it does not give a good representation of the soil behavior and does not follow the Peck formula. The HSM settlement curve is realistic because it describes a good behavior of the soil but it is very broad because it does not manage the variation of the modulus in the small deformations and finally the HSSM settlement curve is the one that is the best because it takes into account the variation of the shear modulus in the zones of small deformations .This work shows that the use of a constitutive soil model adapted to the problem of the excavation of an underground structure (which includes the nonlinearity and the rigidity in the very small deformations), which is none other than the HSSM constitutive soil model, improves considerably the prediction of the displacements around the structure. Regarding the study of the influence of the mechanical characteristics of the soil around the tunnel, we can conclude that the mechanical characteristics of the soil (Young's modulus, internal friction angle and cohesion) around the tunnel (Upper Beauchamp sand) depending on the constitutive soil models used have an influence on the maximum value of the settlement curve . An analysis on the influence of the apparition of plasticized zones around the tunnel on the settlement curve was carried out and it was found that when there is an increase in the plasticized zone using the MC and HSSM models, we observe an increase on the maximum settlement .

This work is based only on the settlement curve. This work needs to be complemented by a study on horizontal displacements in the center of the tunnel and the influence of depth on settlements, the impact of deconfinement rate and constitutive soil models based on the Cam-Clay model.

APPENDIX 1 : RESULTS OF THE INFLUENCE OF MECHANICAL CARACTERISTIC OF UPPER BEAUCHAMP SAND ON THE SETTLEMENT CURVE

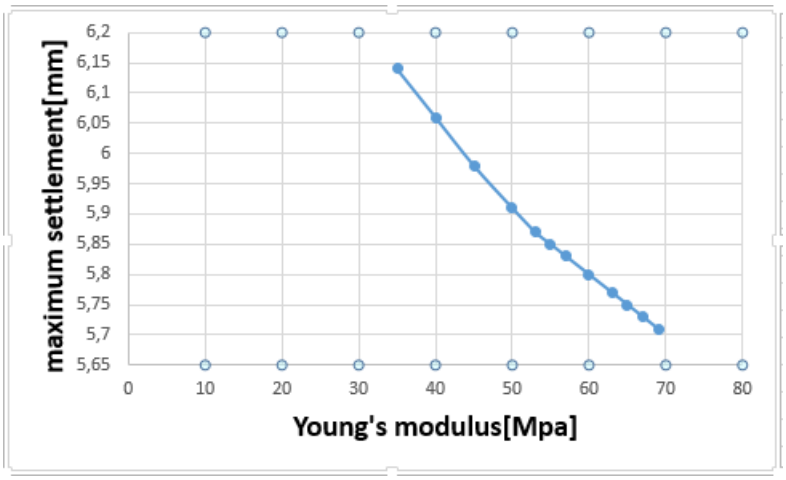

Figure 3.42. variation of maximum settlement function of Young modulus with MC

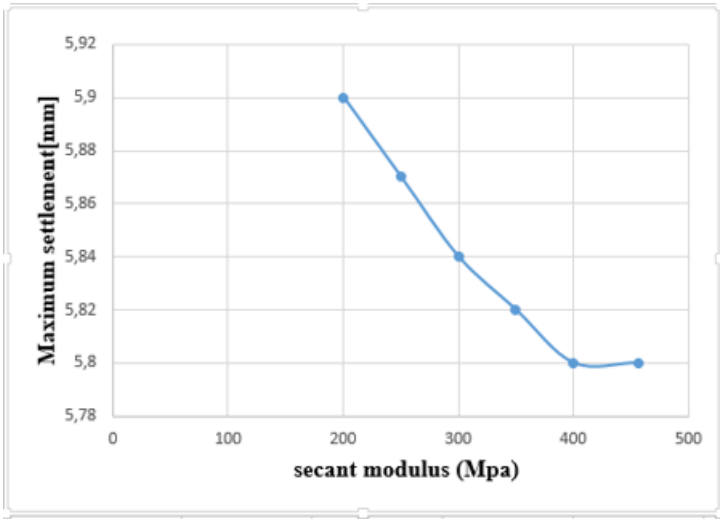

Figure 3.43. variation of maximum settlement function of secant modulus with HSM

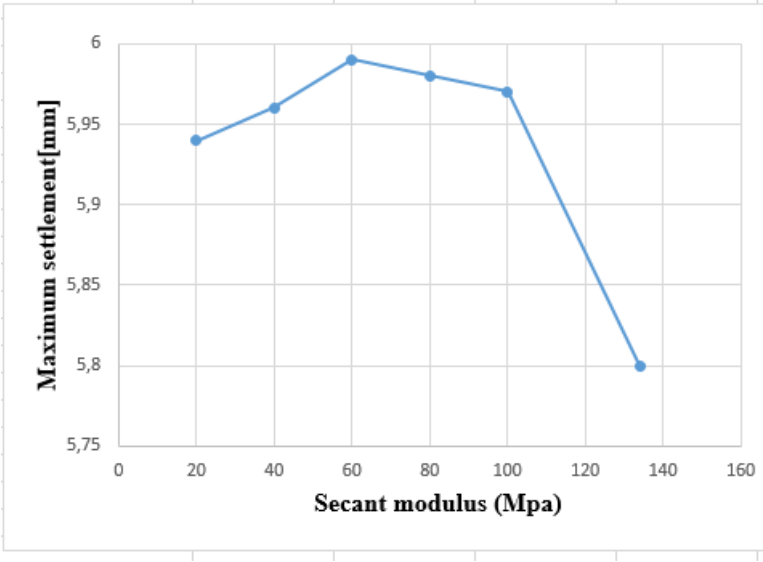

Figure 3.44. variation of maximum settlement function of secant modulus with HSSM

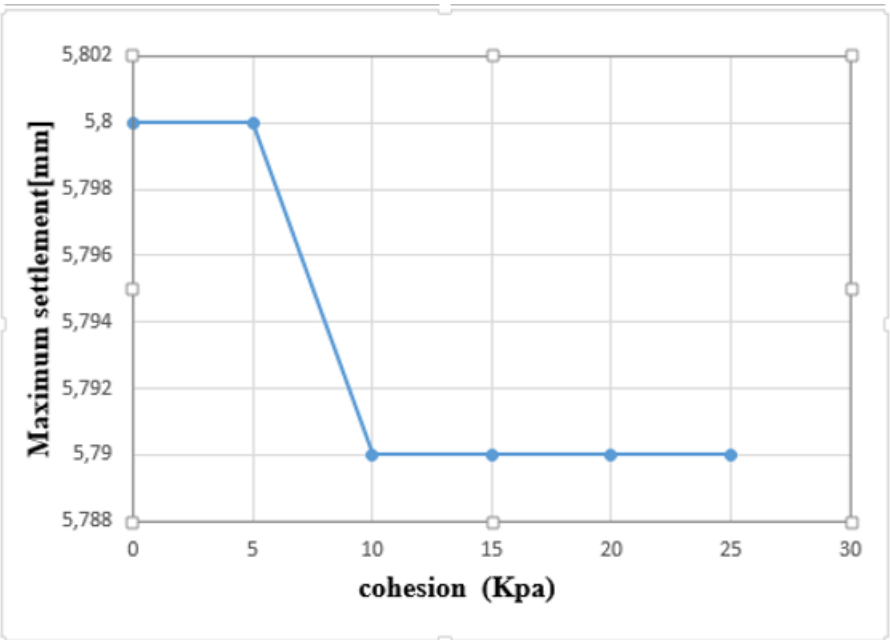

Figure 3.45 . variation of maximum settlement function of cohesion with MC

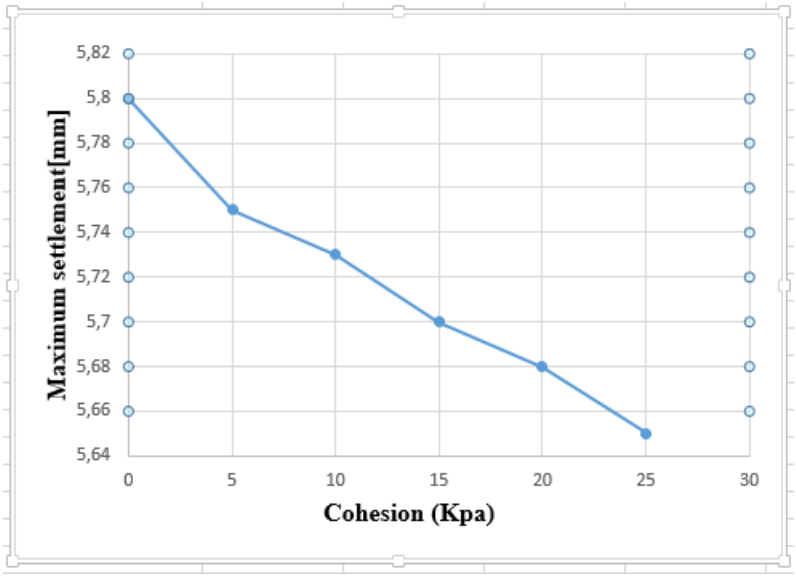

Figure 3.46. variation of maximum settlement function of cohesion with HSM

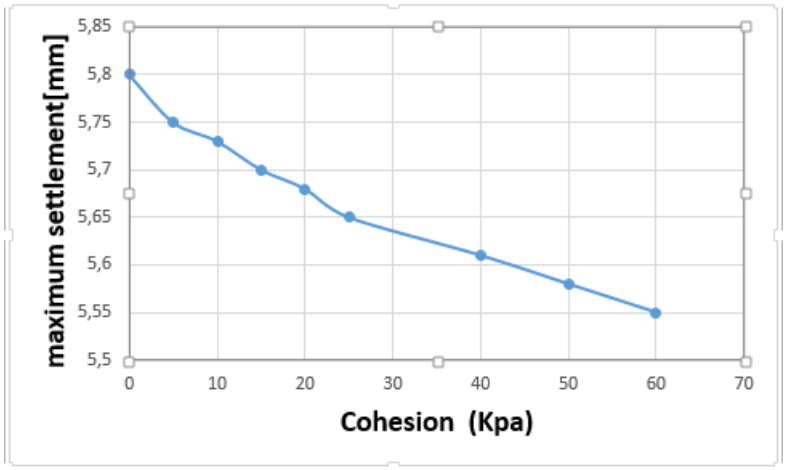

Figure 3.47. variation of maximum settlement function of cohesion with HSSM

References

- Addenbro oke, T., Potts, D., and Puzrin, A. (1997). The influence of pre-failure soil stiffness on the numerical. (Géeotechnique, Éd.)

- AFTES (2002). Recommendations for the convergence–confinement method. GT7R6A1. French Tunnelling and Underground Engineering Association, 16 p.

- Anagnostou, G., & Kovari, K. (1996). Face stability in slurry and EPB shield tunneling. In Proceedings of the symposium on geotechnical aspects of underground construction in soft ground, London (pp. 379–384).

- Aristaghes, P., & Autuori, P. (2003). Confinement efficiency concept in soft ground bored tunnels. Amsterdam: Claiming the Underground Space (pp. 909–913). Amsterdam: Claiming the Underground Space.

- M. Lei, J. Liu, Y. Lin, C. Shi, and C. Liu, "Deformation characteristics and influence factors of a shallow tunnel excavated in soft clay with high plasticity," Advances in Civil Engineering, vol. 2019, Article ID 7483628, 14 pages, 2019.

- Osmański, M. (2016). Numerical analyses of the effects of tunnels construction. Schanz, T. and Vermeer, P. (1998). Pre-failure deformation behaviour of geomaterials. (D. M. R., Éd.) Jardine, 383–387.

- Swoboda, M. B. (s.d.). Rheological analysis of tunnel excavation by means of coupled finite element (FEM)-boundary element (BEM) analysis. International Journal for Numerical and Analytical Methods in Geomechanics 11 (2).

- P. B. Attewell and J. P. Woodman, “Predicting the dynamics of ground settlement and its derivatives caused by tunnelling in soil,” International Journal of Rock Mechanics and Mining Sciences & Geomechanics Abstracts, vol. 15, no. 8, pp. 13–22, 1982.

- PLAXIS 2D (2015). Reference Manual

- R. B. Peck, “Deep excavations and tunnelling in soft ground,” in Proceedings of the Seventh International Conference on Soil Mechanics and Foundation Engineering, pp. 225–290, Mexico City, Mexico, August 1969

- R. J. Mair, R. N. Taylor, and A. Bracegirdle, “Subsurface settlement profiles above tunnels in clays,” Géotechnique, vol. 45, no. 2, pp. 361-362, 1995.

- Z. Wang, W. Yao, Y. Cai, B. Xu, Y. Fu, and G. Wei, “Analysis of ground surface settlement induced by the construction of a large-diameter shallow-buried twin-tunnel in soft ground,” Tunnelling and Underground Space Technology, vol. 83, pp. 520–532, 2019

- Schulz , Mathias “Experts Baffled by mysterious underground chambers”

- Brierley , Gary. “ Tunnelling : A historical perspective” 2020

- “Neanderthals built complex underground structures 175,000 years ago”

- History of tunnelling and underground construction and the factors driving current and future demand

- Think Deep : planning , development and use of underground space in cities

- Meulier , Tom “underground Rome” 2020

- Rigg , Susannah “Mexico city’s secret underground” 2020

- Solly , Meilan “construction on Rome’s Newest subway line is Revealing a Trove of ancient Treasures”2020

- Fitzgerald ,Jr , Joseph E “Safety in the underground construction and operation of the exploratory studies Facility at Yucca Mountain”

- Richelson ,Jeffrey T . “ U.S intelligence : Hiding of Military Assets by “Rogue Nations” and other states a Major security challenge for 21 st century .

- AFTES. La méthode convergence-confinement. Groupe de travail 7, Tunnels et Ouvrages Souterrains, n° 170, 2002, pp. 79-89.

- ARISTAGHES P., AUTUORI PH. Calcul des tunnels creusés au tunnelier. In: AFTES Journées d'études internationales de Chambéry, 1996, pp. 145-150.

- ATKINSON J. H., POTTS D. M. Stability of a shallow circular tunnel in cohesionless soil. Geotechnique, 1977, vol. 27, n° 2, pp. 203-215.

- ATTEWELL P.B. An overview of site investigation and long-term tunnelling induced settlement in soil. Engineering geology of underground movements, Geological Society Engineering Geology Special Publication, 1987, n° 5, pp. 55-61.

- ATTEWELL P.B. Ground movements caused by tunnelling in soil. In: Conference on Large Ground Movements and Structures, 1977, Cardiff, pp. 812-984.

- BARISONE G., PIGORINI B., PELIZZA S. Umbrella arch method for tunnelling in difficult conditions-analysis of Italian cases. In: Proceedings of the Fourth Congress International Association of Engineering Geology, 1982, New Delhi, vol. 4, pp. IV 15–IV 27.

- BARLA G., BARLA M., LEUZZI G. 3D numerical modelling and settlement monitoring during excavation of the Metro-Torino South extension. In: Proc. 7th Int. Symp. on Geotechnical Aspects of Underground Construction in Soft Ground, may 2011, Roma.

- BERNAT S. Modélisation du creusement d'un tunnel en terrain meuble, qualification sur chantier expérimental. Thèse Sci. Lyon : Ecole Centrale de Lyon, 1996, 215 p.

- BERNAUD D., ROUSSET G. Nouvelle méthode implicite pour l'étude du dimensionnement des tunnels. Revue Française de Géotechnique, 1992, n°60, pp. 5-26.

- BRINKGREVE R.B.J., VERMEER P.A. PLAXIS finite element code for soil and rock analysis, 2001, A.A. Balkema, Rotterdam.

- CARRANZA-TORRES C., FAIRHURST C. Application of convergence-confinement method of tunnel design to rock masses that satisfy the Hoek-Brown failure criterion. Tunneling and Underground Space Technology, 2000, vol. 15, n° 2.

- In: Proc. 7th Int. Symp. on Geotechnical Aspects of Underground Construction in Soft Ground, may 2011, Roma.

- CHAPEAU C. Auscultation du sol pendant le creusement. Tunnels et ouvrages souterrains, 1991, Septembre/Octobre, n° 107, pp. 235-245.

- CLOUGH W., SCHMIDT B. Design and performance of excavation and tunnels in soft clay: state of the art report. In: Int. Symp. On Soft Clay, 1977, Bangkok, pp. 980-1032.

- CLOUGH W., SCHMIDT B. Design and performance of excavations and tunnels in soft

clay. Soft Clay Engineering, 1981, pp. 569-634.

- DUNCAN, J.M., CHANG C.Y. Nonlinear analysis of stress and strain in soil. J. Soil Mech.

Found. Div. ASCE96, 1970, pp. 1692-1653.

- FILLIBECK J., VOGT N. Prediction of Tunnel-Induced Settlements in Soft Ground. In:

Proc. 7th Int. Symp. on Geotechnical Aspects of Underground Construction in Soft Ground, may 2011, Roma.

- HEJAZI Y., DIAS D., KASTNER R. Impact of constitutive models on the numerical analysis

of underground constructions. Acta Geotechnica, 2008, vol. 3, n° 4, pp. 251–258.

- Methods in Tunnelling Ruhr University Bochum, 9-11 September 2009. Aedificatio Publishers, pp. 1-4.

- LEBAIS Y., ANDRE D., CHAPEAU C., et al. Tassement lié au creusement des ouvrages en

souterrain. Tunnels et ouvrages souterrains, Novembre/Décembre 1995, n° 132, pp. 379-386.

- LONGANATHAN N., POULOS H.G. Analytical prediction for tunnelling induced ground movements in clays. J. Geotechnical and Geoenvironmental Enging. ASCE, 1998, Vol. 124, n° 9, pp. 846-856.